In vitro and *In vivo* Photodynamic Activities for BAM-SiPc, an Unsymmetrical Bisamino Silicon(IV) Phthalocyanine

LEUNG, Ching Hei

A Thesis Submitted in Partial Fulfillment of the Requirement for the Degree of Master of Philosophy

In

Biochemistry

Department of Biochemistry

August 2007

Thesis/Assessment Committee

Professor Tim-Tak Kwok (Chair)

Professor Wing-Ping Fong (Thesis Supervisor)

Professor Lai-Kwok Leung (Committee Member)

Professor Yun-Chung Leung (External Examiner)

Acknowledgements

I would like to take this opportunity to express my sincere gratitude to my supervisor Prof. Wing-Ping Fong for his patient guidance throughout my M. Phil study. His invaluable advices meant so much to me both in the preparation of the thesis and for my personal growth.

I would also like to express my gratitude to Prof. Tim-Tak Kwok, Prof. Lai-Kwok Leung, Department of Biochemistry, The Chinese University of Hong Kong and Prof. Yun-Chung Leung, Department of Applied Biology and Chemical Technology, The Hong Kong Polytechnic University, for their invaluable comments of my M. Phil thesis.

Special acknowledgement should be given to Prof. Dennis Kei-Pui Ng and Ms Pui-Chi Lo, Department of Chemistry, The Chinese University of Hong Kong. They have kindly provided me the chemical, BAM-SiPc and their knowledge and technical support in the field of Chemistry. Acknowledgement should also be given to Prof. Wing-Keung Liu, Ms Corina Au and Mr. Thomas Wong, Department of Anatomy, The Chinese University of Hong Kong, for their technical support in Histology.

I am particularly grateful to my colleagues Ms. Michel Chan, Ms. Crystal Chan, Mr. Cheung-Wai So, Ms. Judy Wong, Dr. Candy Tang and Ms. Elaine Chan and many others for their patience and cheerful support during my study.

I would like to express my special thanks and immensed gratitude to the one who I deeply treasured in my heart, Ms. Sheila, Sai-Kam Li for her patience, gentle encouragement, unceasing support and forgiveness when I felt frustrated and ill-

tempered which has helped me to overcome the toughest time in these two years of study.

Finally, I should give thanks to the one who I trust in my life, my Lord Jesus.

The bible said: *"The LORD is my shepherd; I shall not want. He maketh me to lie down in green pastures: he leadeth me beside the still waters. He restoreth my soul: he leadeth me in the paths of righteousness for his name's sake. Yea, though I walk through the valley of the shadow of death, I will fear no evil: for thou art with me; thy rod and thy staff they comfort me. Thou preparest a table before me in the presence of mine enemies: thou anointest my head with oil; my cup runneth over. Surely goodness and mercy shall follow me all the days of my life: and I will dwell in the house of the LORD forever."*

Psalms 23

For he is faithful, walking with me no matter what situation, showering me with his greatest mercy and endless love. Thank you, Lord.

摘要

光動力治療(PDT)適應於廣泛的醫療範疇，其中包括抗真菌、抗微生物、抗癌細胞作用等。Photofrin®是現時最廣爲人知及被應用於臨床醫學的感光化合物(Photosensitizer)。但隨著有更多的研究報告指出病人使用 Photofrin®後，都有嚴重的副作用如皮膚感光過敏反應引致的嚴重皮膚灼傷，促使現在有更大的需要去研發新一代能帶有高度的光動力活動但低副作用的感光化合物。

最近，本研究小組研製了一系列嶄新的 Silicon(IV) phthalocyanine 衍生物。在這個系列當中，以 BAM-SiPc (unsymmetrical bisamino substituted silicon(IV) phthalocyanine) 至爲突出。BAM-SiPc 對於不同種類的癌細胞也能展示出其強大的光動力毒害。試管實驗的結果顯示，只需以濃度低至納米單位的 BAM-SiPc 也足以殺死半數的細胞。

在活體實驗的體內分佈分析，高達 98%在後天性免疫力嚴重缺乏小鼠(nude mice)體內的 BAM-SiPc 能於一周後被排出體外。靜脈注射 BAM-SiPc 的一天後，我們發現 BAM-SiPc 能持續積聚於肝癌細胞(HepG2)腫瘤內，但整體而言，BAM-SiPc 沒有選擇性地積聚於肝癌細胞腫瘤內。另一方面在活體實驗的光動力治療中，結果顯示，1 $molkg^{-1}$劑量的 BAM-SiPc 能顯著地殺死(肝癌腫瘤，HepG2)或抑制(腸癌腫瘤，HT29)的癌細胞腫瘤的生長。

H&E 肝臟染片及血清蛋白酶(ALT, AST, CK)活性測示的結果顯示，以

BAM-SiPc 爲中介的光動力治療，不會導致肝臟或心臟中毒及損害。

有關 BAM-SiPc 的代謝研究，實驗結果指出正常的肝臟細胞(WRL-68)能把 BAM-SiPc 分解、代謝，但肝癌細胞(HepG2)卻不擁有相同的功能。當 BAM-SiPc 與老鼠的肝臟提出液混合後，BAM-SiPc 的含量隨著時間而不斷減少，而其中的代謝物分別在黑暗或受到光線照射下，也不會產生毒性。

在分析因爲光動力治療而引發的細胞死亡機制當中，我們發現經光動力治療處理過的癌細胞，會隨著 BAM-SiPc 的濃度增加而在細胞內釋出更多的活性氧分子。細胞周期分析實驗結果顯示，當介乎 0.005 至的 BAM-SiPc 濃度使用於光動力治療，部份細胞的細胞周期會停留於 G_0/G_1 階段。TUNEL 測試及 H&E 腫瘤染片的結果顯示，BAM-SiPc 作中介的光動力治療能在活體實驗中，啓動肝癌腫瘤的細胞自毀系統。

最後，我們發現當 BAM-SiPc 混合了人類低密度脂蛋白(Human low density lipoprotein)，BAM-SiPc 的光動力治療的效率會明顯地被降地。此現象或因低密度脂蛋白抑制了細胞對 BAM-SiPc 的攝取，但由於凝膠層析 (gel filtration) 不能偵測出低密度脂蛋白與 BAM-SiPc 的結合物，所以有關抑制 BAM-SiPc 攝取的原因仍處於未知階段。

Abstract

Photodynamic therapy (PDT) has been found to be useful in many different applications with its anti-fungal, anti-microbial and anti-cancer activities. As serious side effects such as skin photosensitivity have been reported for those patients administered with Photofrin®, it is necessary to search for alternate photosensitzer that exhibits high photodynamic activities but with minimal side effect.

Recently, a novel series of silicon(IV) phthalocyanine derivatives has been synthesized. Among the series, BAM-SiPc, an unsymmetrical bisamino silicon(IV) phthlocyanine, was identified as a promising photosensitizer with an extremely high phototoxicity toward different cancer cell lines. The IC_{50} was in nano-molar concentration.

In the biodistribution study, it was found that BAM-SiPc could be almost cleared (~ 98%) from the nude mice one week after injection. Persistent accumulation of BAM-SiPc in tumor was shown even for 24 hr after BAM-SiPc administration. However, there was no selective uptake of BAM-SiPc in HepG2 tumor. Significant tumor regression (HepG2) or growth inhibition (HT29) was observed after *in vivo* PDT with 1 $\mu molkg^{-1}$ of BAM-SiPc. H & E staining of the liver section and assay of plasma enzyme activities (ALT, AST and CK) showed that no hepatic or cardiac injury was induced by the protocol used in this study.

For the metabolism of BAM-SiPc, it was found that BAM-SiPc could be metabolized by the normal liver cells WRL-68 but not by HepG2 cells. When BAM-SiPc was incubated with the mice liver homogenate, there was a time-dependent decrease in BAM-SiPc content. The metabolite was found to be non-toxic both in the dark and in the presence of light.

There was a dose-dependent increase of intracellular ROS production when cancer cells were PDT-treated with BAM-SiPc. In the cell cycle analysis, arrest in G_0/G1 phase was observed when HepG2 cells were PDT-treated with BAM-SiPc at concentration ranging from 0.005 μM to 0.02 μM. Apoptosis was induced in HepG2 tumor after *in vivo* PDT with BAM-SiPc as shown by the result of Terminal deoxynucleotidyl transferase-mediated dUTP nick end labeling (TUNEL) and H & E staining of the tumor sections.

Finally, it was shown that the PDT efficacy of BAM-SiPc decreased in the presence of LDL. Cellular uptake of BAM-SiPc was inhibited by LDL. However, LDL conjugated BAM-SiPc could not be identified by gel filtration. Therefore, the reason for the decrease in BAM-SiPc uptake has yet to be determined.

List of Abbreviations

ALA	δ-aminolaevulinic acid
AlPc	Aluminum(III) phthalocyanines
$AlPcS_4$	Aluminum tetrasulfophthalocyanine
ALT	Alanine aminotransferase
ANOVA	Analysis of variance
AST	Aspartate aminotransferase
ATCC	American type culture collection
BAM-SiPc	Unsymmetrical bisamino substituted silicon(IV) phthalocyanine
BPD	Benzoporphyrin derivative
BSA	Bovine serum albumin
cdk	Cyclin-dependent kinase
CK	Creatine kinase
DCFDA	2',7'-Dichlorofluorescein diacetate
DISC	Death inducing signaling complex
FITC	Fluorescein isothiocyanate
GSH	Reduced glutathoine
H & E staining	Haematoxylin and eosin staining
HpD	Hematoporphyrin derivatives
HSP	Heat shock protein
ID	Initial dose
i.v.	Intravenous
LC-MS	Liquid chromatography-mass spectrophotometry

LDL	Low density lipoprotein
MALDI-TOF	Matrix-assist laser deionization-time of flight
m-THPC	5, 10, 15, 20-Tetra [m-hydroxyphenyl] chlorin$_{e6}$
NAD^+	β-nicotinamide adenine dinucleotide
NO	Nitric oxide
PARP	Poly ADP ribose polymerase
Pc	Phthalocyanine
PDT	Photodynamic therapy
PI	Propidium iodide
PS	Photosensitizer
ROS	Reactive oxygen species
SiPc (Pc 4)	Silicon(IV) phthalocyanine
TdT	Terminal deoxynucleotidyl transferase
TNF-α	Tumor necrosis factor-α
TUNEL	Terminal deoxynucleotidyl transferase-mediated dUTP nick end labeling
ZnPc	Zn(II) phthalocyanine

List of Figures

List of Tables

Table of Content

CHAPTER 1

Introduction

1.1 History and development of photodynamic therapy

Photodynamic therapy (PDT) is a treatment which combines the administration of photo-reactive agent and illumination on target area to remove the unfavourable tissues. Its medical value could be dated back to ancient Egypt and India. At that time, a photosensitive chemical called psoralens, extracted from some seeds and fruits, was utilized to treat some skin diseases[1]. However, the medical value of PDT was not realized in the modern era until the beginning of 20th century. Nieis Finsen won the Nobel Prize for his work on using "phototherapy" to treat smallpox and tuberculosis[2]. Later, Herman von Tappeiner and A. Jesionek have successfully treated tumors on skin by activating the topical eosin with sunlight[3, 4]. Despite the promising discovery of the anti-cancer effect of PDT, the use of photosensitizers (PS) was better known for the photo-detection of tumor tissue because of the fluorescent property of PS[5].

Until 1960s and 1970s, Lipson *et al.* [6] and Dougherty[7] used hematoporphyrin derivatives (HpD) and fluorescein respectively to destroy tumor tissue. Since then, PDT has been studied extensively, including the basic mechanism of PDT-induced cytotoxic effect, formulation of novel PS or PS derivatives and most importantly the medical application of this mode of treatment. Particularly, the anti-cancer activity of PDT has drawn the most of the attention from the researchers. In the late 1990s, Porfimer Sodium or commercially called Photofrin® (Fig. 1.1a), a purified version of HpD, was approved for clinical use in United States and Canada. Photofrin® was found to be useful in treating early and late-stage lung cancer and also esophageal cancer[5]. Since then, several more PS, for example, methyl-tetrahydroxyphenyl

(a)

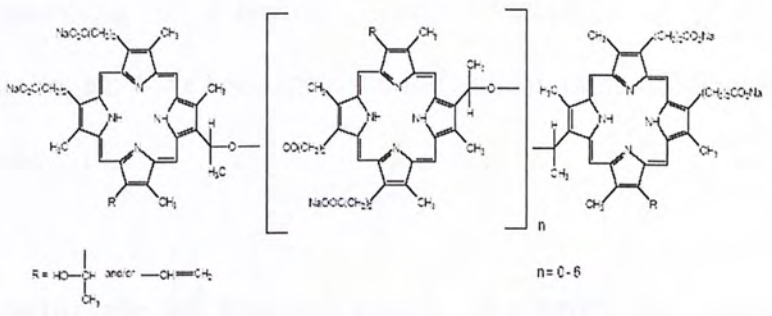

(b)

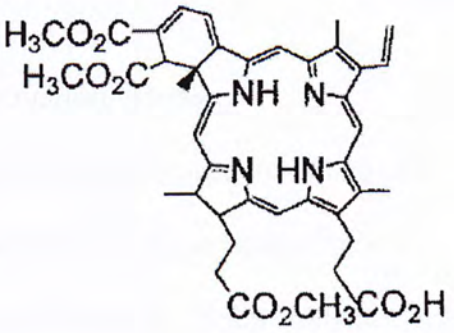

(c)

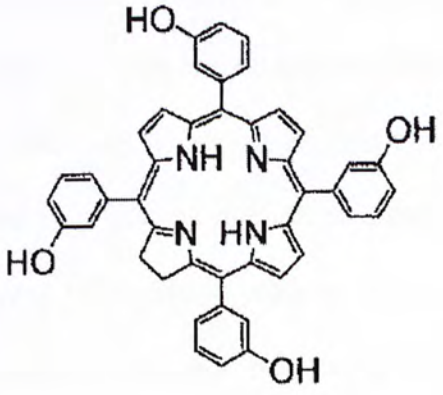

(d)

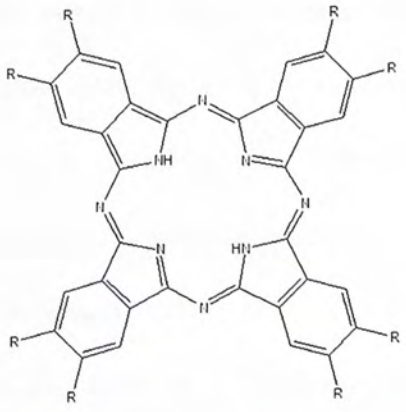

Fig. 1.1 Chemical structures of some photosensitizers used in photodynamic therapy: (a) Photofrin®, (b) Benzoporphyrin derivatives, (c) Foscan® and (d) Phthalocyanines.

chlorine (Temoporfin or Foscan®), 5-aminolevulinic acid (5-ALA), methyl 5-aminolevulinate, etc. have been approved for clinical use in different countries (e.g. U.S.A. and Canada).

1.2 Basic principle of photodynamic therapy: the beauty of the treatment

- ***Oxidation as a potent killing weapon***

PDT can kill cells rapidly because it can greatly increase the intracellular oxidative pressure. The sudden increase in oxidative stress will trigger a cascade of death signaling events inside the cells. Such oxidation is accomplished by a cascade of the energy transferring processes. There are two types of photo-oxidation reaction, Type I and Type II photoreaction. In an anoxic or hypoxic intracellular environment, Type I photoreaction will dominate which means that the excited PS will directly oxidize an organic substrate (e.g. plasma membrane components). The reduced PS will further react with oxygen molecules to produce reactive oxygen species (ROS) such as superoxide anion and hydroxyl radical ($OH^{\cdot}$). ROS is such a highly reactive free radical that its oxidative power can cause serious intracellular damage, leading to cell death. However, in most cases, the Type II photoreaction is the dominant type in PDT, which means the energy of the excited PS will be transferred to molecular oxygen and produce an extremely reactive substance, singlet oxygen which is believed to be the key cytotoxic agent during PDT[5] (Fig. 1.1).

As singlet oxygen is highly reactive, it has a very short life time ranging from 10-100 μs. The oxidative damage towards the cells will only be confined within a small region and within an individual cell because singlet oxygen can only travel a very short distance.

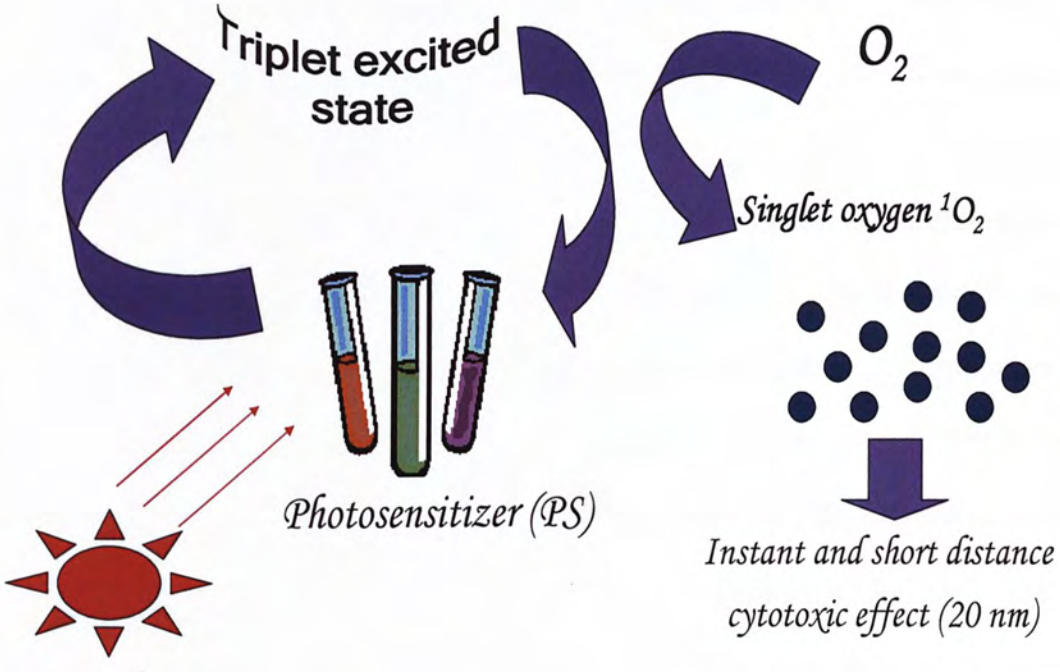

Fig. 1.2 Schematic diagram showing the basic principle for the generation of ROS.

- ***Light delivers highly specific and localized therapy***

PDT consists of two non-cytotoxic components, light and PS. Singlet oxygen will only be produced when light is delivered to excite the PS. By virtue of this property, photodynamic effect can be localized to the target area simply by manipulating the light source. Currently, surgery, radiotherapy and chemotherapy are the major treatments for cancer. However, different degrees of side effects had been reported in patients who received these treatments.

Surgery involves the removal of a large part of the organ and takes a very long time for patients to recover. Situations would become more complicated for those patients who suffered from advanced stage or late stage cancers. Chemotherapy is usually used as a last resort to control the progress of the disease, but a great discomfort has to be tolerated by the patient because of the non-discriminative cytotoxic effect on both normal and cancer cells. In radiotherapy, there is a limiting dose for application on each patient because of its carcinogenic effect. Due to these drawbacks of the other treatments, PDT emerges as a very attractive alternative. Endoscope equipped with optical fibers is commonly used for delivering light to activate the PS when the target tissue is located deep inside the body[8]. Recently, Moseley *et al.* [9] has introduced a novel device called "sticking plaster" which makes application of PDT more convenient and without time-constraint. "Sticking plaster" is actually a portable light emitting diode array which can be placed firmly on the target area of the patient. This allows the continuous activation of the PS which has been smeared on the skin surface. It has been proved to be effective in treating superficial basal cell carcinoma and actinic keratosis.

1.3 Photosensitizers: From discovery, synthesis to modifications

The discovery of photodynamic activity was rather accidental. After Lipson *et al.* [6] had recognized the anti-tumor activities of HpD, many researchers started to search or synthesize new PS for application on cancer treatment. After decades of experience, it is widely accepted that an ideal photosensitizer should fulfill several basic criteria:

1. Cytotoxicity should only be exerted with light activation but the PS should remain non-toxic in the dark.
2. PS with an absorption maximum (excitation wavelength) at a wavelength greater than 600 nm is preferred because red light or light with wavelength near the infra-red region can penetrate deeper into the skin.
3. PS should preferentially accumulate in tumor tissue rather than normal tissue and singlet oxygen can be effectively generated in the target cells.

Throughout the decades of investigation, many different kinds of PS have been reported to be potential photosensitizing agents. HpD (first generation PS), chlorins, cacteriochlorins and phthalocyanines (second generation PS) are highly valued compounds in various applications. Photofrin®, the first clinically approved PS, was thought to be a promising agent because it could effectively treat oncological diseases such as advanced stage of lung cancer. However, there were also many reports stating the drawbacks of using Photofrin® which were not expected at the very beginning.

Skin photosensitivity is the most adverse and significant side effect suffered by the patients who received Photofrin®- PDT. Some clinical reports suggested that the selectivity of Photofrin® to tumor tissue was low and the drug could be retained in the healthy tissue, especially skin, for up to several weeks or even months. Much

inconvenience arises because patients have to avoid sunlight or high intensity light during this period[2, 5, 10]. The wavelength of absorption maximum for Photofrin® is 630 nm. Only a relatively small portion of light at this wavelength can transmit through the skin to activate the PS. Another drawback is that patients have to wait for 48-72 h and protect from light after administration of Photofrin® in order to allow selective accumulation of PS in tumor tissue before illumination can be applied. Due to these reasons, using Photofrin® for PDT is not a favourable choice which is why its prevalence has been limited. Therefore, searching for a better PS is still an ongoing task in the field of PDT.

- ***Other commercially available PS: Benzophorphyrin derivatives and Foscan®***

Benzoporphyrin derivative (BPD) (Fig. 1.1b) is photodynamically active with an absorption maximum around 690 nm. However, it is not suitable for cancer treatment because it is rapidly cleared from the body, only 3 hours after intravenous administration. Also, the tumor selectivity is relatively low[11]. Nevertheless, Verteporfin, one of the BPDs, was found to be effective in destroying the neovasculature on the retina and has been approved for clinical use in treating age-related macular degeneration[12, 13].

A commercially available PS called Foscan® (Fig. 1.1c) has been used in treating palliative head and neck cancer. It is the most active PS among the series of tetrahydroxyphenyl analogues with an excitation wavelength at 652 nm. In terms of photodynamic efficacy, Foscan® is better than Photofrin® as it can produce similar extent of cellular damage with a lower drug and light dose[14] (Foscan®: ~0.1 mg/kg, < 20 J/cm^2; Photofrin: 2 mg/kg, ~200 J/cm^2). However, the unusual high phototoxicity of Foscan® has made the optimization of treatment protocol very difficult. Also, large

lesion would be left for those patients who have received the treatment. Skin photosensitivity could still be suffered 20 days after PS administration[15]. These make the choice of Foscan® as a photo-activating agent unfavourable in some circumstances.

- ***Phthalocyanines***

Phthalocyanine (Pc) is another class of PS which has gained much attention. Similar to hematoporphyrin, phthalocyanine possesses a tetra-pyrrolic ring (Fig. 1.1d) which allows PS excitation by light and results in the production of singlet oxygen. Physically, it has a longer wavelength of absorption maximum than Photofrin® at around 670 ~ 680 nm. A lower intensity of light can thus be used to activate the PS because light with longer wavelength can travel deeper under the skin. Metal chelation to the central core of the ring is often done in order to lengthen the time of the triplet excited state and hence the amount of singlet oxygen produced. Aluminum(III) phthalocyanines (AlPc), Zn(II) phthalocyanines (ZnPc) and Silicon(IV) phthalocyanines (SiPc or Pc 4) are examples of the Pc series of photosensitizer. In the last decade, the *in vitro* and *in vivo* photodynamic activities of Pc, especially for ZnPc and SiPc, have been intensively studied. One study has shown that significant tumor regression can be observed in a murine EMT-6 tumor bearing Balb/c mice model treated with fluorinated ZnPc derivatives[16]. Another study suggested that ZnPc may be effective in suppressing skin cancer activities by demonstrating the *in vitro* phototoxicity to three different skin-derived cell lines, namely, HT-1080 transformed human fibroblasts, 3T3 mouse embryo fibroblasts and HaCaT human keratinocytes[17]. Beside anti-cancer activity, ZnPc has also been reported to be able to inactivate bacterial growth[18].

SiPc is one of the most photoactive PS among the Pc series. The usefulness of SiPc in cancer therapy has been reflected by its tumoricidal activities in a wide variety of cancer cells. George *et al.* [19] suggested that Pc 4 could suppress the proliferation of glioma. They found that Pc 4 mediated PDT can induce apoptosis (low light dose) or necrosis (high light dose) of U87-derived human glioma in nude rat as revealed in the histological study. Whitacre *et al.* [20] have revealed that there is a significant tumor regression when human colon cancer xenografts (SW 480) were treated with Pc 4 and illuminated with a diode laser of wavelength at 672 nm. Colussi *et al.* [21] has also found that Pc 4 was effective in eradicating human ovarian epithelial carcinoma (OVCAR-3) in nude mice.

- ***Obstacles for PDT to gain popularity in medical field***

Currently, testing on phthalocyanines has already entered preclinical or Phase I clinical trial. Borgatti-Jeffreys *et al.* [22] used zinc phthalocyanine tetrasulfonate to successfully obtain complete or partial tumor regression response in mice and dogs with naturally occurring neoplasms. Although a lot of PS is available and some have already been approved for clinical use, adjusting the optimum drug and light doses to maximize treatment efficacy but with minimal side effect is still a very difficult issue to tackle[10]. One major reason is that the selective accumulation of PS in tumor tissue instead of healthy tissue is not apparent. To solve this problem, researchers have tried to synthesize derivatives of PS with high phototoxicity but low dark toxicity, examples included the BPD derivatives, ZnPc derivatives and SiPc derivatives. The PDT efficacy of the derivatives is better than their parental PS as modification of their chemical properties allows better diffusion into abnormal tissue. In recent years, attempts have been made to modify PS by conjugation with biomolecules so as to

increase the selective uptake which is based on the biological properties of the target tissues.

1.4 Enhancement of selective retention of PS in cancerous tissue

PDT is an attractive therapeutic option for cancer treatment because it can exert cytotoxicity specifically by manipulating the light source. Also, it is believed that PS can selectively accumulate in the rapidly proliferating tissue especially the malignant cells. Such belief is based on the abnormal properties of malignant tissues including large interstitial space, a leaky vasculature, compromised lymphatic drainage and lower intracellular pH, etc. when compared with their normal counterpart. These properties facilitate the diffusion of PS especially those PS which are amphiphilic in nature[14]. However, some researchers has reported that there is actually no preferential uptake of PS by cancerous tissue compared to normal tissue. One typical example is Photofrin® where the PS is selectively taken up by the skin and causes photosensitivity with symptoms such as burn and skin rashes.

- ***Amphiphilic PS is photodynamically more active than ordinary PS***

Molecules with both hydrophobic and hydrophilic regions at different positions are regarded as amphiphilic. The hydrophobic region and hydrophilic region of an amphiphilic PS can interact with the surrounding environment independently. So, it exerts greater phototoxicity on the target cells because amphiphilic PS can readily insert into the membrane structure or the surface of protein where oxidative attack and cell death can be rapidly produced[5, 23-26]. Margaron *et al.* [27] suggested that the amphiphilicity of the tetraphenylporphine will increase with the number of sulfonic acid substitution. They found that the higher the amphiphilicity of

tetraphenylporphine, the greater was the phototoxicity generated. Later, Cauchon *et al.*[28] supported the same argument by substituting zinc trisulfophthalocyanines with an alknyl side chain. They found that substitution with hexynyl or nonynyl groups would increase the amphiphilicity of the compound which enhanced the cellular uptake, mitochondrial membrane insertion and potency of the PS.

- ***Increase cell targeting by biological modification of PS***

Malignant cells usually possess abnormal biological properties which the normal cells do not have. Many researchers have designed modification of PS which can target those abnormal features in order to increase the PS uptake specificity. At the very beginning when such idea had just emerged, many researchers tried to conjugate PS with common biomolecules such as bovine serum albumin (BSA), low density lipoprotein (LDL) or saccharides to see whether there is any increase in PS uptake in tumor cells. Brasseur *et al.* [29] has successfully demonstrated that BSA conjugation with $AlPcS_4$ allows the drug to accumulate more in the cancer cells. As a result, the phototoxicity towards J774 mouse mammary tumor cells of monocyte-marcrophage origin can be significantly increased. In addition, they found that maleyated BSA conjugation could further enhance the photodynamic activity because the negative charge on maleyated BSA could increase the binding of the conjugated PS to scavenger receptor. Similar observation was also reported in the studies by Hamblin *et al.* [30] and Huang *et al.* [31]. Hamblin *et al.* showed that conjugating $chlorin_{e6}$ with maleylated BSA could enhance its phototoxicity towards J774 cells while Huang *et al.* demonstrated that the phototoxic effect of BSA conjugated dicationic silicon(IV) phthalocyanine towards HepG2 hepatocarcinoma cells was greater than that of the unconjugated PS.

Lipoproteins, especially LDL, is another class of biomolecule where the efficiency in increasing selective uptake of PS by tumor cells has been cited in many reports. It is believed that LDL conjugation can increase the selective uptake mainly through LDL receptor recognition. The role of LDL receptor in enhancing PS uptake has been studied by using human and rat transformed fibroblasts. The results showed that both Hematoporphyrin-LDL and ZnPc-LDL conjugated complexes were accumulated more than the unconjugated PS. The LDL conjugated Hp was internalized through LDL receptor uptake whereas the LDL conjugated ZnPc entered the cells by non-specific endocytosis[32]. When chlorin$_{e6}$ was covalently attached with LDL molecule, the cellular uptake was greater than those of free chlorin$_{e6}$ and non-covalently attached complex: 80% of the targeted cells was killed compared with only 10% by using the same amount of free or non-covalent complexed chlorin$_{e6}$[33]. Although there are much evidence supporting that LDL conjugation can enhance the potency of a PS, many studies have only proved such idea in *in vitro* cell culture system. The usefulness of LDL conjugation in an *in vivo* or clinical system remained uncertain. van Lier *et al.* [34] had even found that LDL conjugation could not significantly increase the phototoxicity of aluminum (dodecylaminosulfonyl) tetrasulfophthalocyanine in an animal model. Such phenomenon was thought to be due to the natural distribution of PS to LDL in the blood stream when intravenous injection was employed. On the other hand, they had also found that the photodynamic activity would be abolished after the covalent attachment of LDL to AlPcS$_4$. It seems that the effect of LDL conjugation will vary depending on different PS, cell types or type of conjugation. Further studies are still required to confirm under what circumstances will LDL conjugation increase the potency of a PS.

- ***Other drug delivery systems to enhance PDT specificity***

In addition to LDL and serum albumin, molecules such as transferrin and steroids have also been reported to increase PS uptake in tumor cells[35]. These modifications are based on the fact that malignant tissues have a higher demand of resources for maintaining cell integrity, cell division and energy production. Besides, some researchers have designed modifications which can manipulate the subcellular localization of PS. With the importance of singlet oxygen contributing to cell death and realizing that it can only travel within a short distance (~45 nm), the subcellular localization of PS would be a key factor to determine the magnitude of PS photodynamic activities[35]. Delivering PS to the cell nucleus is a promising approach in improving PDT specificity because nucleic acids are very photosensitive and their damage will readily induce cell death. Akhlynina *et al*.[36-38] tried to covalently attached chlorin$_{e6}$ with BSA and insulin molecule and found that chlorin$_{e6}$ would be localized to cell nucleus and produced significant phototoxcity to the cell. Later, they have also tried to link the bio-conjugated chlorin$_{e6}$ with a nuclear localization signal so as to facilitate the transport of PS to the nucleus through the nuclear pore complex. Results showed that the photodynamic efficacy of chlorin$_{e6}$ could be increased by more than 2400 fold.

Recently, a novel approach to enhance PDT specificity has been developed. It involves the design of a PS covalently attached with a macromolecule such that the PS will only become activated when the macromolecule is cleaved away. This idea is similar to the concept of "magic bullet". PS attached with macromolecules such as a polypeptide will only become activated within tumor tissues where there is an over-expression of tumor-associated protease, for example, cathepsins and matrix metalloproteinase[39-41]. These proteases can cleave away the polypeptide chain and

leave the free PS within the cancer cells. This method is called protease-mediated PDT[42].

Currently, many molecules have been identified to be useful in increasing the selective accumulation of PS. However, each bio-conjugation is only workable in several types of cell due to the diverse cellular characteristics between different kinds of cell. Moreover, each kind of PS was often reported to be effective in curing some diseases but not the other[35]. Also, difficulty in optimizing the drug and light doses has not yet been solved. Therefore, there is still a need to look for a novel class of PS or PS derivatives.

1.5 Development of silicon (IV) phthalocyanine (SiPc) derivatives

Previously, we have investigated the *in vitro* photodynamic activities of a series of phthalocyanine derivatives. The compounds are mostly ZnPc derivatives and SiPc derivatives. Derivatives were synthesized aiming at improving tumor targeting and hence the PDT efficacy when compared with their parental PS. Derivatives were often formed by chemically replacing the substituent at the axial position with chemical groups or well-known biomolecules. These modifications can either alter the chemical properties of the parental PS (from hydrophobic / hydrophilic to amphiphilic) to facilitate the diffusion and accumulation of PS within malignant cells or the biomolecule can be selectively uptaken by malignant cells through receptor-mediated endocytosis.

$SiPc(py)_2$, $SiPc(Gal)_2$, $SiPc[C_3H_5(NMe_2)_2O](OMe)$, $SiPc[C_3H_5(NMe_2)_2O]_2$ are members of a series of SiPc derivatives in which their *in vitro* photodynamic activities have been reported previously[45] (Fig. 1.3). The details of these compounds are as follows:

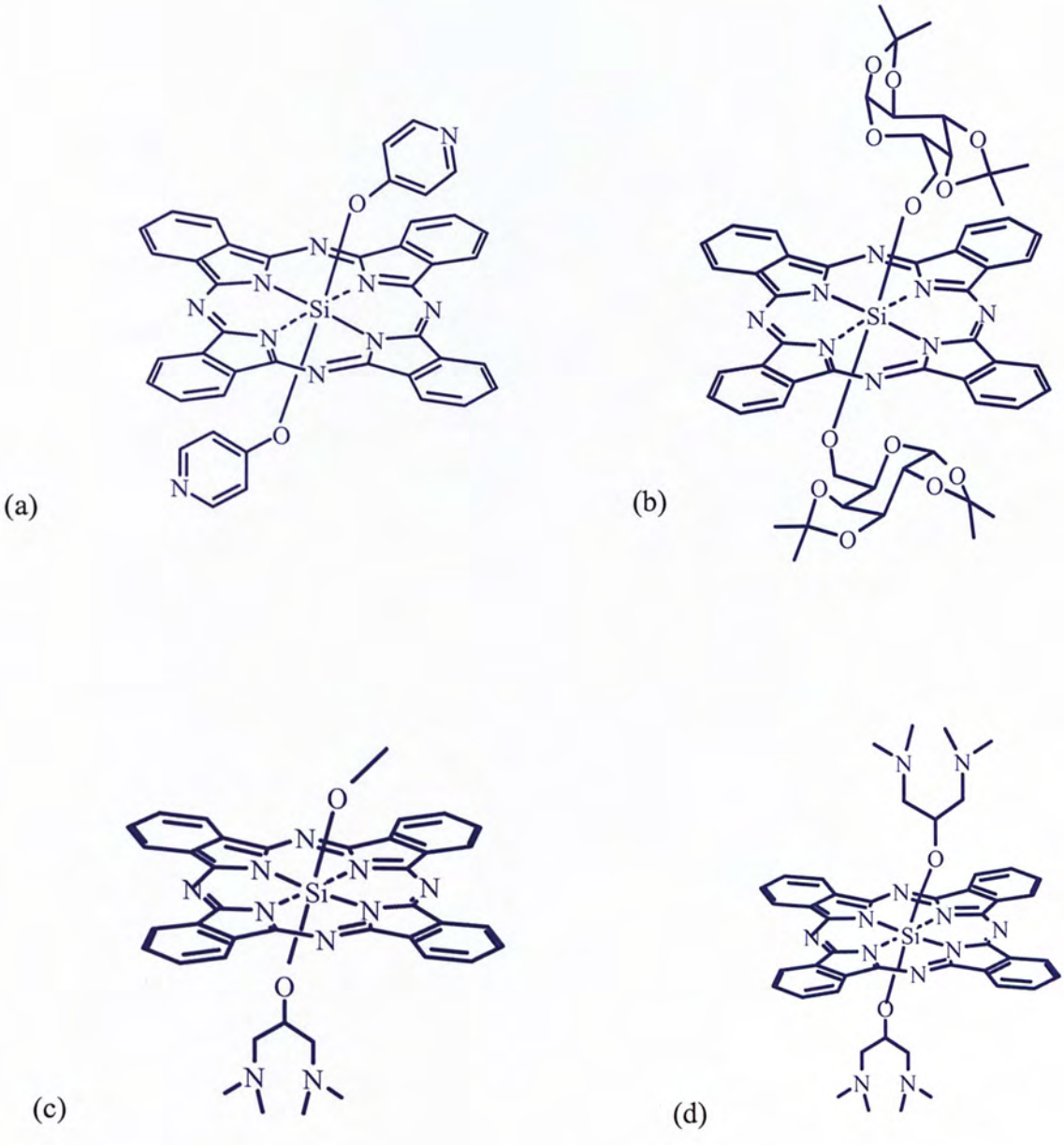

Fig. 1.3 Chemical structures of SiPc derivatives: a) $SiPc(py)_2$; b) $SiPc(Gal)_2$; c) BAM-SiPc; d) $SiPc[C_3H_5(NMe_2)_2O]_2$.

1. $SiPc(py)_2$: The axial positions of SiPc were symmetrically substituted with pyridine group. The pyridine groups mimic the structure of pyrimidine ring. This modification was designed based on the fact that malignant cells have an extra nucleotide demand for rapid DNA synthesis and cell proliferation. Selective uptake of the PS by cancer cells could be conferred by recognizing the substituent and endocytosed by the cancer cells.
2. $SiPc(Gal)_2$: This derivative was axially substituted with two acetal-protected galactose groups symmetrically. As there is an over-expression of glucose transporter in tumor cells[43-44, 46], such modification has been designed in a way to enhance the accumulation of PS in cancer cells through the glucose transporter uptake mechanism. On the other hand, the bulky acetal-protected galatose substituents would increase the hydrophilicity and inhibit the self aggregation of the PS[47].
3. $SiPc[C_3H_5(NMe_2)_2O](OMe)$ or BAM-SiPc: unsymmetrical substitution with 1,3-bis(dimethylamino)-2-propoxy and methyl groups which make SiPc more amphiphilic in nature. This compound was believed to diffuse more readily across and insert into the membrane of the cell[45].
4. $SiPc[C_3H_5(NMe_2)_2O]_2$: the parental compound in the synthesis of BAM-SiPc. It was formed by the symmetrical axial linkage of two 1,3-bis(dimethylamino)-2-propoxy groups.

The IC_{50} (i.e. the concentration of drug that results in 50% cell viability) of $SiPc(Gal)_2$, BAM-SiPc and $SiPc[C_3H_5(NMe_2)_2O]_2$ against the cultured cancer cells were found to be at nano-molar level using HepG2 and J774 as the cell models[45,47]. In particular, BAM-SiPc appeared as the most potent PS. In this series of SiPc derivatives, amphiphilicity seems to play an important part to the phototoxicity of

PS.

1.6 Death mechanisms in photodynamic therapy

PDT can induce cell death either by necrosis because of the extensive cellular damage or by triggering the death signal and switch on the apoptotic pathway. Drug and light dose, subcellular localization of PS and cell type are the factors which control the mode of cell death[48]. There are two different pathways of apoptosis, the death-receptor mediated apoptosis (extrinsic pathway) and mitochondria-mediated apoptosis (intrinsic pathway). PDT can induce apoptosis by triggering either pathway. Ahmad *et al.* [49] reported that human epidermoid carcinoma A431 cells underwent apoptosis after photosensitization with Pc 4. They found that Pc 4 mediated PDT could transiently increase the level of cell surface Fas-receptor and Fas receptor binding ligand, FasL which play crucial roles in the induction of the extrinsic pathway. Moreover, multimerization of the Fas protein and binding of the Fas receptor with the adaptor molecule FADD (Fas associated protein with a death domain) were observed after Pc 4 mediated PDT. Such interaction is known to trigger the downstream pathway of apoptosis, i.e. the binding and proteolytic cleavage of pro-caspase 8.

- ***BAM-SiPc triggers the intrinsic pathway of apoptosis by a direct mitochondrial action***

Lo *et al.* [46, 47] have reported that BAM-SiPc is predominantly localized in mitochondria of HepG2 and HT29 cells. The death mechanism of PDT with BAM-SiPc was studied by using HepG2 cells as a model. Apoptosis was induced after BAM-SiPc mediated PDT, as shown by the result of the Terminal deoxynucleotidyl transferase-mediated dUTP nick end labeling (TUNEL) assay and

Annexin V staining. In the same study, Western blot analysis revealed that there were release of cytochrome C from mitochondria to cytosol and cleavage of poly-ADP-ribose polymerase (PARP). This confirms that the PDT treated cells had undergone the intrinsic pathway of apoptosis. For the extrinsic pathway, 10 μM caspase 8 inhibitor z-IETD-fmk was used but it could not significantly inhibit the death of cells. This indicates that the extrinsic pathway could play at best a minor role in causing cell death in BAM-SiPc mediated PDT. Other results such as down-regulation of Bcl-2 and translocation of Bax from cytosol to mitochondria both shed light on the mechanisms which regulate the PDT-mediated apoptosis[50]. However, there is only very limited information about the detail signaling pathway of how PDT rapidly triggers the death signal.

1.7 Objectives of the present study

According to the result of *in vitro* photodynamic activity assay of SiPc-derivatives, BAM-SiPc was the most potent PS among the series. Therefore, BAM-SiPc was chosen for further investigation. HepG2 and HT29 tumor bearing nude mice was employed as models to study the *in vivo* photodynamic efficacy of BAM-SiPc. Since tumor selectivity and skin photosensitivity due to persistent retention of a PS in skin tissue were the major issues concerned in using PDT, biodistribution of BAM-SiPc was performed so that the uptake of BAM-SiPc by the tumor as well as drug clearance could be determined. Haematoxylin and eosin (H & E) staining of the histological liver section and assay of plasma enzyme activities were performed in order to assess the level of intrinsic toxicity induced by BAM-SiPc mediated PDT and evaluate the safety use of BAM-SiPc in cancer therapy.

Although the usefulness of PDT has been known for decades, the death mechanism and the intracellular signaling events involved are still uncertain. The intracellular ROS production and cell cycle distribution of PDT-treated HepG2 cells were determined to get an insight into the detail of how the BAM-SiPc mediated PDT triggers apoptosis. Due to the fact that different kinds of PS and dosage of treatment will execute different pathways of cell death, H & E staining and *in vivo* TUNEL staining have been performed to see whether apoptosis has been triggered after *in vivo* PDT with BAM-SiPc.

Apart from that, metabolism of BAM-SiPc was also studied so as to investigate whether BAM-SiPc could be metabolized by liver cells and to see whether the metabolite is toxic to the host. Finally, low density lipoprotein was used as a carrier for BAM-SiPc to see whether the uptake of BAM-SiPc by tumors and hence the PDT efficacy of BAM-SiPc could be further increased in the presence of LDL.

With all these information, we can assess the potential of using PDT with BAM-SiPc for cancer treatment in clinical trial.

CHAPTER 2

Materials and Methods

2.1 Synthesis of BAM-SiPc

SiPc[$C_3H_5(NMe_2)_2O$](OMe), BAM-SiPc, an unsymmetrical bisamino silicon(IV) phthalocyanine was kindly provided by Prof. Dennis K.P. Ng from Department of Chemistry, The Chinese University of Hong Kong. The procedures of the synthesis were summarized as follow[47]: MeOH was slowly added to the top of a solution of SiPc[$C_3H_5(NMe_2)_2O]_2$ (1.42 g, 1.71 mmol) in $CHCl_3$. The bilayer system was left under ambient condition for 3 days. The precipitate formed was filter off and subjected to a basic alumina column (Merck, 70–230 mesh ASTM) with $CHCl_3$/hexane (1:2) as the eluent to give a greenish blue solid (0.92 g, 75%) with R_f ($CHCl_3$/hexane 1:2) =0.86.

2.2 Preparation of BAM-SiPc solution for photodynamic treatment

Solid BAM-SiPc was dissolved in dimethyl formamide (DMF) by means of ultrasonication. The concentration of the stock solution was adjusted to 800 μM with reference to the standard curve obtained by spectrophotometric measurement. Then, the BAM-SiPc solution was diluted to 80 μM with 0.01 M aqueous Cremophor EL (0.047 g in 1 ml of distilled water) as the solvent. T he 80 μM BAM-SiPc was then diluted to 8 μM and was sterilized by filtering through 0.2 μm *Acrodisc*® Syringe Filters. The solution was finally diluted to appropriate concentrations with cell culture medium. *Acrodisc*® Syringe Filters (0.2 μm) with *Supor*® Membrane were purchased from Pall Gelman Laboratory, USA. DMF and

Cremophor EL were obtained from Sigma-Aldrich, USA.

2.3 Cell line and culture conditions

The human hepatocellularcarcinoma cells HepG2 and Hep3B, the human colorectal adenocarcinoma cells HT29 as well as the liver cells WRL-68 (Table 2.1) were originally obtained from American Type Culture Collection (ATCC). HepG2 was maintained in RPMI 1640 medium supplemented with 10% fetal bovine serum, penicillin (50 units/ml) and streptomycin (50 μg/ml) in 5% CO_2, 95% air in a humidified incubator at 37°C. Hep3B, WRL-68 and HT29 were maintained in Dulbecco's Modified Eagle's Medium (DMEM) supplemented with 10% fetal calf serum, and penicillin-streptomycin (Penicillin, 100 units/ml; Streptomycin, 100 μg/ml). Culture medium for HT29 was further supplemented with L-glutamine and transferrin to give a final concentration of 1.5 mM and 10 μg/ml respectively. Fetal bovine serum, L-glutamine, penicillin-streptomycin solution, RPMI 1640 medium and DMEM were all purchased from Invitrogen Corporation, HK, Ltd while transferrin was obtained from Sigma-Aldrich, USA.

	ATCC number	Origin
HepG2	HB-8065	Liver with hepatocelullar carcinoma
	Description: The cells demonstrate decreased expression of apoA-I mRNA and increased expression of catalase mRNA in response to gramoxone (oxidative stress). They express insulin-like growth factor II. There is no evidence of a Hepatitis B virus genome in this cell line.	

	ATCC number	Origin
Hep3B	HB-8064	Liver with hepatocellular carcinoma
	Description: This cell line contains an integrated hepatitis B virus genome.	

	ATCC number	Origin
WRL-68	CL-48	HeLa contaminant
	Description: Cells contain Human Papilloma Viral DNA sequences and express some hepatocyte-like functional properties in culture.	

	ATCC number	Origin
HT29	HTB-38	Colon with colorectal adenocarcinoma
	Description: The cells express urokinase receptors, but do not have detectable plasminogen activator activity. HT-29 cells are negative for CD4, but there is cell surface expression of galactose ceramide (a possible alternative receptor for HIV). The cell line is positive for expression of c-myc, K-ras, H-ras, N-ras, Myb, sis and fos oncogenes.	

Table 2.1 Properties of the cell lines used in the present study.

2.4 Animal tumor model

Balb/c nude mice (20 - 25 g) were obtained from the Laboratory Animal Services Center (LASEC) at The Chinese University of Hong Kong. All experiments on tumor-bearing nude mice were approved by the Animal Experimentation Ethics Committee, The Chinese University of Hong Kong. In developing the tumor model, ten million tumor cells (HepG2 or HT29) were subcutaneously inoculated into the back of the nude mice (Fig. 2.1). Measurement of the tumor size was started on Day 6 after tumor cells inoculation. Three parameters of the tumor, namely, length, width and thickness were measured by using the micrometer digital caliper (SCITOP Systems Ltd.). The tumor volume was calculated by the following formula:

$$\text{Tumor volume} = \pi \times (\text{Length} \times \text{Width} \times \text{Thickness}) / 6$$

Mice were bred under pathogen-free condition with free access of food and water.

2.5 PDT laser source

Continuous wave laser was generated from the Ceralas PDT 675 medical laser system (bandwidth 675 nm ± 3 nm, power range 0.1 – 1 W) coupled with a frontal light distributor (Fig. 2.2). This medical laser system and the frontal light distributor were purchased from CeramOptec GmbH, a company of Biolitec group, Germany.

2.6 *In vitro* photodynamic activity assay

2.6.1 Pr eparation of cells for photodynamic treatment

Cells were seeded in 96-well plate at appropriate density (HepG2 and Hep3B: 2×10^4 cells per well; HT29: 3×10^4 per well) and incubated overnight in a 5% CO_2, 95% air humidified incubator at 37 °C. After incubation, the culture medium was removed and cells in each well were rinsed with 100 μl of phosphate buffer

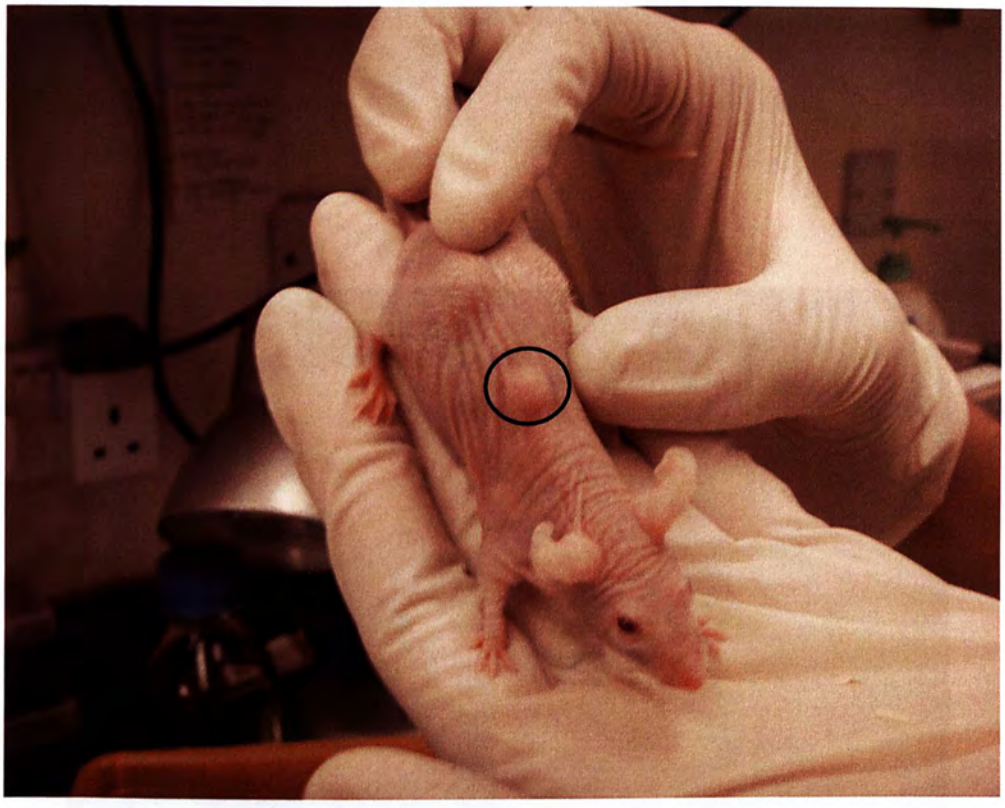

Fig. 2.1 Tumor bearing nude mouse (9 days after inoculation).

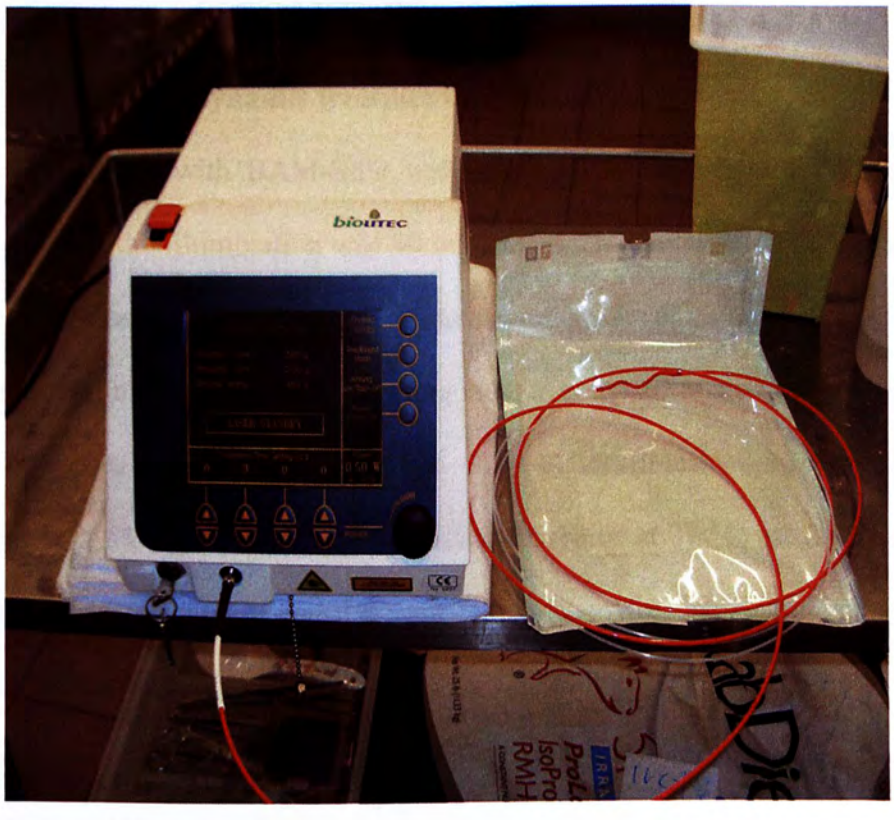

Fig. 2.2 Setup of the PDT laser system.

saline (PBS, pH 7.4). One hundred μl of different concentrations of BAM-SiPc in culture medium was added. Samples were allowed to incubate in a 5% CO_2, 95% air humidified incubator for 2 h at 37 °C. Finally, solution in each well was aspirated and cells in each well were rinsed with 100 μl PBS. Samples were ready for illumination after filling with 100 μl of fresh culture medium per well.

2.6.2 In vitro photodynamic treatment

Cells treated with BAM-SiPc were illuminated with light for 10 min. The fluence rate for the illumination was 40 $mWcm^{-2}$ such that an illumination of 10 min led to a total fluence rate of 24 Jcm^{-2}. The illuminating set up consisted of a 300 W halogen lamp, a water tank for cooling and a color filter cutting off light with wavelength < 610 nm (Newport) (Fig. 2.3). After illumination, the cells were incubated in a 5% CO_2, 95% air humidified incubator at 37 °C for 24 h to provide sufficient time for the recovery of the survived cells. After incubation, samples were ready for cell viability determination.

2.6.3 Cell viability assay[51]

The culture medium of the cell sample was aspirated. Cells were then washed with PBS and mixed with 50 μl 3-(4,5-Dimethylthiazol-2-yl)-2,5-diphenyltetrazolium bromide (MTT) solution (3 mg/ml). Samples were allowed to incubate in a 5% CO_2, 95% air humidified incubator at 37 °C for 2 h. Afterwards, cells were lysed with 50 μl 10% (w/v) sodium dodecyl sulphate (SDS) in 0.04 M hydrochloric acid in each well. The plate was then placed in a 60 °C oven for 30 min to lyse the cell and release the purple formazan crystal formed inside the viable cells.

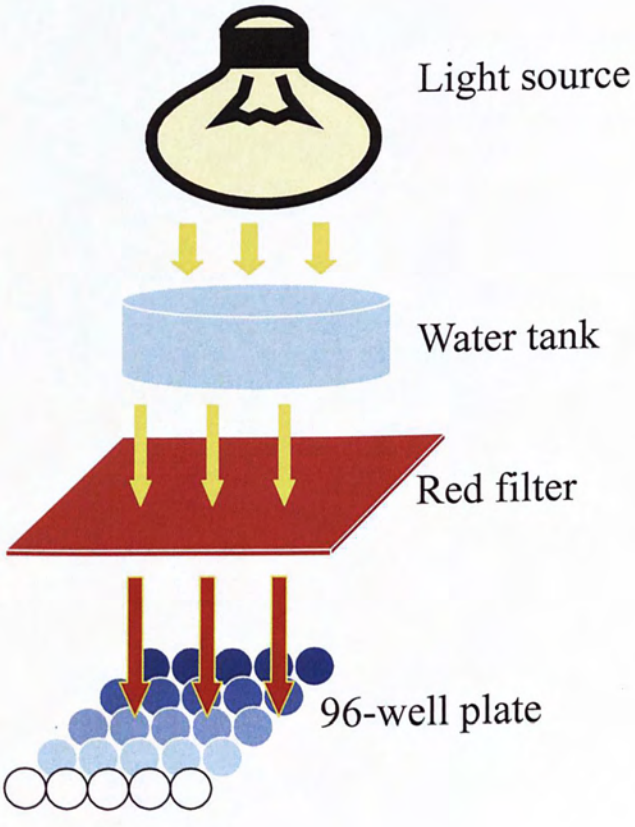

Fig. 2.3 Schematic diagram showing the set-up for illumination of the cancer cells.

Eighty μl of iso-propanol was then added to dissolve the formazan crystal. The samples were ready for spectrophotometric measurement. Absorbance at 540 nm for each well was recorded by the ELISA plate reader (Bio-Rad). Percent cell viability was calculated by the following formula:

$$\% \text{ Cell Viability} = [(OD_{540 \text{ treated sample}} - OD_{540 \text{ Blank}}) / (OD_{540 \text{ control}} - \text{Blank})] \times 100\%$$

SDS and MTT solid were USB products purchased from GE medical systems, HK Ltd. Iso-propanol was obtained from Sigma-Aldrich, USA.

2.7 Determination of ROS production by 2',7'-dichlorofluorescein diacetate (DCFDA) assay

ROS production was determined by using 2',7'-dichlorofluorescein diacetate (DCFDA). After PDT, the culture medium of the sample was aspirated and cells (2 x 10^4/well) were washed with PBS. One hundred μl of 100 μM DCFDA solution in PBS was added to each well of cells and the mixture was allowed to incubate in a 5% CO_2, 95% humidified incubator at 37 °C for 1 h in dark. Fluorescence measurements were then made in a fluorescence plate reader (TECAN Polarion, Tecan UK Ltd., Theale, UK) using a 485 nm excitation filter and a 535 nm emission filter set at a gain of 60. DCFDA powder was purchased from Molecular Probes, CA, USA.

2.8 Propidium iodide (PI) staining for analysis of cell cycle arrest

HepG2 cells (1 x 10^6) were seeded in 35 mm Falcon dish and allowed to grow overnight. After overnight incubation, the cell culture medium was aspirated and cells were rinsed with PBS, pH 7.4. Cells were taken for *in vitro* photodynamic treatment as described in Section 2.6.2. After the illumination, cells were further

incubated in the dark for 24 h. On the next day, cells were harvested by trypsinization and fixed with 70% ethanol at -20 °C for another 24 h. Afterwards, cells were pelleted by centrifugation at 1500 rpm for 3 min. Cell pellets were washed with PBS and resuspended in 1 ml PI staining solution (20 μg/ml PI, 8 μg RNase in PBS, pH 7.4). Samples were further incubated for 15 - 30 min at 37 °C in the dark. Finally, cells were transferred for cell cycle analysis in the FASCanto Flow Cytometer (BD Biosciences, France). PI (crystal form) was purchased from Sigma-Aldrich, USA. RNase was purchased from Roche Diagnostics, Hong Kong Ltd.

2.9 Biodistribution study of BAM-SiPc

One μmol (~ 0.7 mg) BAM-SiPc/kg of mice body weight was intravenously (i.v.) injected into the tumor-bearing nude mice. At different time intervals, the mice was anesthetized with an intra-peritoneal injection of 0.2 ml ketamine/xylazine cocktail solution (0.1 mg ketamine and 0.01 mg xylazine per gram of body weight; 0.5 ml ketamine and 0.25 ml of xylazine were mixed with PBS to make a 5 ml cocktail solution). The major organs/tissues of the mice were excised, rinsed with PBS, pH 7.4 and blotted dry. The excised organs/tissues were homogenized with DMF by a Biospec Biohomogenizer (Fisher Scientific, USA). Homogenates were centrifuged at 2450 x g for 20 min to remove the large debris. Supernatants were collected and subjected to fluorescence measurement. The peak fluorescence intensity was recorded by scanning the fluorescence emission spectrum from 610 nm to 900 nm using an excitation wavelength at 608 nm. Amount of BAM-SiPc present in the sample was determined with reference to the standard curve. The amount was expressed in % initial dose (ID) per gram of tissue as calculated by the following formula.

$$\% \text{ ID per gram of tissue} = \frac{(\text{amount of BAM-SiPc / weight of the tissue})}{\text{Initial injection dose}} \times 100\%$$

Ketamine and xylazine solution were obtained from LASEC, The Chinese University of Hong Kong.

2.10 *In vivo* photodynamic treatment

In vivo photodynamic treatment was started on Day 9 after tumor cells inoculation. By that time, the tumor has reached a size of 40 mm^3 to 100 mm^3. One μmol BAM-SiPc/kg of body weight was i.v. injected into the tumor-bearing nude mice as described in Section 2.9. Twenty-four hour after the injection, the nude mice were anesthetized with the ketamine / xylazine cocktail solution. PDT laser was directly spotted onto the tumor with a fluence rate of 0.1 Wcm^{-2} for 300 sec, giving a total fluence of 30 Jcm^{-2}. Tumor sizes of the nude mice were followed for the next 15 days.

2.11 Assay for plasma enzyme activities

Blood was obtained by intra-cardiac puncture. Heparin (1250 USP units/ml) was added to prevent blood coagulation. The blood samples were centrifuged at 4000 rpm for 5 min to obtain the supernatants which represent the plasma. The activities of alanine aminotransferase (ALT), aspartate aminotransferase (AST) and creatine kinase (CK) were assayed by the commercially available assay kits. In the assay of ALT and AST activities, 50 μl of plasma was allowed to incubate with 1 ml of assay reagent for 1 min at 37 °C. Enzyme activities were then determined by monitoring the absorbance change at 340 nm for 2 min. To assay CK activity, 50 μl of plasma was allowed to incubate with 1 ml of assay reagent for 3 min at 37°C. Similarly,

enzyme activity was determined by monitoring the absorbance change at 340 nm for 2 min. The amount of enzyme activity was expressed as U/L. ALT and AST enzyme activities assay kit were Infinity™ products purchased from Thermo Electron Corporation, Australia while CK enzyme activity assay kit was the product of Biosystems, Spain. Heparin was purchased as the sodium salt which was the product of Sigma-Aldrich, USA.

2.12 Determination of cellular uptake of BAM-SiPc

HepG2 cells (1 x 10^6) were seeded in 35 mm Falcon dish and allowed to incubate overnight in a 5% CO_2, 95% air humidified incubator at 37°C. After that, cells were incubated with 0.5 μM BAM-SiPc in RPMI medium. At different time intervals, cells were washed with PBS, pH 7.4 to remove the unbound BAM-SiPc. Cells were then harvested by trypsinization. Cells were washed twice with PBS and then lysed in DMF so as to release BAM-SiPc from the cells. Cells debris was removed by centrifugation at 2450 x g for 20 min. The amount of BAM-SiPc present inside the cells was determined by measuring the peak fluorescence intensity as described in Section 2.9 with reference to the standard curve of BAM-SiPc. The BAM-SiPc content was expressed in nmol per million of cells. The number of cells was counted under the bright-field microscope with the aid of a hematocytometer. Falcon dish was the product from BD Bioscience, France.

2.13 Metabolism of BAM-SiPc

2.13.1 Comparsion between normal liver cells WRL-68 and the hepatocarcinoma HepG2 cells in their ability to metabolize BAM-SiPc

HepG2 cells (1 x 10^6) and WRL-68 cells (3 x 10^5) were seeded in 35 mm

Falcon dish. After overnight incubation, cells were treated with 1 ml of 0.5 μM BAM-SiPc in respective cell culture medium for 2 h during which cells could maximally accumulate BAM-SiPc. BAM-SiPc solution was then removed from the cells and the dish was re-filled with fresh culture medium. After that, samples were allowed to incubate in a 5% CO_2, 95% air humidified incubator at 37 °C for 24 h to allow the cells to metabolize BAM-SiPc. The residual amount of BAM-SiPc was determined by the methods described in Section 2.9.

2.13.2 Catabolism of BAM-SiPc by mice liver homogenate

Liver was homogenized with 10-fold (w/v) PBS by using a Tissue Tearor on ice. The homogenate was then centrifuged at 2450 x g for 20 min to remove the large debris. Approximately 7 mg (protein content as determined by Bradford assay) of liver homogenate was mixed with BAM-SiPc such that the latter concentration was 8 μM. Samples were then incubated at 37 °C for different periods of time. After that, samples were mixed in a 1:1 (v/v) ratio with DMF in order to extract the metabolite. The protein content was removed by centrifugation at 2450 x g for 20 min. Supernatants were collected and subjected to *in vitro* photodynamic activity assay (Section 2.6) after serial dilution with the RPMI cell culture medium. Residual amount of BAM-SiPc was determined by scanning the absorption spectrum from 610 nm to 800nm. The reading at the absorbance peak (674 nm) was taken for calculation.

2.14 Histochemical staining

2.14.1 Preparation of paraffin-embedded tissue section

Liver and tumor excised from the nude mice were fixed in 4% paraformaldehyde, pH 7.4 overnight at 4 °C. On the next day, tissues were processed

by standard protocol for preparing histological section and embedded in paraffin. Tissue sections were cut with a thickness of 5 μm and then placed on 24 x 50 mm microscopic slides. The sections were allowed to dry completely by incubating in a 60 °C oven. After overnight incubation, the sections were dewaxed and rehydrated by immersing in xylene solution and a series of alcohol solutions of descending concentration from 100% down to 70% before proceeding for further histochemical staining.

2.14.2 Haematoxylin and Eosin (H & E) staining

After dewaxing and rehydration, the paraffin embedded tissue sections were immersed in a 5% Mayer's Haematoxylin solution for 2 min to stain the cell nuclei with purple colour. Sections were then washed in running water to remove the excess staining solution. After that, sections were immersed in 2% Eosin for 5 min to counter-stain the cytoplasm with pink color. Tissue sections were immersed in a series of alcohol of ascending concentration from 70% to 100% and finally in xylene solution in order to dehydrate the sections completely. The stained tissue sections were finally mounted with a coverslip and viewed under the bright field of a Zeiss Axioskop II Plus microscope. Images were captured by the coupled AxioCam digital camera.

2.14.3 Terminal deoxynucleotidyl transferase-mediated dUTP nick end labeling (TUNEL) assay for studying apoptosis

After dewaxing and rehydration with alcohol, the paraffin embedded tissue sections were taken for the detection of DNA strand breaks by the TUNEL assay. The experimental procedures were similar to that described in the protocol of *In Situ Cell Death Detection Kit, Fluorescein* (Roche Diagnostics, HK LTD). Briefly, tissue

sections were first immersed in freshly prepared permeabilization solution (0.1% v/v Triton X-100, 0.1% w/v sodium citrate) at room temperature for 8 min in order to inactivate any nuclease which could lead to false positive results. Sections were then rinsed twice with PBS, pH 7.4. The area around the samples was dried thoroughly. Fifty μl of TUNEL reaction mixture (terminal deoxynucleotidyl transferase and nucleotide mixture) provided in the kit was added to cover the whole tissue section. Sections were then incubated at 37 °C in humidified incubator for 60 min. After the incubation, sections were rinsed with PBS for 3 times. At this moment, the samples were ready for examination under the Fluorescence module of Zeiss Axioskop II Plus microscope with excitation wavelength 450-500 nm and emission wavelength ranging from 515-565 nm. Images were captured by the coupled AxioCam digital camera. Green fluorescence colour indicates positive staining of the cells.

2.15 Conjugation of BAM-SiPc with LDL[31]

2.15.1 Analysis of the phototoxicity and cellular uptake of BAM-SiPc in the presence of LDL

Human plasma low density lipoprotein LDL was mixed with BAM-SiPc at different ratio in serum-free RPMI 1640 medium. The mixture was incubated in the dark for 90 min at 37 °C with constant agitation. After that, one hundred μl of LDL-BAM-SiPc mixture was added to HepG2 cells (2 x 10^4 per well) in each well. *In vitro* photodynamic activities assay were carried out as stated in Section 2.6.2. In cellular uptake experiment, 0.2 nmol of BAM-SiPc was mixed with 2 nmol of LDL and allowed to incubate with HepG2 (1 x 10^6) for 2 h. BAM-SiPc content was determined by the method stated in Section 2.12. Human plasma LDL was a Calbiochem product purchased from MERCK Biosciences, Germany.

2.1 5.2 Gel filtration

A solution of human LDL (2 nmol), BAM-SiPc (0.2 nmol) or β-nicotinamide adenine dinucleotide (NAD^+, 0.625 nmol) was chromatographed in a G-100 Sephadex column (dry bead diameter = 40 – 120 μM; 1.8 x 21 cm) using 20 mM aqueous NH_4HCO_3 as the eluent with a flow rate of 0.5 ml per minute. After mixing BAM-SiPc with LDL and incubating for 90 min in dark, the mixture was also chromatographed in a G-100 Sephadex column but in a smaller scale (1.8 x 9 cm). The presence of human LDL was determined by Bradford protein assay. BAM-SiPc content was monitored by fluorescence spectrometry as described in Section 2.9 and NAD^+ content was monitored by measuring the absorbance at 260 nm.

2.16 Statistical analysis

Analysis of Variance (ANOVA) test was used for comparing the means between different treatment conditions. Statistically significant difference between each individual treatment group was further analyzed by the Bonferroni post hoc test. All the statistical comparison was accomplished by using the SPSS 14.0 for windows software.

CHAPTER 3

Results

3.1 *In vitro* photodynamic activities assay

The *in vitro* photodynamic activities assay was performed to investigate the potency of BAM-SiPc in killing cancer cells and see whether BAM-SiPc mediated photodynamic activity was in a dose-dependent manner (Fig. 3.1). In the dark, there was no cytotoxic effect towards the cancer cells. In the presence of light, a dose-dependent cytotoxicity of BAM-SiPc towards different cancer cell lines could be observed. The cancer cells remained unaffected when treated either with BAM-SiPc or light alone but were effectively killed when a combined treatment was employed. The IC_{50} values of BAM-SiPc could reach nano-molar level in the presence of light (Table 3.1). Based on the IC_{50} values, it can be concluded that the murine macrophage J774, the colon adenocarcinoma HT29 and T84 and the hepatocarcinoma HepG2 have similar susceptibility towards BAM-SiPc mediated PDT. The hepatocarcinoma Hep3B cells was less susceptible with the IC_{50} of BAM-SiPc about two-fold higher than those of the other cancer cell lines.

Table 3.1 IC_{50} values of BAM-SiPc mediated PDT towards different cancer cell lines

Cultured cancer cell lines	IC_{50} values (μM)
J774	0.020*
HT29	0.017^{+}
T84	0.027^{+}
HepG2	0.025*
Hep3B	$0.051^{\triangle}$

* (Lo *et al.*, 2004.); $^{+}$(Lo *et al.*, 2007); $^{\triangle}$(Lai *et al.*, 2006)

(a)

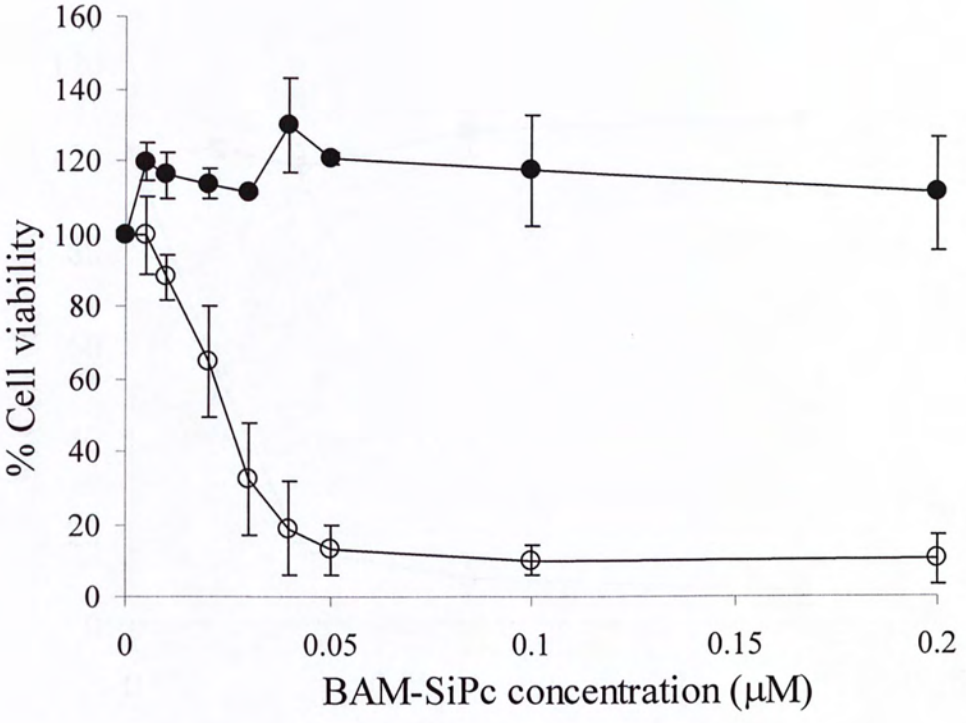
160
140
120
100
80
60
40
20
0
% Cell viability
0
0.05
0.1
0.15
0.2
BAM-SiPc concentration (μM)

(b)

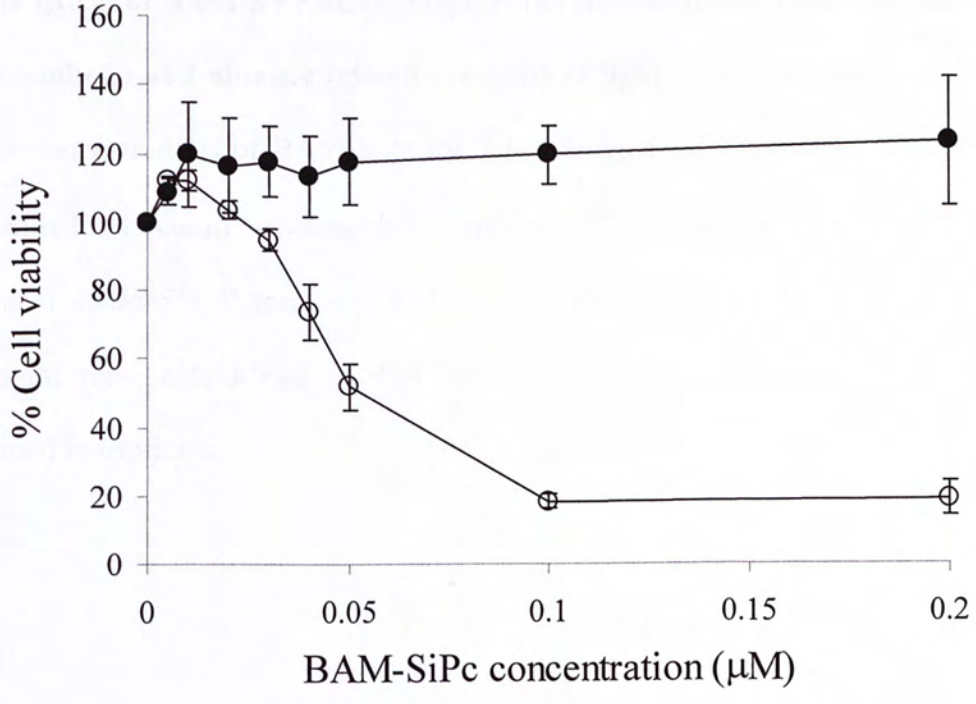
160
140
120
100
80
60
40
20
0
% Cell viability
0
0.05
0.1
0.15
0.2
BAM-SiPc concentration (μM)

(c)

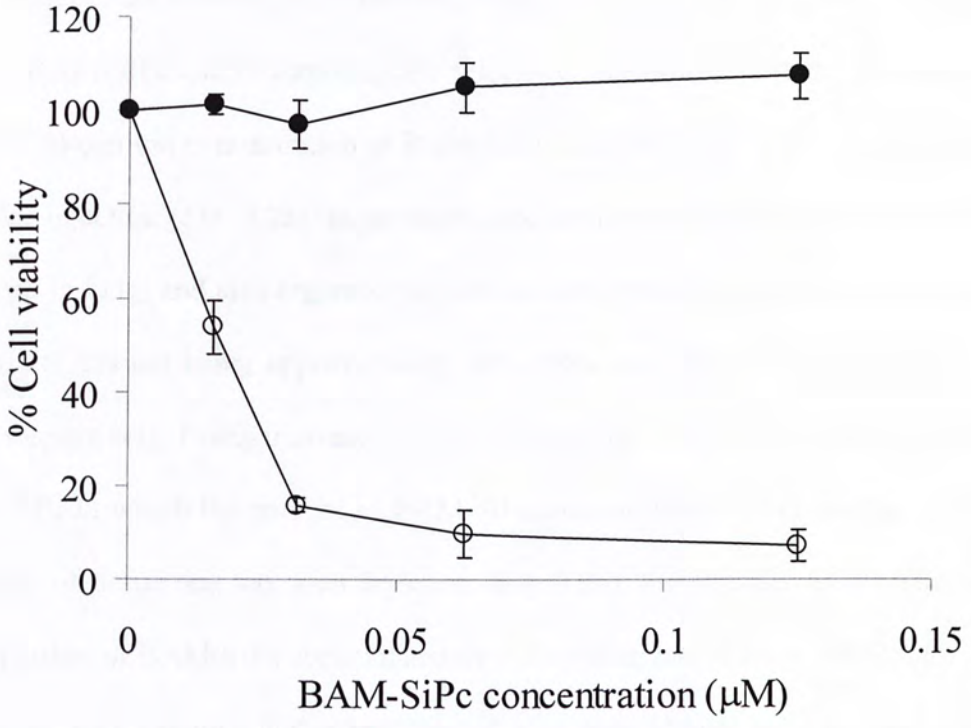

Fig. 3.1 Effect of BAM-SiPc on (a) HepG2; (b) Hep3B; (c) HT29 in the presence (open symbols) and absence (closed symbols) of light. Cells were incubated with various concentrations of BAM-SiPc for 2 h, followed by illumination of halogen lamp with filter (cutoff wavelength $\lambda < 610$ nm, fluence rate at 24 $mWcm^{-2}$, total fluence of 48 Jcm^{-2}). Percent cell viability was determined by MTT assay. Each data point represents Mean ± SEM from three independent experiments, each performed in triplicate.

3.2 Tissue distribution of BAM-SiPc in HepG2 bearing nude mice

Biodistribution study of BAM-SiPc was performed to investigate the retention time of BAM-SiPc and its tumor uptake selectivity. Result of the study was shown in Fig. 3.2. Maximum concentration of BAM-SiPc could be found in most of the tissues 2 h after injection (Fig. 3.2a). In particular, the greatest retention of BAM-SiPc was observed in lung, and also organs of the reticulo-endotheial system namely liver and spleen, the amount being approximately 70%, 58% and 52% of the ID per gram of tissue respectively. Comparatively, liver and kidney had the fastest clearance rate of BAM-SiPc in which the amount of BAM-SiPc present dropped to less than 25% ID per gram of tissue one day after injection (Fig. 3.2a). For muscle, only a relatively small portion of BAM-SiPc accumulated in it. The pharmaco-kinetic profiles for skin and tumor, both having a higher proliferating rate, were similar to each other. Unlike other tissues, amount of BAM-SiPc present in skin and tumor kept increasing until 6 hr after the injection and remained relatively constant afterwards. The maximal amount of BAM-SiPc accumulated in tumor was only about 2% of the ID per gram of tissue.

The BAM-SiPc content in different tissues at 2 h and 1 week after injection were compared (Fig 3.2b). It could be observed that most of the BAM-SiPc had been removed from the host after 1 week. Less than 2% ID per gram of tissue of BAM-SiPc remained in all the examined tissues, except for kidney where ~ 5% of the ID per gram of tissue remained.

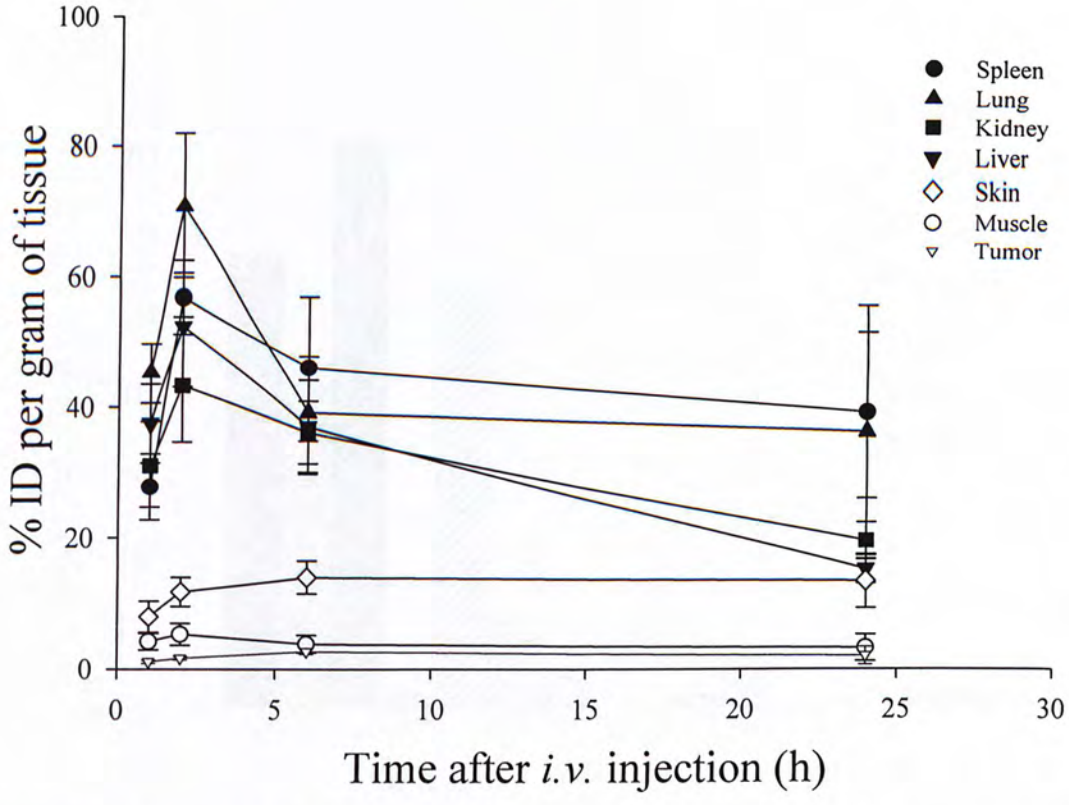

Fig. 3.2a. Tissue distribution of BAM-SiPc. One μmolkg^{-1} of BAM-SiPc per body weight was injected intraveneously into the HepG2-bearing nude mice. At different time intervals, mice were sacrificed and tissues were homogenized with DMF to extract BAM-SiPc. Fluorescence measurement was taken to quantify the amount of BAM-SiPc. Data were expressed as Mean ± SD, n=5.

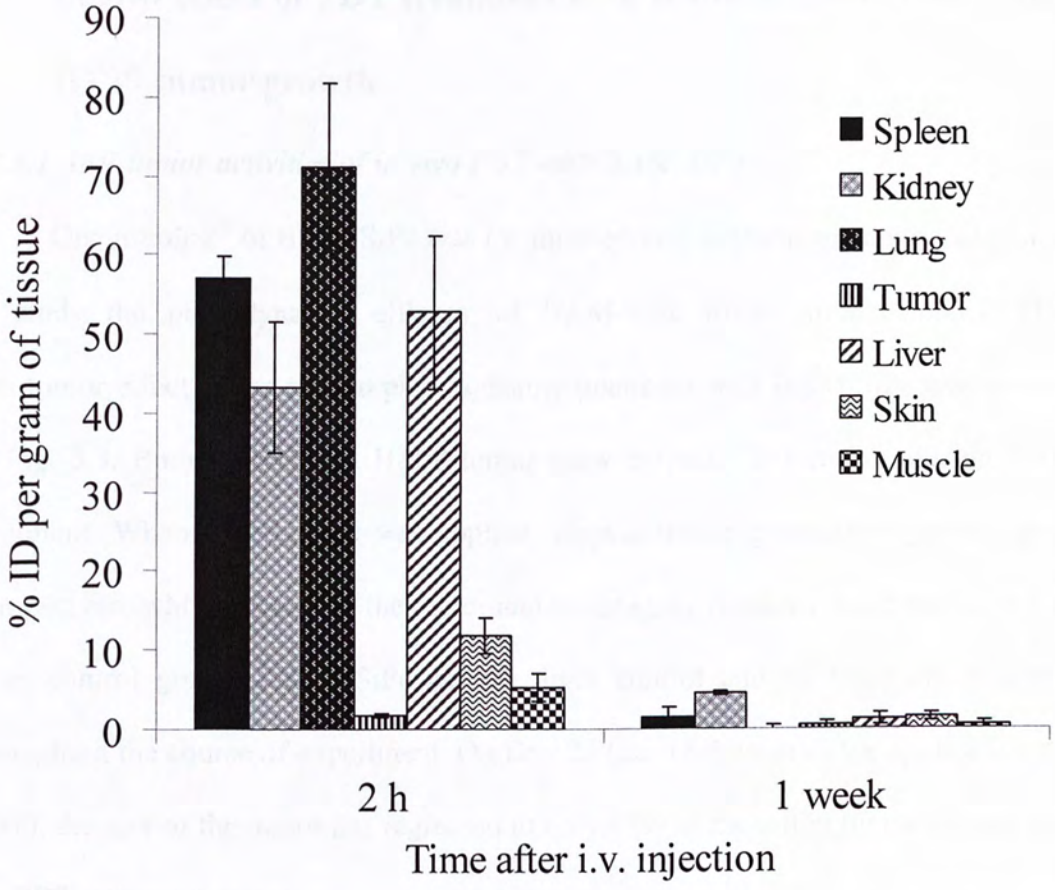

Fig. 3.2b Comparsion of the BAM-SiPc content in different tissues at 2 h and 1 week after i.v. injection. Data were expressed as Mean ± SD, n=5.

3.3 *In vivo* effect of PDT treatment with BAM-SiPc on HepG2 and HT29 tumor growth

3.3.1 Anti-tumor activities of in vivo PDT with BAM-SiPc

One $\mu molkg^{-1}$ of BAM-SiPc was i.v. injected into the tumor-bearing nude mice to study the photodynamic efficacy of BAM-SiPc in an animal model. The anti-tumor effect of the *in vivo* photodynamic treatment with BAM-SiPc was shown in Fig. 3.3. Both HepG2 and HT29 tumor grew normally before introducing PDT treatment. When illumination was applied, HepG2 tumor gradually regressed at a constant rate while the size of the tumor and its integrity remained unchanged for the three control groups (BAM-SiPc control, light control and no treatment control) throughout the course of experiment. On Day 25 (i.e. 15 days after the application of PDT), the size of the tumor has regressed to only 15% of the initial tumor volume for the PDT treatment group.

For HT29, growth of the tumor was significantly retarded for the first 10 days after BAM-SiPc mediated PDT. Thereafter, HT29 tumor resumed normal growth. For the three control groups, normal tumor growth could be observed. The doubling time for the tumor size of the control groups was about 15 days, using the days for the start of the measurement (Day 6) as the reference point. For the PDT-treated group, the tumor size only increased in ~ 80% at the end of the experiment (Day 25). All the treated and control mice had normal activities and did not show any observable discomfort.

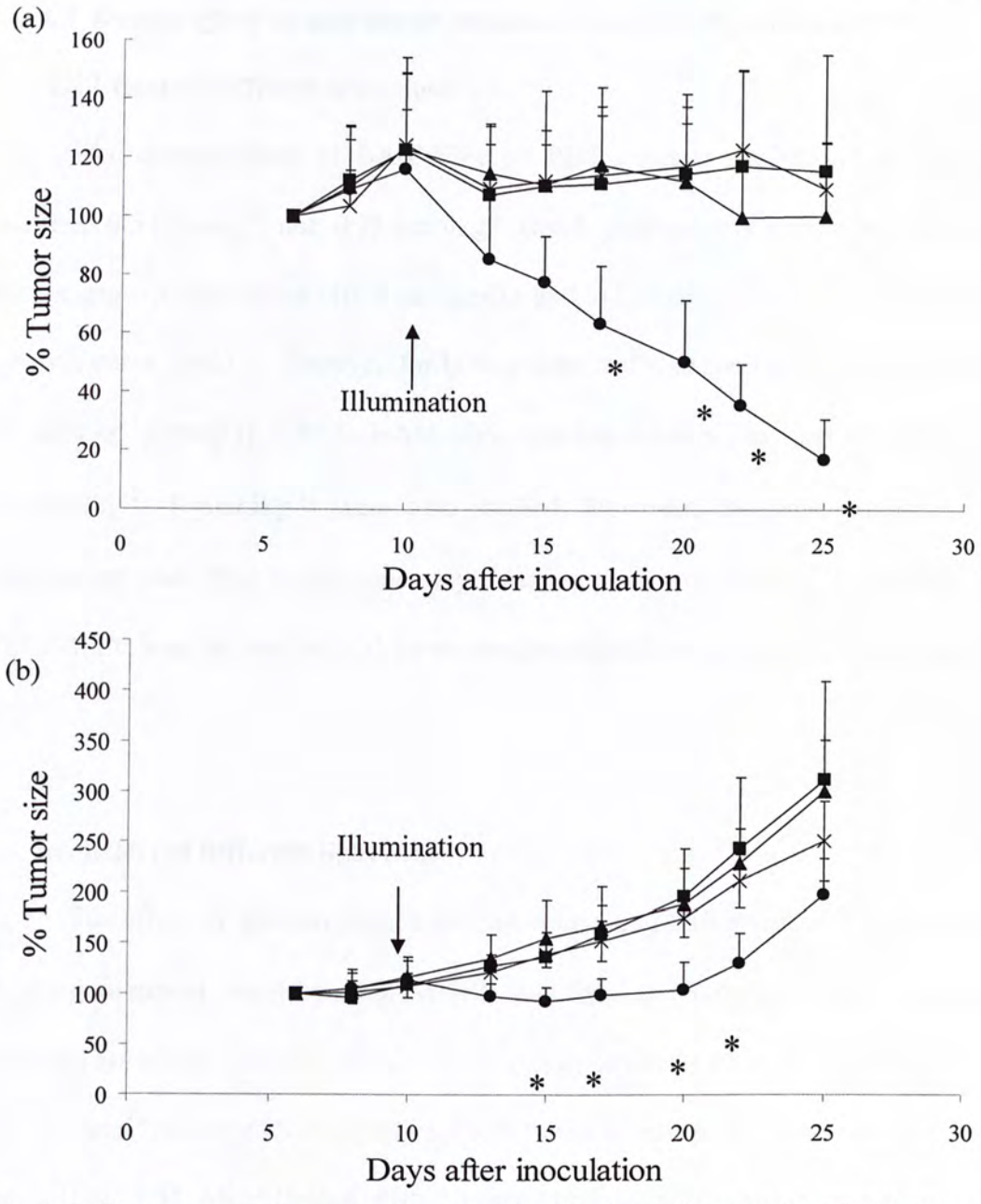

Fig. 3.3 Tumor growth curve for (a) HepG2 (n = 8) and (b) HT29 (n = 6) tumor-bearing nude mice treated with BAM-SiPc mediated PDT. Experiments were divided into four different groups, PDT- treated (●); BAM-SiPc control (x); Light control (▲) and No treatment control (■). The dose of BAM-SiPc used was 1 $\mu molkg^{-1}$ while the laser fluence was at 30 Jcm^{-2}. Data represent Mean ± SD of the % tumor size. Percent tumor size referred to the relative volumes of the solid tumor developed on the nude mice. *, $p < 0.05$ (One–way ANOVA) when compared with all other groups.

3.3.2 Dosage effect on anti-tumor activities by BAM-SiPc mediated PDT

a. Effect of different drug dose

The dosage effect of BAM-SiPc on PDT efficacy was shown in Fig. 3.4. Neither 0.5 $\mu molkg^{-1}$ nor 0.25 $\mu molkg^{-1}$ could produce any tumor regression or tumor growth retardation effect on HepG2 and HT29 solid tumor. A normal tumor growth curve could be observed for both groups and was similar to the light control (0 $\mu molkg^{-1}$) group ($p > 0.05$). BAM-SiPc injection doses higher than 1 $\mu molkg^{-1}$ (i.e. 2 $\mu molkg^{-1}$, 4 $\mu molkg^{-1}$) were also studied. However, the mice suffered great discomfort and died within one day (data not shown). Hence, 1 $\mu molkg^{-1}$ of BAM-SiPc was the optimum dose to produce significant anti-tumor effect used in PDT.

b. Effect of different light dose

The effect of different light doses on eradicating tumor was also investigated. In the experiment, the dose of BAM-SiPc was fixed at 1 $\mu molkg^{-1}$. When compared with the BAM-SiPc control group (0 Jcm^{-2}), fluence rate at 30 Jcm^{-2} and 60 Jcm^{-2} but not 15 Jcm^{-2} could produce significant anti-tumor effect in the HepG2-bearing nude mice (Fig. 3.5). Mice treated with 30 Jcm^{-2} of light were free of any observable physical damage while skin burning was obvious when the light dose was increased to 60 Jcm^{-2} (Fig. 3.6). Nevertheless, the physical activity of the mice was not inhibited regardless of the fluence rate of light used in the experiment.

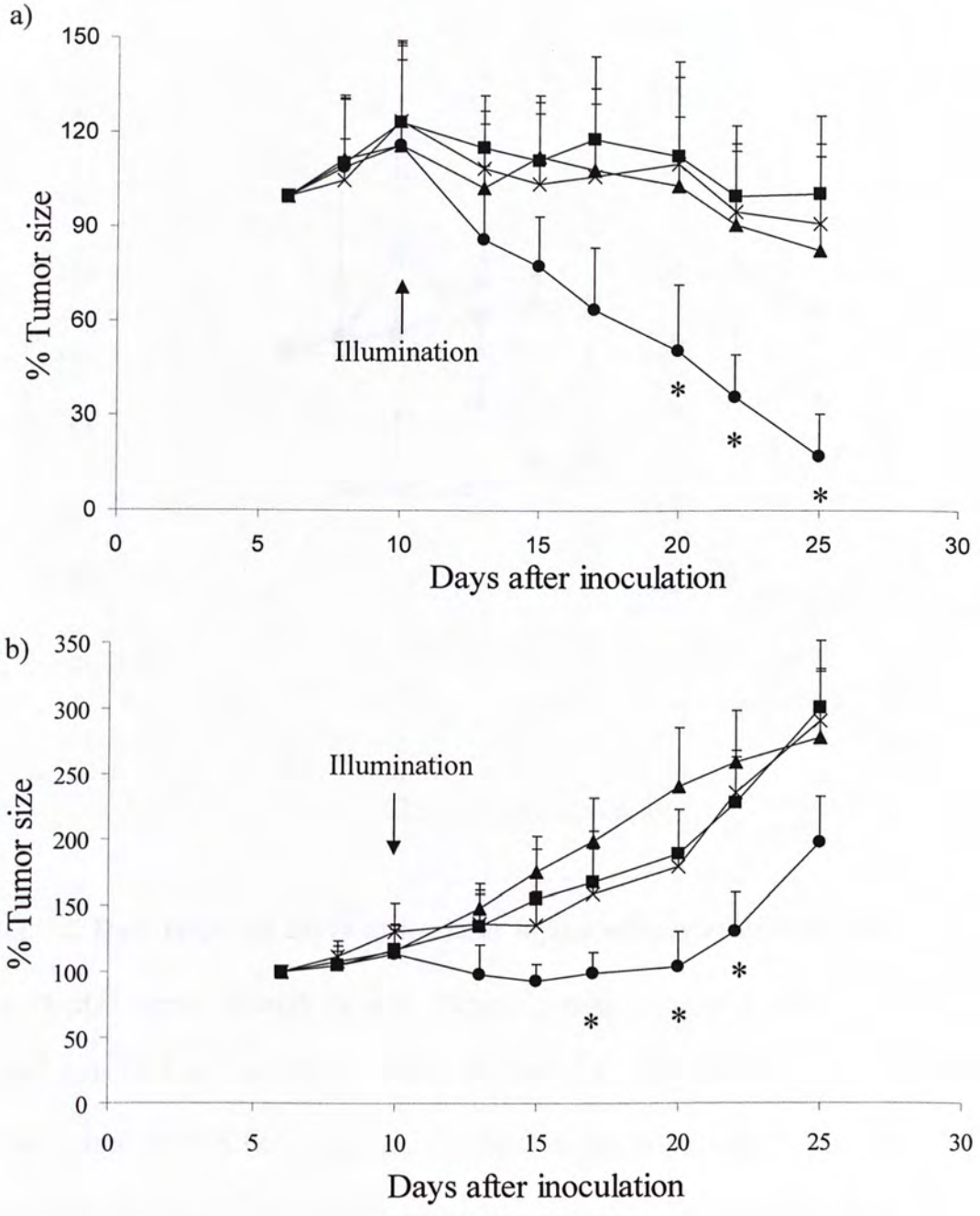

Fig. 3.4 Dose response curve of BAM-SiPc on (a) HepG2 and (b) HT29 tumor growth (n = 5). Experiments were divided into four groups, 0 $\mu molkg^{-1}$ (■); 0.25 $\mu molkg^{-1}$ (▲; 0.5 $\mu molkg^{-1}$ (x) and 1 $\mu molkg^{-1}$ (●). All animals were illuminated with laser wavelength 675 ± 3 nm, (0.1 W, 5 min, total fluence rate ~ 30 Jcm^{-2}) at 24 hr post injection. Data represent Mean ± SD. *, $p < 0.05$ (One–way ANOVA) when compared with all other groups.

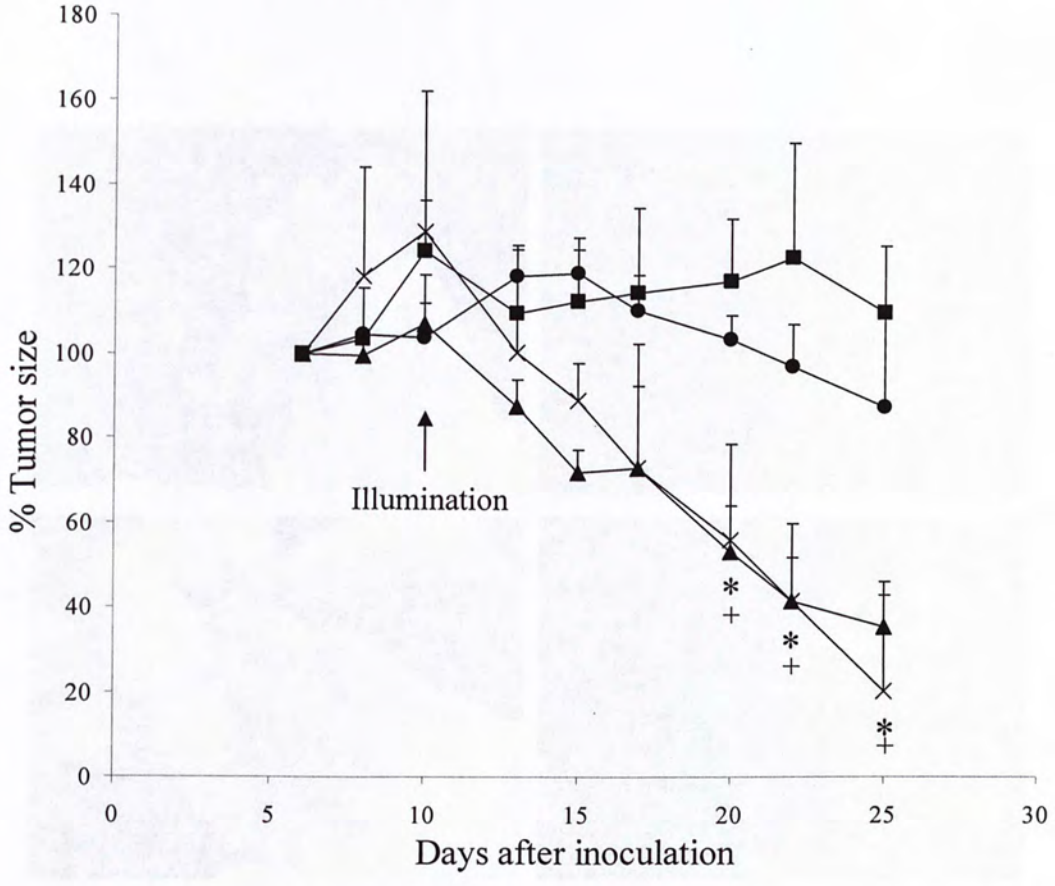

Fig. 3.5 Dose response curve of the laser light source (wavelength 675 ± 3 nm) on HepG2 tumor growth (n = 3). Experiments were divided into four groups, 0 Jcm^{-2} (■); 15 Jcm^{-2} (●); 30 Jcm^{-2} (x); 60 Jcm^{-2} (▲). All animals were i.v. injected with 1 μmol BAM-SiPc per kg body weight. Data points represent Means ± SD. *, $^{+}$, $p < 0.05$ (One–way ANOVA) referred to the statistical significant difference for 30 Jcm^{-2} and 60 Jcm^{-2} when compared with the dark control group.

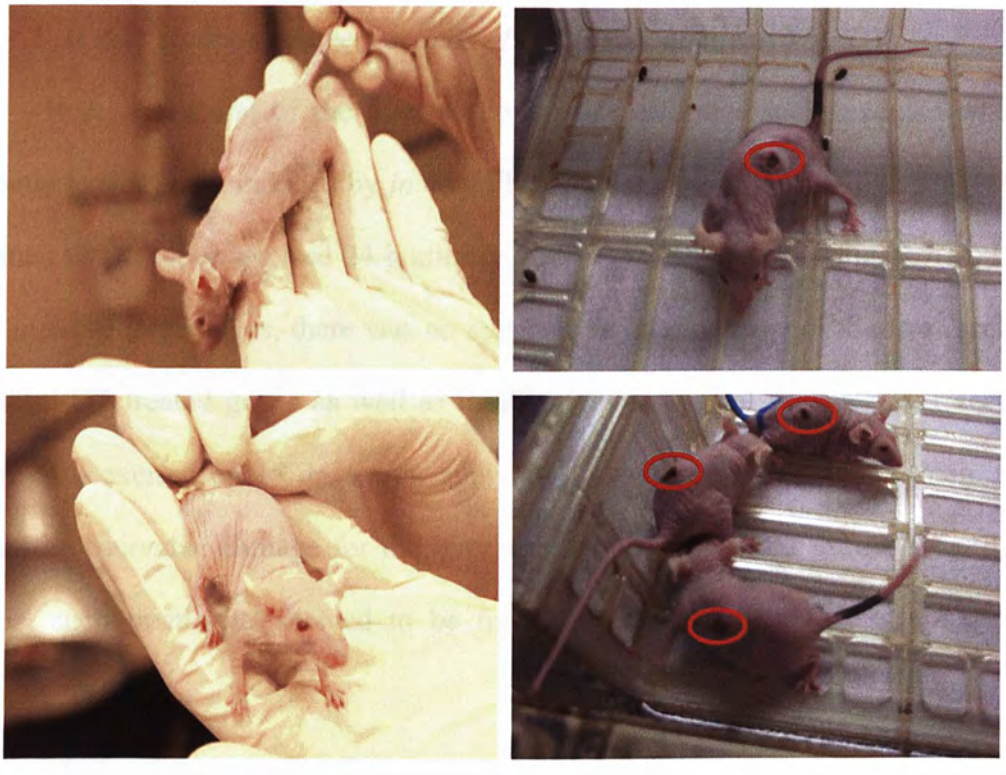

Fig. 3.6 Snapshots for the PDT treated mice. HepG2 bearing nude mice were treated with either 30 Jcm^{-2} (Left) or 60 Jcm^{-2} (Right) laser.

3.4 Analysis of intrinsic toxicity induced by BAM-SiPc mediated PDT

3.4.1 H & E staining of liver sections of nude mice after in vivo PDT

H & E staining of the liver sections was performed to investigate whether hepatic toxicity was induced by *in vivo* PDT treatment with BAM-SiPc. The H & E stained liver section excised 24 h after *in vivo* PDT was shown in Fig. 3.7(a). From the microscopic images, there was no apparent cellular damage of the liver sections in the PDT treated group as well as in all the three control groups. Liver sections were also excised on 15 days after applying photodynamic treatment. Again, there was no observable damage for the liver sections in all the four groups (Fig. 3.7b). Thus, such treatments seemed to be free from inducing both acute and chronic hepatic toxicity.

3.4.2 Enzyme activities assay for the plasma of in vivo PDT treated mice

Elevation of ALT and AST activities will suggest the presence of liver damage while elevation of CK activity will suggest that significant heart damage is induced. The level of these enzyme activities in plasma were assayed to analyze whether there was any hepatic or cardiac injury induced by BAM-SiPc mediated PDT. Plasma of the nude mice was obtained 15 days after *in vivo* BAM-SiPc mediated PDT. Plasma enzyme activities assay showed that there was no statistically significant difference among the four treatment groups (Fig. 3.8, $p > 0.05$, One-way ANOVA analysis), suggesting that there was no significant chronic heart and liver damage after PDT with BAM-SiPc.

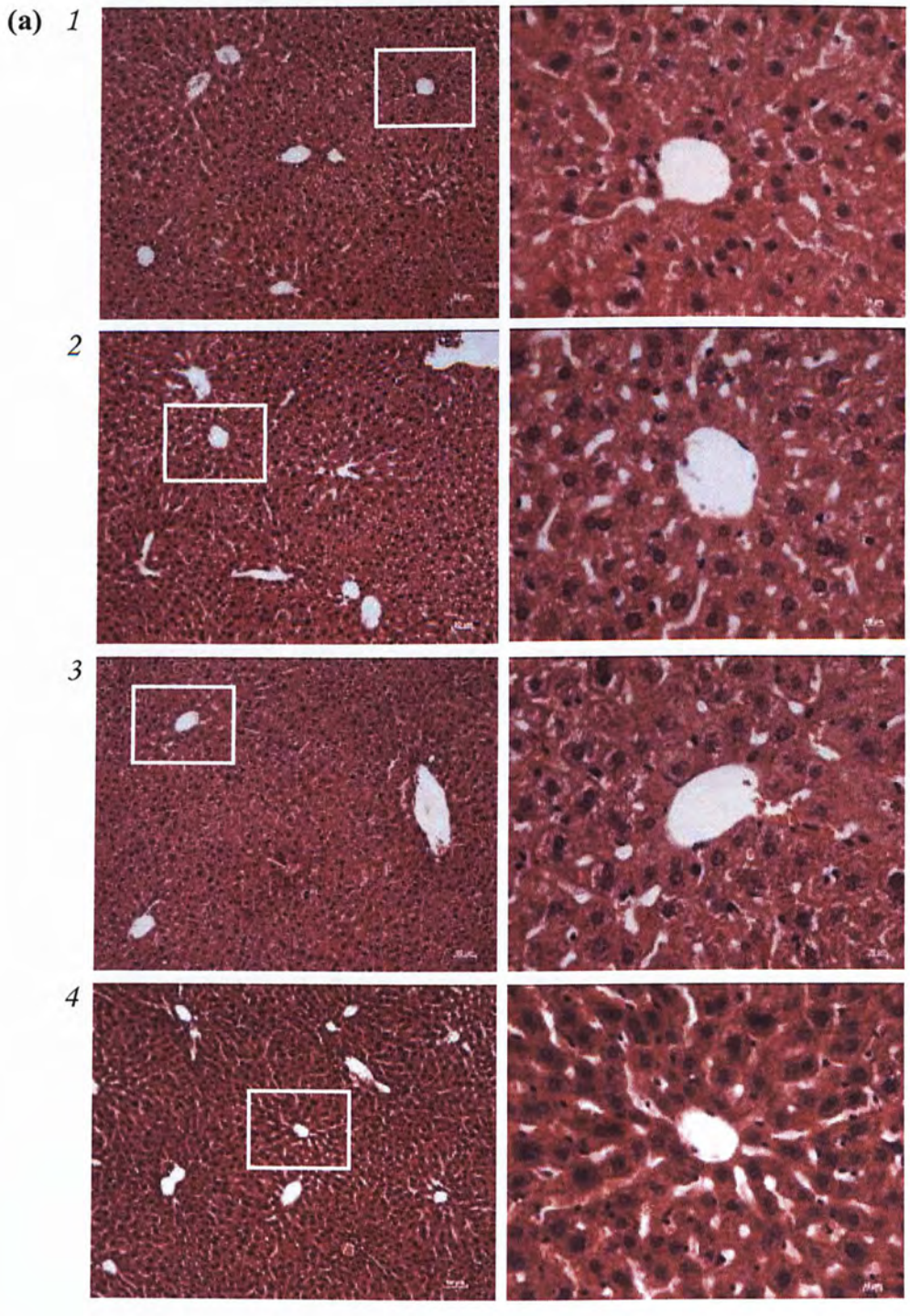
(a)
1
2
3
4

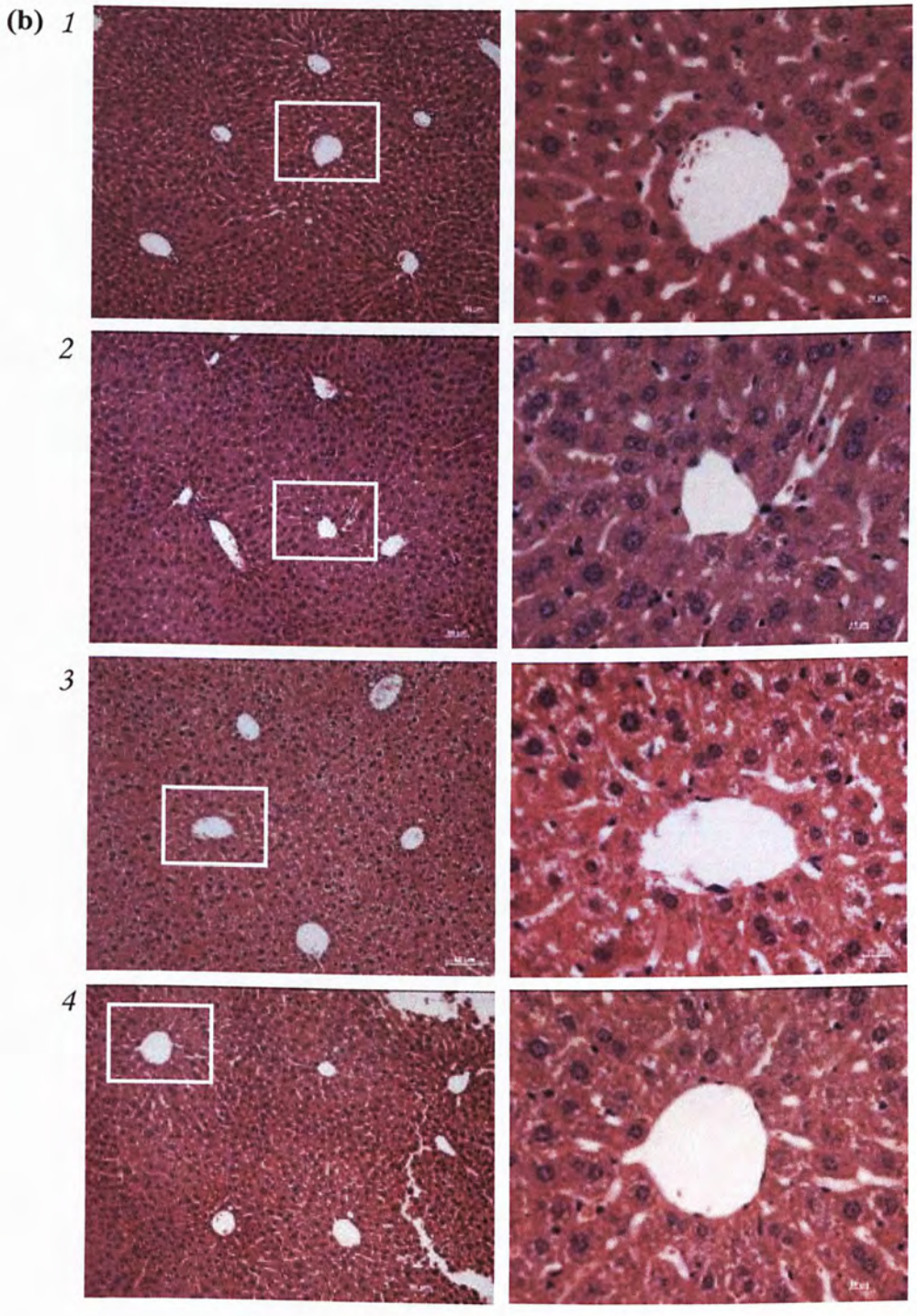
(b)
1
2
3
4

Fig. 3.7 Representative microscopic images (from three independent experiments) of H & E staining for liver sections of BAM-SiPc mediated PDT treated mice. Livers were excised from the nude mice (a) 24 hr and (b) 15 days after treatment. 1-4: PDT-treated; BAM-SiPc control; Light control and No treatment control, respectively. Left: lower magnification (10x); Right: higher magnification (40x) of images enclosed in the white frame showing the region around the hepatic artery.

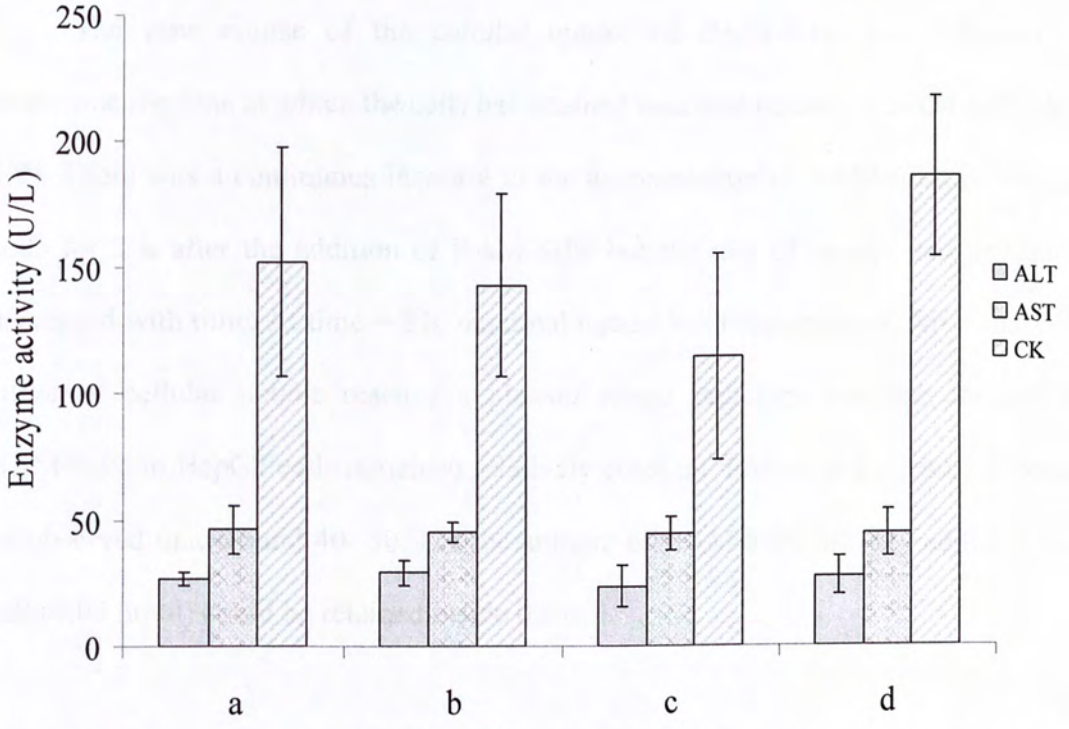

Fig. 3.8 Plasma enzyme activities of nude mice which has undergone various treatments. Plasma samples were obtained 15 days after *in vivo* BAM-SiPc mediated PDT and their ALT, AST (n = 8) and CK (n = 5 or 6) activities were assayed by commercial enzyme assay kits. (a) – (d): PDT-treated; BAM-SiPc control; Light control and No treatment control, respectively. Data represent Mean ± SD.

3.5 BAM-SiPc metabolism in the *in vitro* culture cells and liver homogenate

3.5.1 Cellular uptake of BAM-SiPc

The time course of the cellular uptake of BAM-SiPc was followed to determine the time at which the cells has attained maximal uptake of BAM-SiPc (Fig. 3.9). There was a continuous increase in the accumulation of BAM-SiPc in HepG2 cells for 2 h after the addition of BAM-SiPc but the rate of uptake had gradually decreased with time. At time = 2 h, maximal uptake has been attained. After that, the curve of cellular uptake reaches a plateau which indicates that the amount of BAM-SiPc in HepG2 cells remained relatively constant. Based on the result, it could be observed that around 40- 50% of the amount of BAM-SiPc initially added to the cell (0.05 nmol) could be retained inside the cell.

3.5.2 BAM-SiPc metabolism in cultured normal liver cells and cancer cells

The ability in metabolizing BAM-SiPc was compared between the liver cancer cells HepG2 and the normal liver cells WRL-68. As maximal uptake of BAM-SiPc could be achieved at time = 2 h, it was chosen as a reference point for the study of BAM-SiPc metabolism. In this experiment, the confluency of the cell samples had reached around 80% to 90%. The residual amount of BAM-SiPc present in different samples was shown in Fig. 3.10. The intrinsic fluorescence given by the cell lysate (sample a) and the culture medium (sample f) were negligible. Comparison of the fluorescence given by the mixture of cell lysate and BAM-SiPc (sample d) with that of BAM-SiPc only (sample e) showed that the fluorescence intensities were similar to each other. It indicates that the cell lysate would not cause any reduction in the fluorescence intensity.

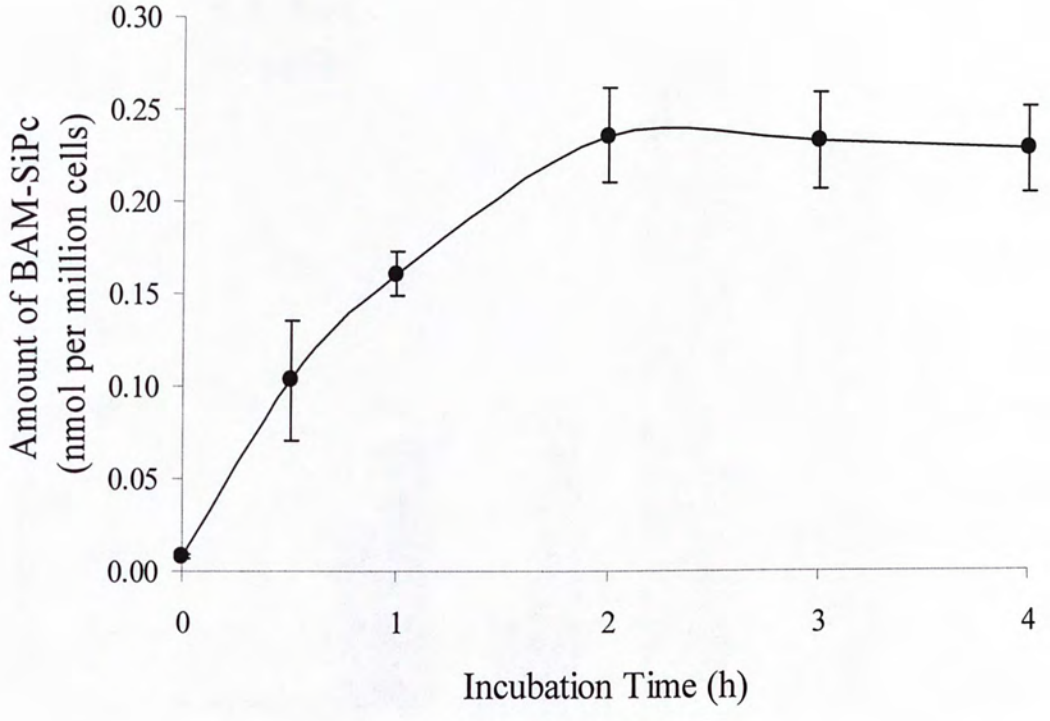

Fig. 3.9 Time course of the cellular uptake for BAM-SiPc by hepatocarcinoma HepG2 cells. BAM-SiPc (0.5 μM) was incubated with HepG2 cells (1 x 10^6) for different periods of time. BAM-SiPc was extracted from the cells by DMF. Amount of BAM-SiPc was quantified by fluorescence measurement. Data represent mean ± SD from three independent experiments.

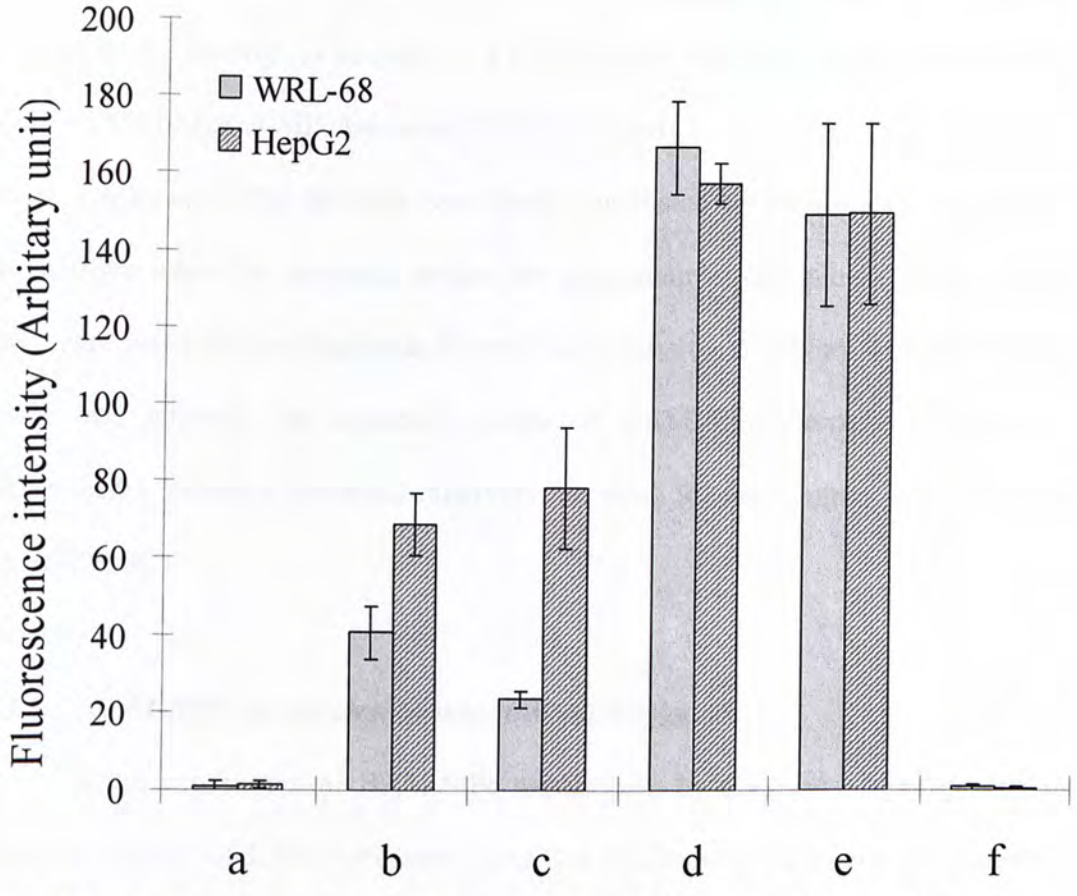

Fig. 3.10 Comparison of the ability of metabolizing BAM-SiPc between the hepatocellular carcinoma HepG2 cells (shaded) and the liver cells WRL-68 (filled). Cells were incubated with 0.5 μM BAM-SiPc for (a) 0 hr; (b) & (c) 2 h. After removing BAM-SiPc solution, samples were then washed with PBS. Samples (a) & (b) were immediately extracted with DMF while sample (c) was allowed to further incubate for 24 h with culture medium before DMF extraction. Sample (d) represents the control experiment in which 0.5 μM BAM-SiPc was incubated with cell lysate while sample (e) represents the sample with 0.5 μM BAM-SiPc only; Sample (f) refers to the sample of the intrinsic fluorescence given by the cell lysate only. Data represent Mean ± SD, n=3.

At time = 2 h, there was 40% of BAM-SiPc taken up by HepG2 cells which was similar to the findings in Section 3.5.1 (~ 0.2 nmol out of 0.5 nmol) while there was only ~ 25% of BAM-SiPc taken up by WRL-68 cells.

HepG2 cells and WRL-68 cells were further incubated for 24 h after the removal of BAM-SiPc when the maximal uptake has been attained (sample c). Result showed that there was a 40% reduction in fluorescence intensity comparing with the WRL-68 cells that attained the maximal uptake of BAM-SiPc (sample b). However, fluorescence intensity remained relatively the same for the samples incubating with HepG2 cells.

3.5.3 BAM-SiPc metabolism by mice liver homogenate

In the experiment of BAM-SiPc metabolism by mice liver homogenate, the residual amount of BAM-SiPc was quantified by spectrophotometric measurement. When BAM-SiPc was mixed with liver homogenate, there was a time-dependent decrease of BAM-SiPc. After 24 h of incubation, less than 20% of BAM-SiPc remained in the samples (Fig. 3.11a). Heat-denatured liver homogenate was used in the control experiment, assuming that all the enzyme activities present in liver homogenate were abolished after the heat treatment. Amount of BAM-SiPc present in the samples remained approximately the same even after 24 h incubation with the denatured liver homogenate (Fig 3.11b).

The phototoxicity of the metabolite was analyzed by *in vitro* photodynamic activities assay. In the dark, supernatant of the samples after incubating for 24 h with either native or denatured liver homogenate remained non-toxic (Fig. 3.12a and Fig. 3.12b).

In the presence of illumination, normal phototoxicity of BAM-SiPc was

observed for the samples incubated with denatured liver homogenate even after 24 h. Normal phototoxicity of BAM-SiPc for different samples was indicated by similar IC_{50} values and the dose-dependent cytotoxicity curve (Fig. 3.12c). However, there was a time-dependent decrease in phototoxicity of the samples which had been incubated with native liver homogenate. The dose-dependent cytotoxicity curve gradually shifted to the right with increase in the incubation time of BAM-SiPc with native liver homogenate. When the time of incubation was more than 18 hr, the phototoxicity of BAM-SiPc was completely abolished (Fig. 3.12d).

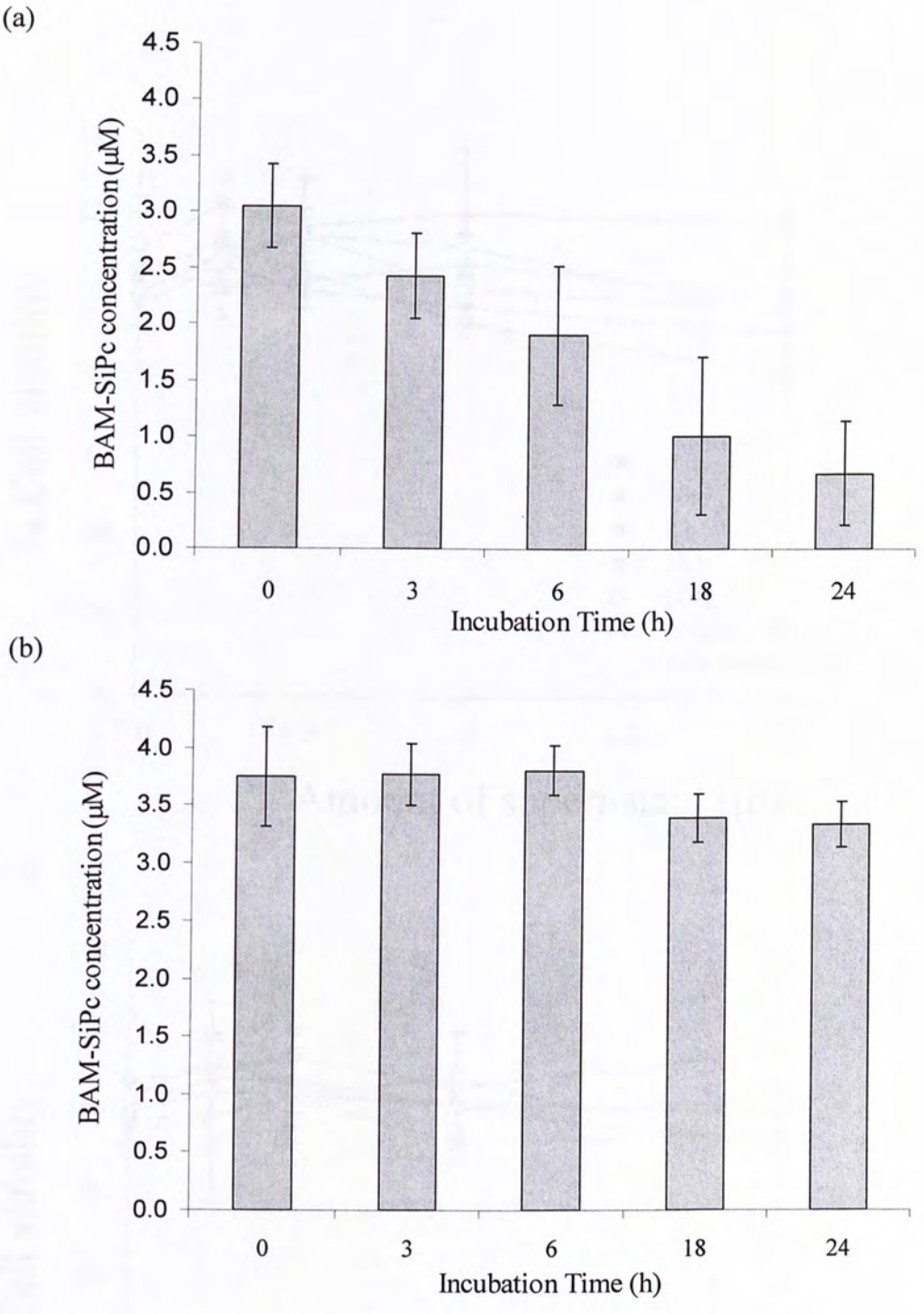

Fig. 3.11 Time course of the residual BAM-SiPc content after pre-incubation with (a) native and (b) heat-denatured liver homogenate. Residual amount of BAM-SiPc was determined by scanning the absorption spectrum from 600 nm to 800 nm, reading of the absorbance peak (674nm) was taken for calculation. Data represent mean ± SEM from three independent experiments.

(a)

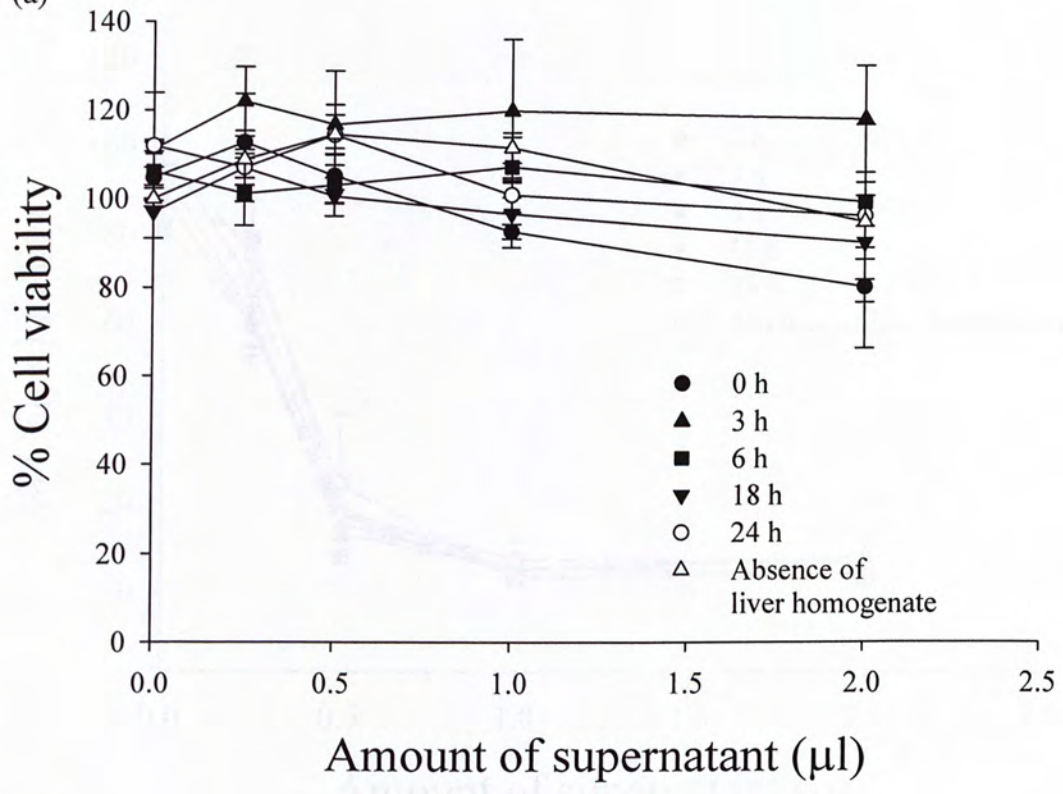
% Cell viability
140
120
100
80
60
40
20
0
0.0
0.5
1.0
1.5
2.0
2.5
Amount of supernatant (µl)
0 h
3 h
6 h
18 h
24 h
Absence of liver homogenate

(b)

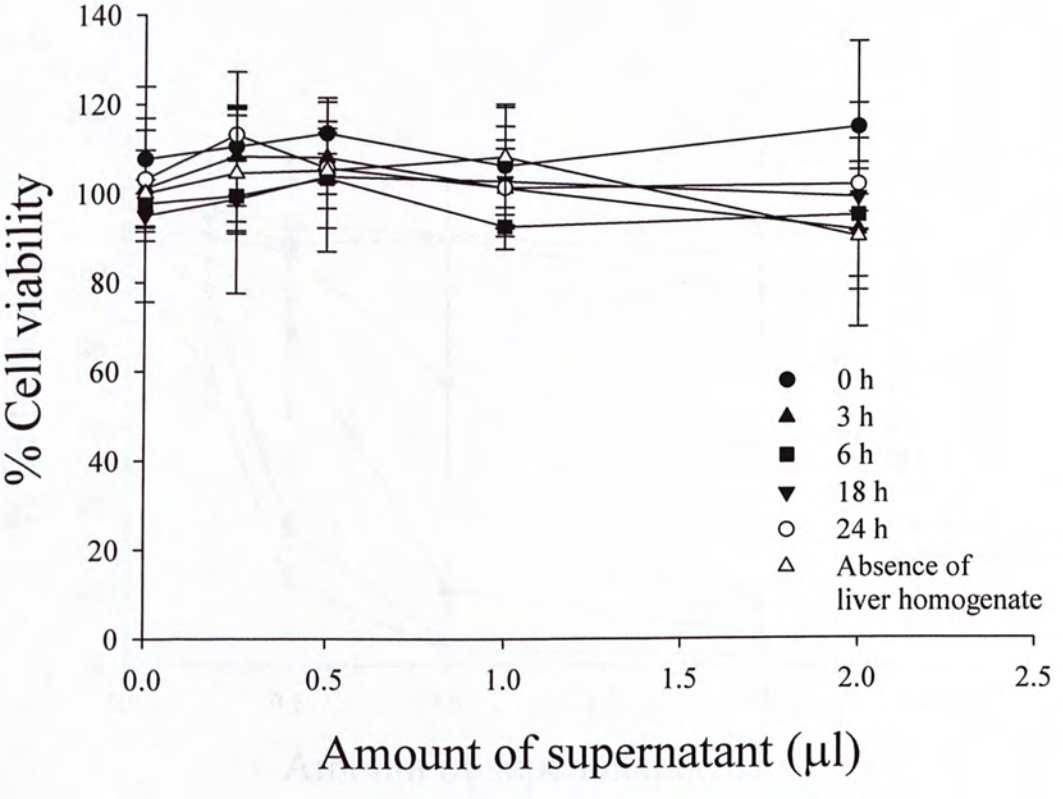
% Cell viability
140
120
100
80
60
40
20
0
0.0
0.5
1.0
1.5
2.0
2.5
Amount of supernatant (µl)
0 h
3 h
6 h
18 h
24 h
Absence of liver homogenate

(c)

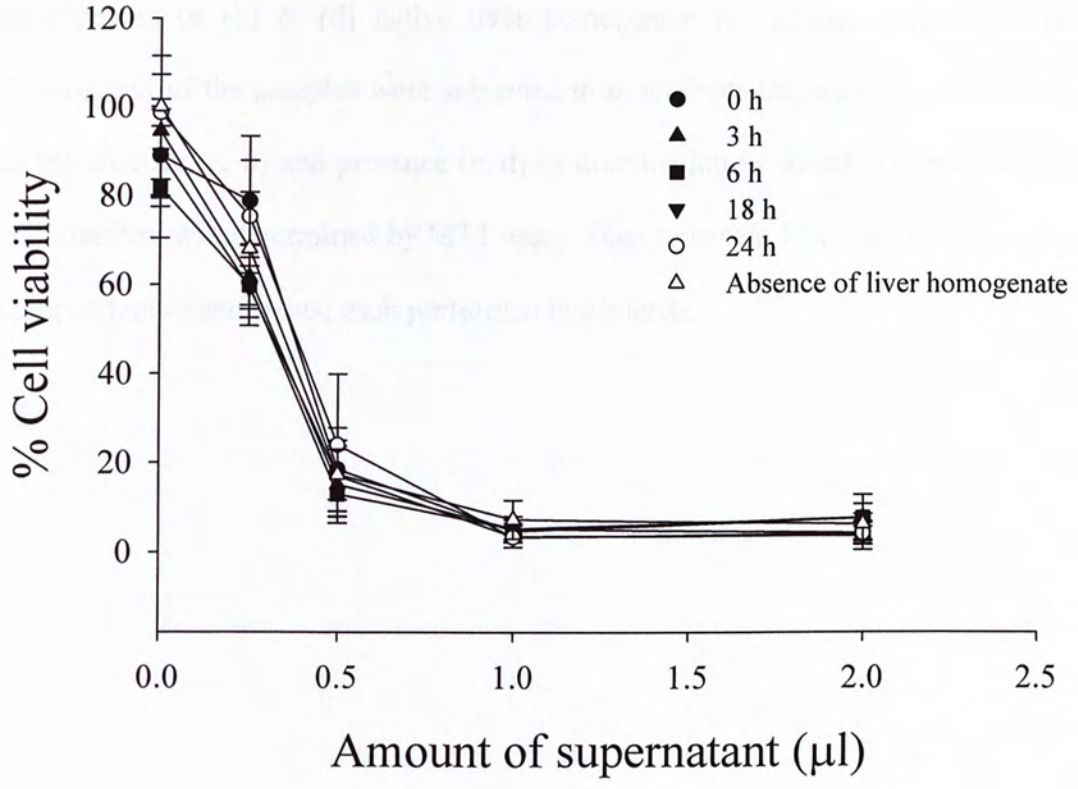
% Cell viability
120
100
80
60
40
20
0
0.0
0.5
1.0
1.5
2.0
2.5
Amount of supernatant (µl)
0 h
3 h
6 h
18 h
24 h
Absence of liver homogenate

(d)

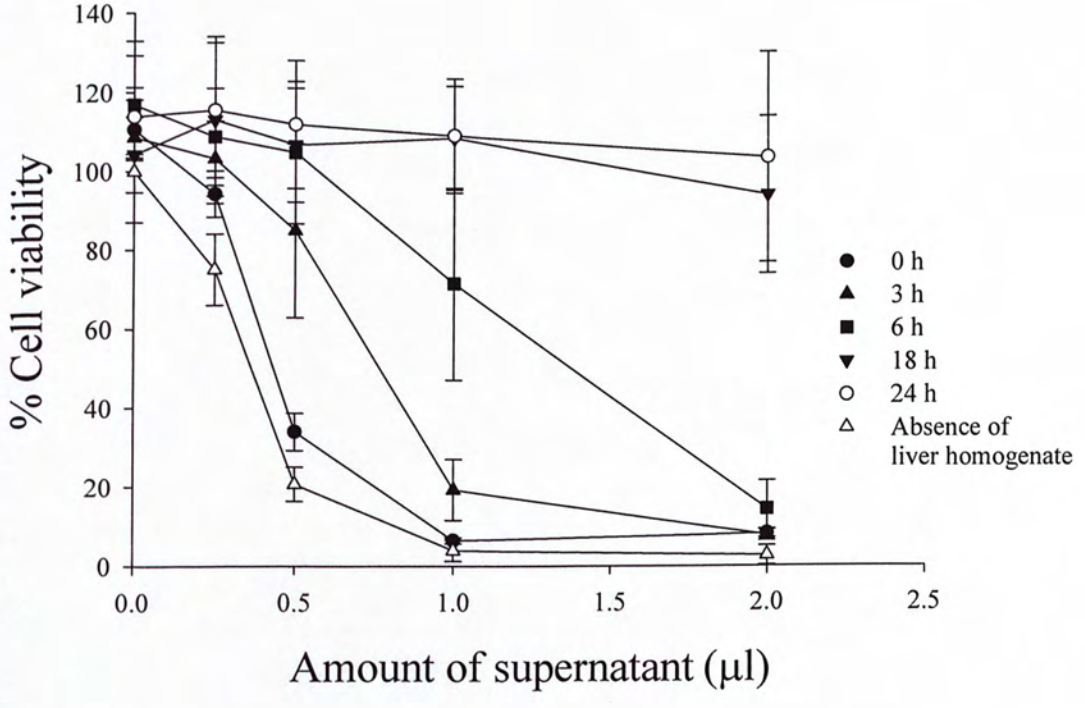
% Cell viability
140
120
100
80
60
40
20
0
0.0
0.5
1.0
1.5
2.0
2.5
Amount of supernatant (µl)
0 h
3 h
6 h
18 h
24 h
Absence of
liver homogenate

Fig. 3.12 Effect of pre-incubation with liver homogenate on phototoxicity of BAM-SiPc. BAM-SiPc (8 μM) was incubated with (a) & (c) heat denatured liver homogenate or (b) & (d) native liver homogenate for various periods of time. Supernatant of the samples were subjected to *in vitro* photodynamic activities assay in the absence (a, b) and presence (c, d) of illumination as stated in Section 2.6 and cell viability was determined by MTT assay. Data represent Mean ± SEM from three independent experiments, each performed in triplicate.

3.6 Death mechanism induced by BAM-SiPc mediated PDT

3.6.1 Events related to cell death induced by in vitro BAM-SiPc mediated PDT

The intracellular ROS production and cell cycle analysis were performed to study the biochemical mechanism of cell death induced by BAM-SiPc mediated PDT. Upon illumination, there was a dose-dependent increase in the relative ROS production. In particular, intracelluar ROS production increased by more than 3-, 2- and 4-fold for HepG2, Hep3B and HT29 respectively at 0.1 μM BAM-SiPc (Fig. 3.13) where the cell viability after photodynamic treatment was below 20%. On the contrary, no apparent increase in intracellular ROS could be observed in the absence of light.

PI staining for cell cycle analysis of the PDT treated cells was performed to see whether cell cycle arrest was induced at 24 h after PDT with BAM-SiPc (Fig. 3.14). There was no obvious change in distribution of cells in cell cycle for the BAM-SiPc control and light control groups when compared with the untreated HepG2 cells. Arrest in G_0/G1 phase of the cell cycle after PDT with BAM-SiPC could be observed. The treatment caused an accumulation of 79%, 82%, 85% cells in G_0/G1 phase at 0.005 μM, 0.01 μM, 0.02 μM BAM-SiPc, a slight increase when compared with the 77% for the solvent control. The increase in G_0/G1 cell population was accompanied with a decrease in cell number in S-phase. When a BAM-SiPc concentration greater than 0.02 μM was used, the cell cycle distribution continued to shift from G_0/G1 peak to the region "Debris" with increasing concentration of BAM-SiPc. At 0.1 μM of BAM-SiPc, almost the entire (98%) cell population had fell into the "Debris" region. The "Debris" region represents the necrotic cells or those cells with fragmented DNA or DNA strands break. In other words, cells treated with 0.02 μM BAM-SiPc had immediately undergone necrosis or apoptosis.

(a)

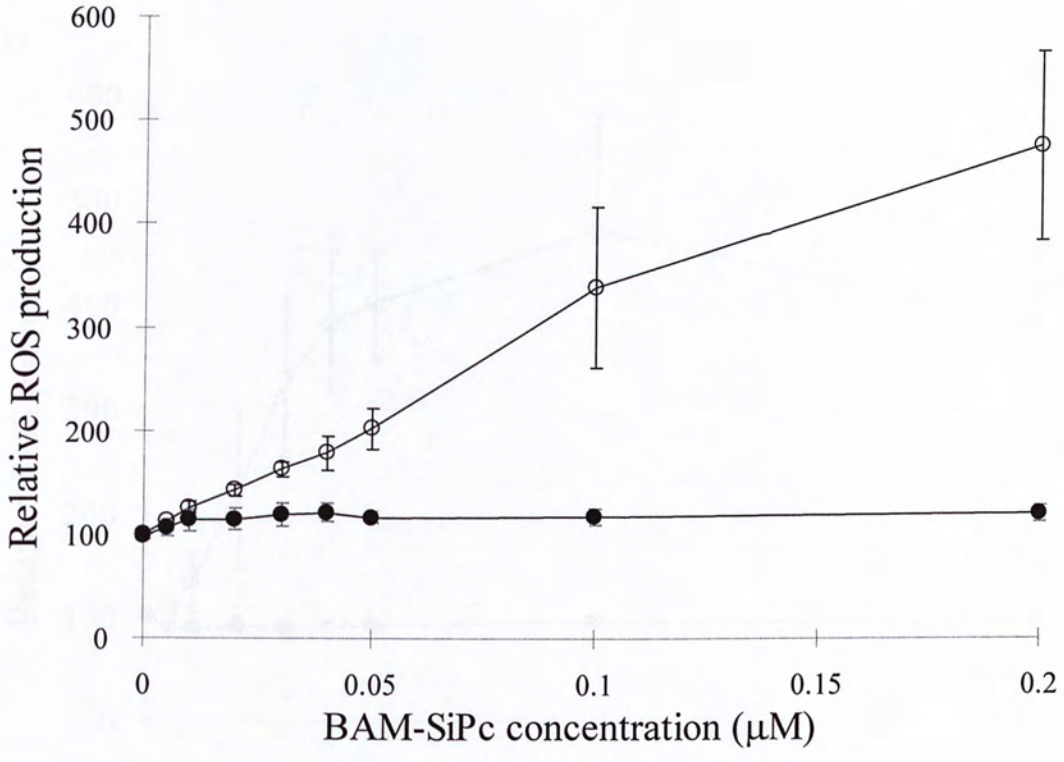
600
500
400
300
200
100
0
Relative ROS production
0
0.05
0.1
0.15
0.2
BAM-SiPc concentration (μM)

(b)

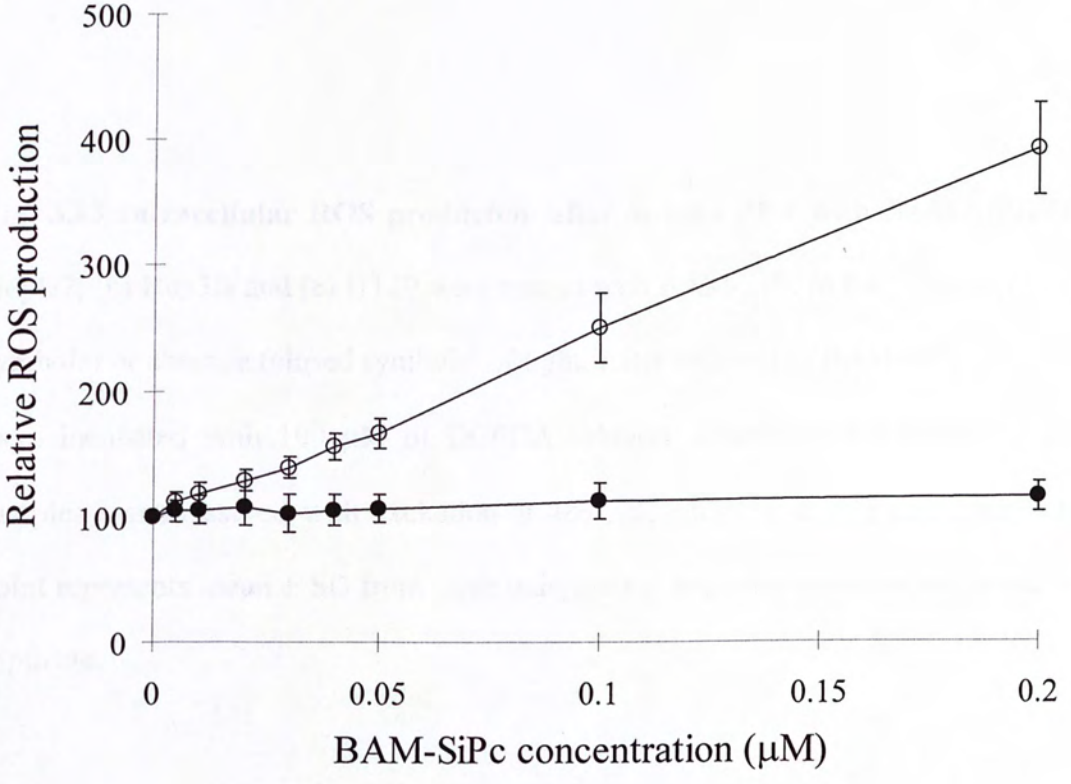
500
400
300
200
100
0
Relative ROS production
0
0.05
0.1
0.15
0.2
BAM-SiPc concentration (μM)

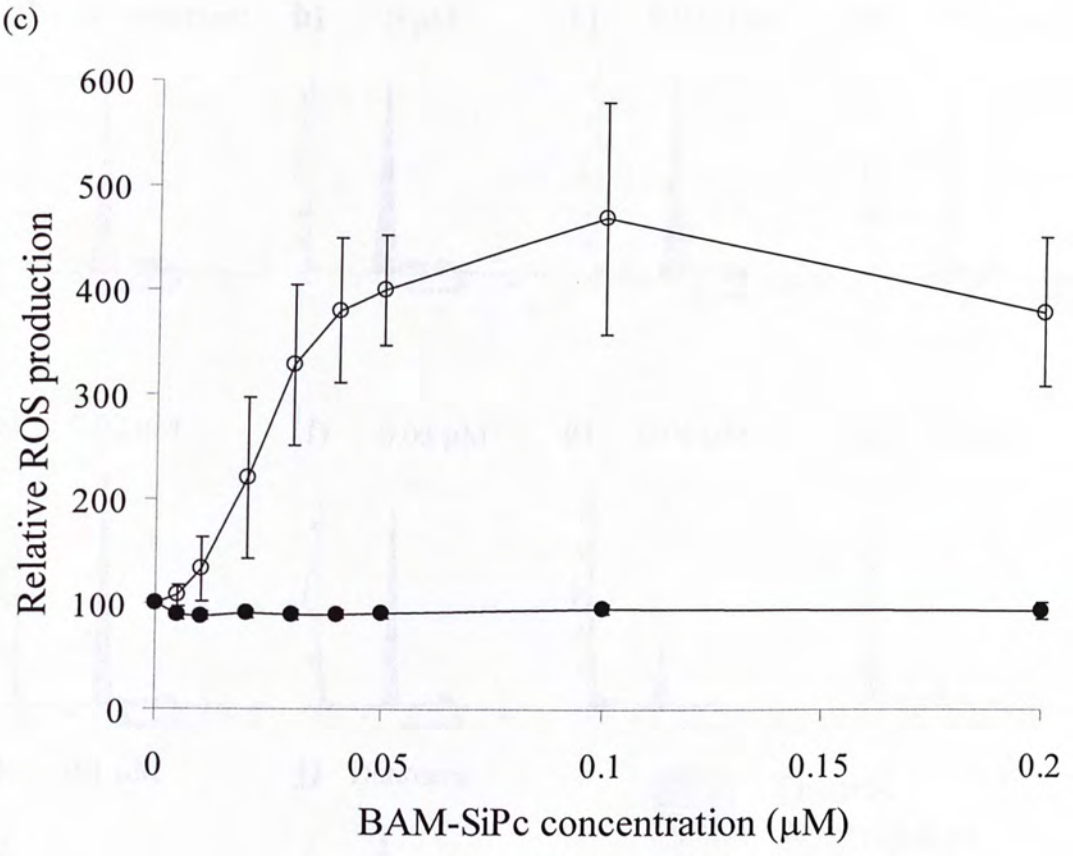

Fig. 3.13 Intracellular ROS production after *in vitro* PDT with BAM-SiPc. (a) HepG2; (b) Hep3B and (c) HT29 were treated with BAM-SiPc in the presence (open symbols) or absence (closed symbols) of light. After removal of BAM-SiPc, samples were incubated with 100 μM of DCFDA solution. Fluorescence intensity of the samples was measured with excitation at 485 nm, emission at 535 nm. Each data point represents mean ± SD from three independent experiments, each performed in triplicate.

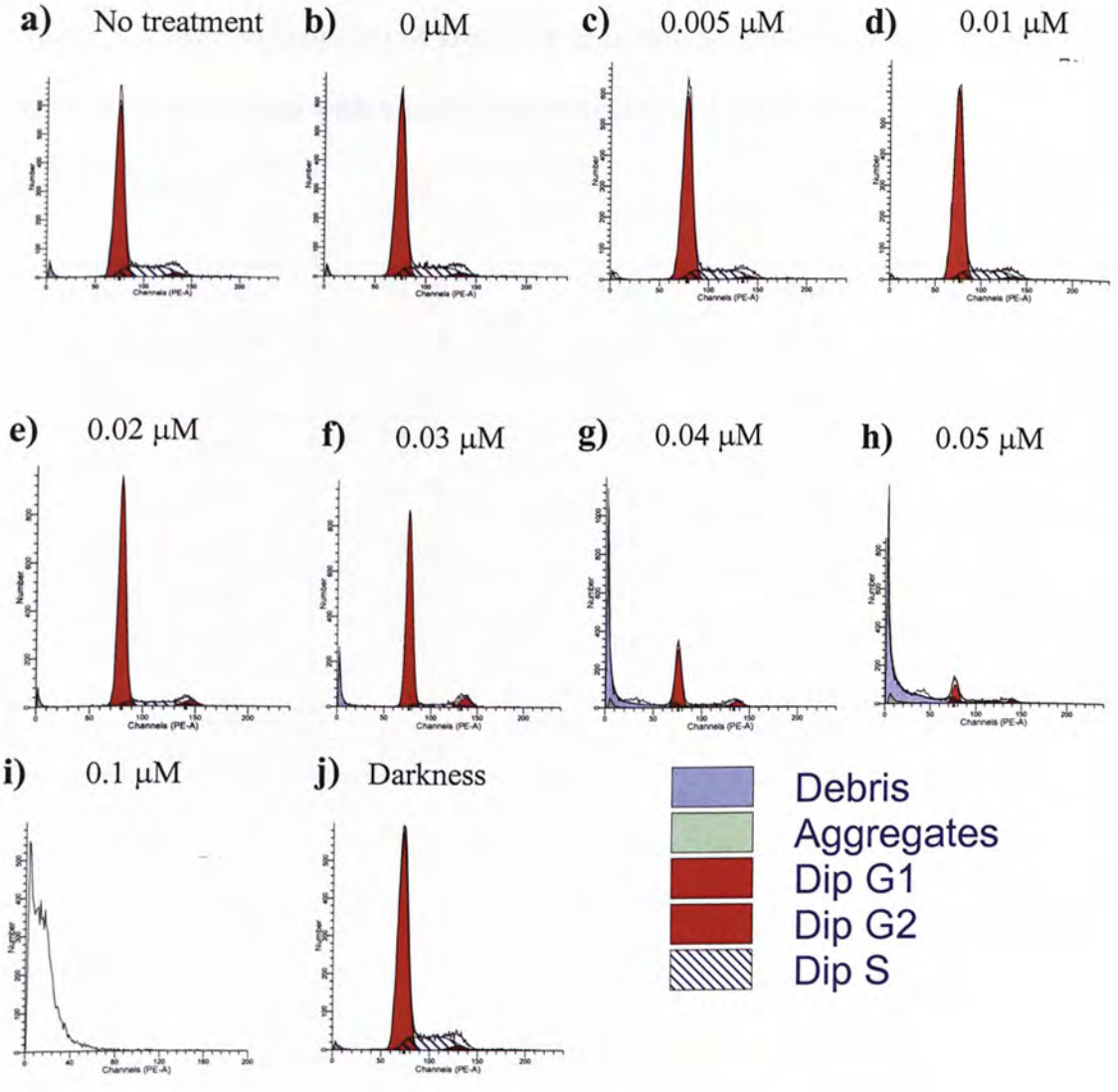

Fig. 3.14 Cell cycle patterns of BAM-SiPc mediated PDT treated HepG2 cells. HepG2 cells underwent *in vitro* PDT with the indicated BAM-SiPc concentrations (b to i). (j) represents the HepG2 cells incubated with 0.1 μM BAM-SiPc but without light treatment. Samples were then stained with PI solution (20 μg/ml) for 15-30 min. Fluorescence from individual cells was recorded by a FASCanto flow cytometer with PE-A (ex 488nm; em 585nm). "Dip" referred to diploid.

Table 3.2 Distribution (%) of HepG2 population in different stages of cell cycle after PDT treatment with various concentrations of BAM-SiPc.

Treatment	G1	S	G2	Debris
Untreated cells	74.90	13.79	8.40	3.03
Solvent control	77.18	13.61	7.44	1.97
0.005 μM	78.91	12.37	6.51	2.48
0.01 μM	82.40	10.80	5.70	1.28
0.02 μM	84.72	7.27	5.40	2.70
0.03 μM	76.64	6.47	7.41	9.68
0.04 μM	29.82	8.54	6.42	55.48
0.05 μM	14.12	6.44	4.27	75.34
0.1 μM	1.44	0.36	0.19	98.04
Dark	77.18	14.2	6.99	1.90

3.6.2 Death mechanism exerted by in vivo BAM-SiPc mediated PDT

TUNEL and H & E staining of HepG2 tumors were performed to investigate the death mechanism induced by *in vivo* BAM-SiPc mediated PDT. HepG2 tumors were excised at 24 h after different treatments and their histological sections were taken for TUNEL staining. A large population of TUNEL-positive nuclei was detected for the PDT treated tumors (Fig. 3.15a). It indicated that BAM-SiPc mediated PDT could induce DNA fragmentation in HepG2 tumor. However, when HepG2 tumors were either treated with BAM-SiPc or light alone, very little or negligible fluorescence signal could be observed, similar to HepG2 tumors with no treatment (Fig. 3.15 b-d). Nuclear fragmentation is one of the hallmark features in apoptosis. The fragmented nuclei are enclosed in nuclear envelope and form apoptotic bodies with other organelles. The microscope images of the H & E staining of the HepG2 tumors were shown in Fig. 3.16. Nuclear fragmentation was detected in the solid tumors excised 15 days after *in vivo* PDT with BAM-SiPc. This confirms the induction of apoptosis by BAM-SiPc mediated PDT. For the three control groups, the majority of the cancer cells in the solid tumor maintained their spherical intact nuclei. It means that HepG2 tumor grew normally and was not affected by treatments either with BAM-SiPc or light alone.

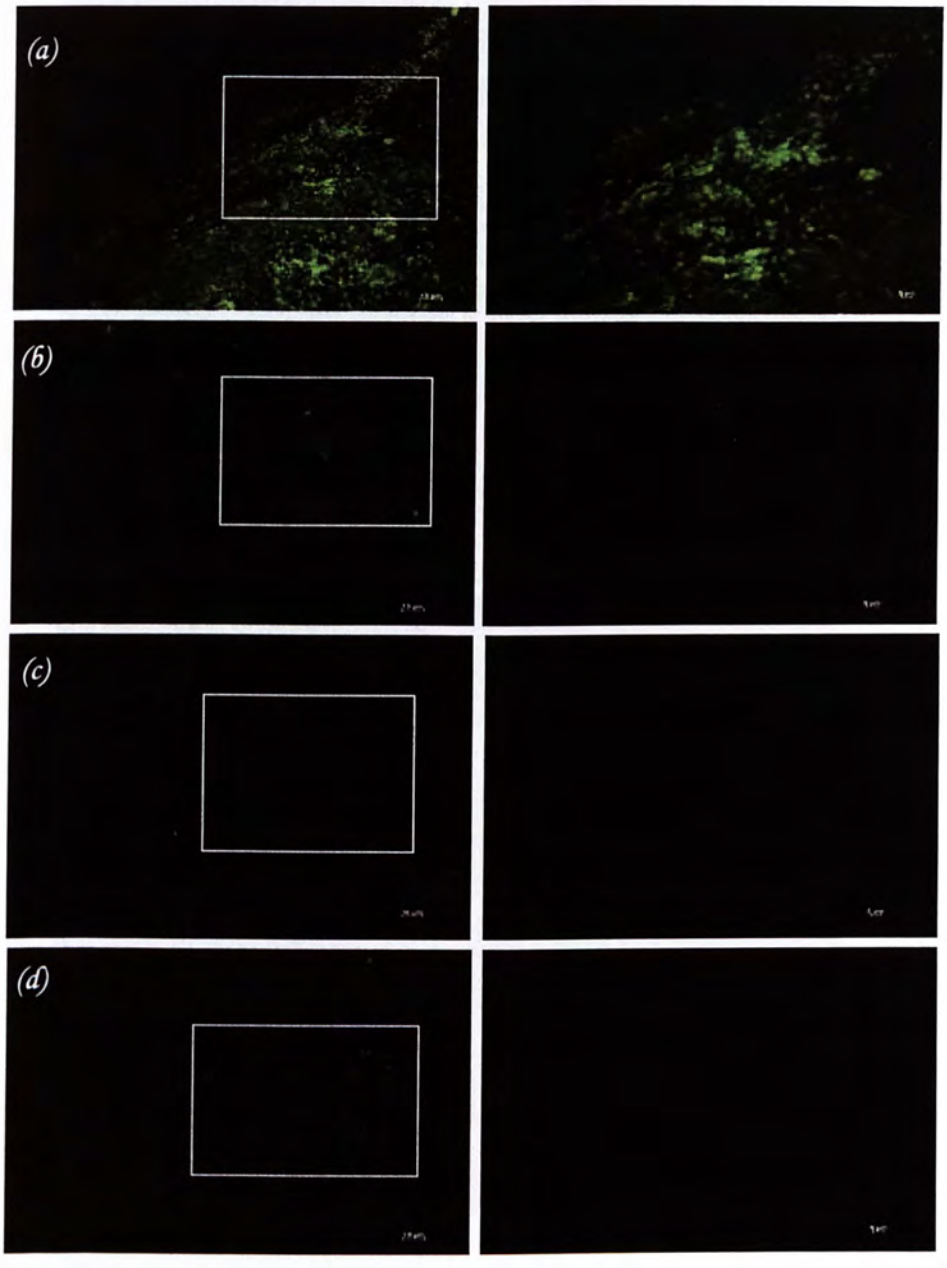

Fig. 3.15 Representative microscopic images (from three independent experiments) of TUNEL staining for solid tumor of BAM-SiPc mediated PDT treated mice. HepG2 solid tumors were excised from the nude mice 24 h after BAM-SiPc mediated PDT and their histological sections were stained by the TUNEL reaction mixture for 1 h. (a) - (d): PDT-treated tumor; BAM-SiPc control; Light control and No treatment control respectively. Left: lower magnification (20x); Right: higher magnification (40x) of images enclosed in the white frame.

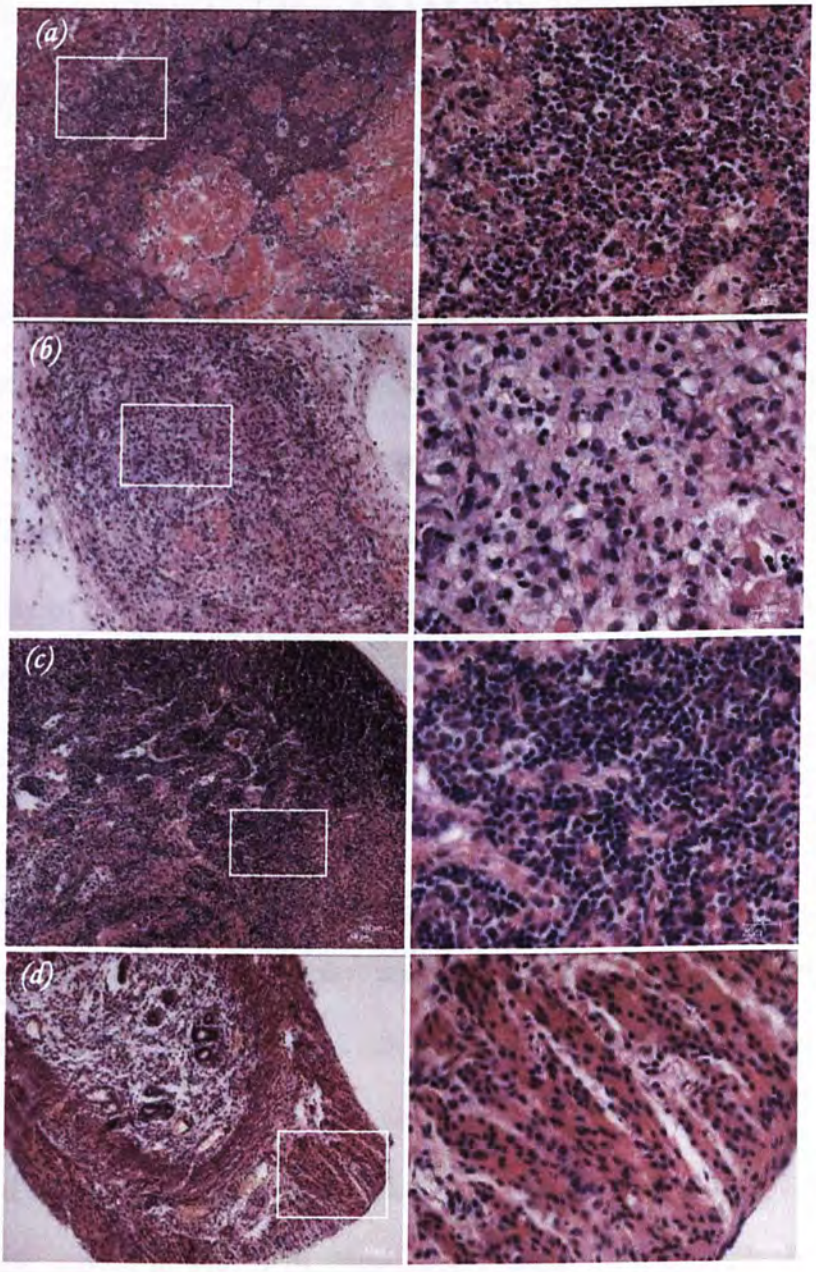

Fig. 3.16 Representative microscopic images (from three independent experiments) of H & E staining for solid tumor of BAM-SiPc mediated PDT treated mice. HepG2 solid tumors were excised from the nude mice 15 days after treatment. Nuclei of the tumors were stained by Mayer's haematoxylin solution (purple) for 2 min and the cytoplasm was counterstained by eosin solution (pink) for 5 min. (a) – (d): PDT-treated tumor; BAM-SiPc control; Light control and No treatment control, respectively. Left: lower magnification (10x); Right: higher magnification (40x) of images enclosed in the white frame.

3.7 Effect on phototoxicity of BAM-SiPc in the presence of LDL

3.7.1 Effect on phototoxicity of BAM-SiPc after mixing BAM-SiPc with LDL

HepG2 was used as a model to study the phototoxicity of the mixture of BAM-SiPc and LDL. In the dark, no cytotoxic effect was exerted even in the presence of the highest concentration of BAM-SiPc and LDL (Fig. 3.17). Thus, viability of HepG2 cells was not affected by adding LDL to the samples. When illumination was employed, normal phototoxicity was exerted against HepG2 cells in the absence of LDL with BAM-SiPc concentration fixed at IC_{50}, i.e. 0.025 μM. The phototoxicity of BAM-SiPc decreased with increasing amount of LDL added into the samples. Cytotoxic effect could not be observed when a 1:40 molar ratio of BAM-SiPc to LDL was used for incubating with HepG2 cells

3.7.2 Gel filtration for analysis of the LDL-BAM-SiPc mixture

Gel filtration chromatography was performed to determine whether LDL conjugated BAM-SiPc was formed after mixing BAM-SiPc with LDL. The gel filtration elution profiles for (a) mixture of BAM-SiPc and LDL in a small scale column and the elution profile of (b) NAD^+, (c) BAM-SiPc, and (d) LDL in larger column were shown in Fig. 3.19. When the mixture of BAM-SiPc and LDL was chromatographed on a gel filtration column, peaks representing BAM-SiPc and LDL overlapped with each other. One explanation was that all the BAM-SiPc was conjugated with LDL. Using a larger column, it could be observed that the elution profiles of both LDL and BAM-SiPc showed peaks at the same elution volume (16 ml). This was unexpected as LDL is a large molecule with a molecular weight 2.25 x 10^6 whereas BAM-SiPc is a small molecule of 717.89 dalton. NAD^+ (molecular weight 685.4) was used as a reference to estimate the retention time for the small

molecules. The elution profile for NAD^+ showed a peak at a much larger elution volume of 35 ml. Based on the results, it could be concluded that the resolution of the gel filtration column used in this experiment was able to retain small molecule for a longer time and separated them from large molecule (e.g. LDL). Surprisingly, LDL and BAM-SiPc could not be resolved by using this gel filtration column.

(a)

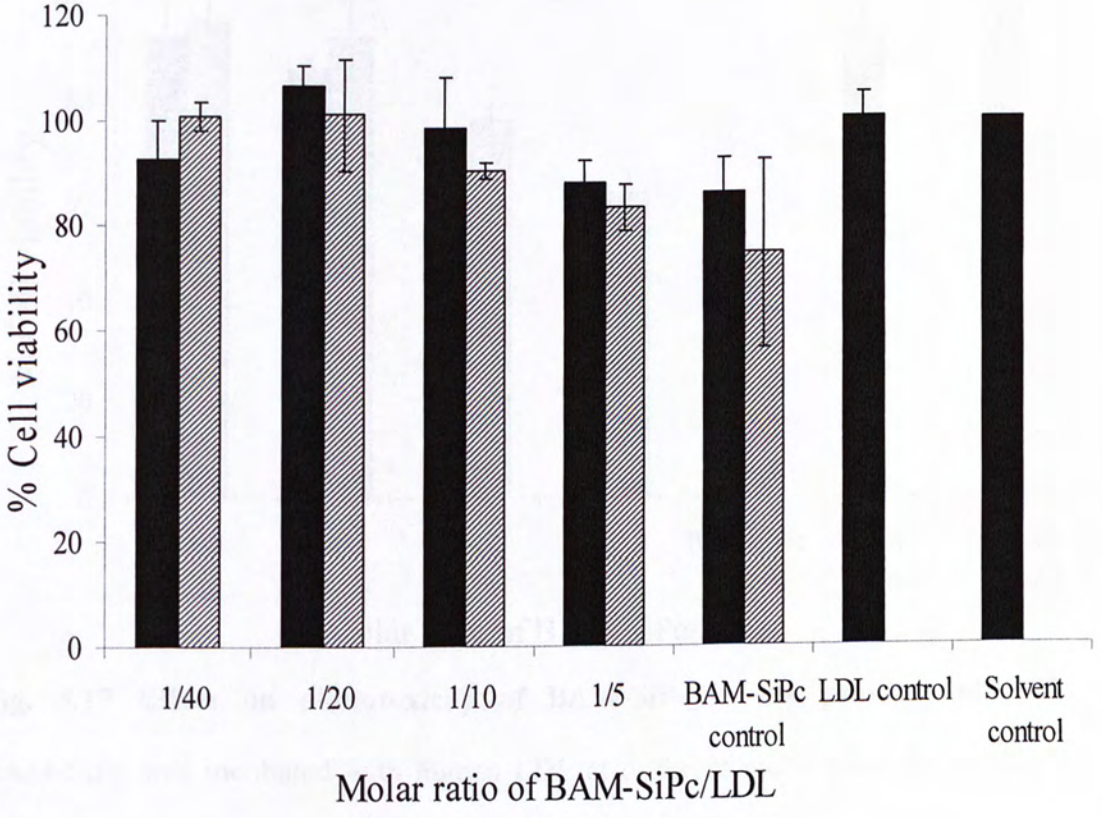
120
100
80
60
40
20
0
% Cell viability
1/40
1/20
1/10
1/5
BAM-SiPc control
LDL control
Solvent control
Molar ratio of BAM-SiPc/LDL

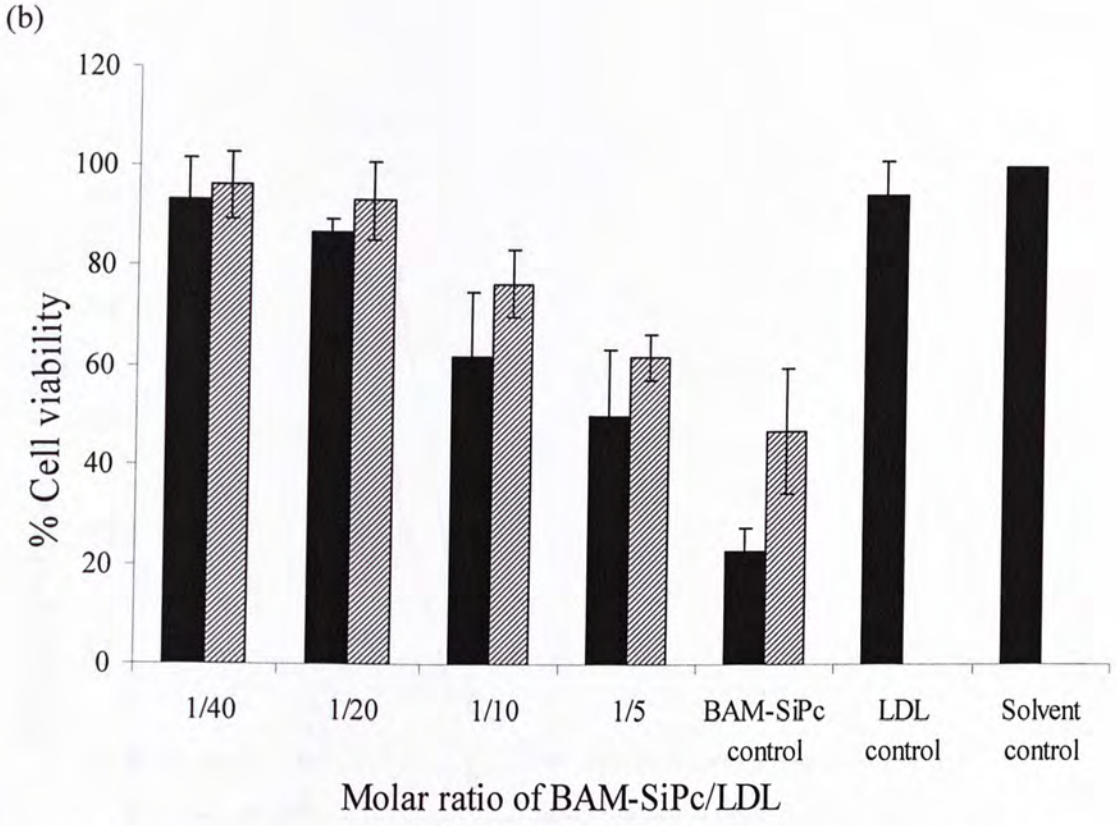

Fig. 3.17 Effect on phototoxicity of BAM-SiPc in the presence of LDL. BAM-SiPc was incubated with human LDL at different molar ratio for 90 min in dark. Then, the phototoxicities of the samples were analyzed by *in vitro* photodynamic activities assay. Two different BAM-SiPc concentrations, one at IC_{50} i.e. 0.01 μM (shaded) and the other at 0.025 μM (filled), were used to incubate with various amount of LDL in this experiment. BAM-SiPc control and LDL control referred to samples of 0.025/0.01 μM BAM-SiPc and amount of LDL used in the 40:1 sample respectively. (a) & (b) represent the samples treated in the absence or presence of light respectively. Data express as mean ± SEM from three independent experiments, each performed in triplicate.

(a)

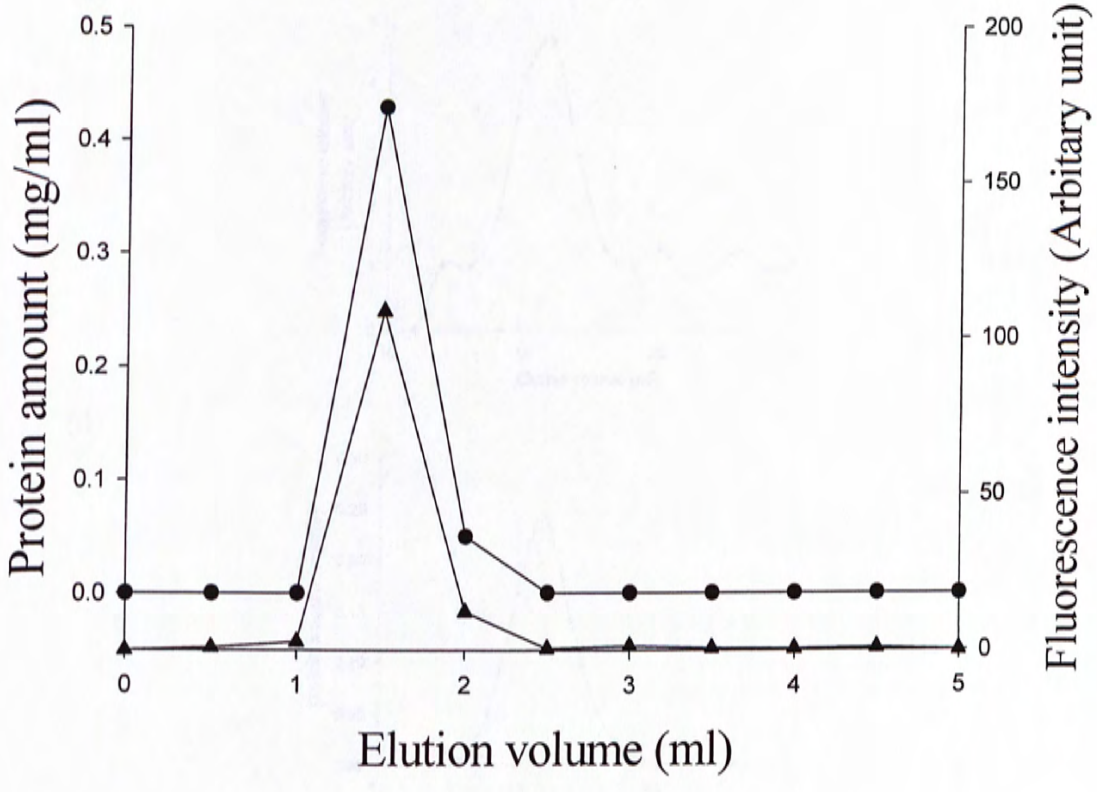
Protein amount (mg/ml)
0.5
0.4
0.3
0.2
0.1
0.0
Fluorescence intensity (Arbitary unit)
200
150
100
50
0
0
1
2
3
4
5
Elution volume (ml)

(b)

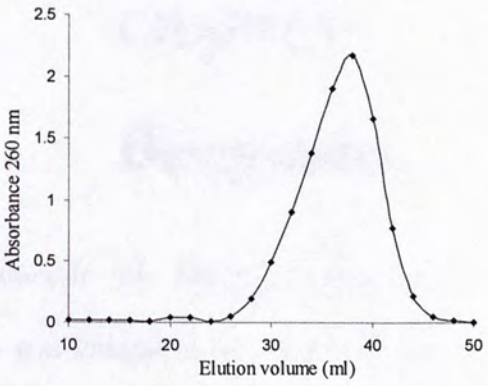

(c)

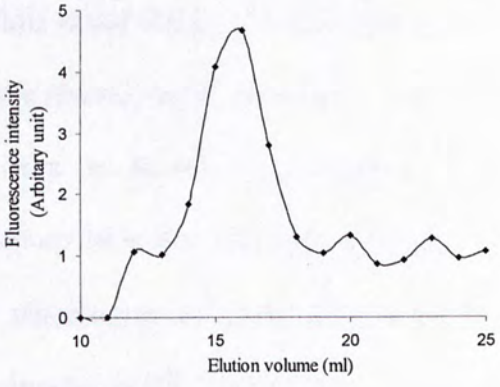

(d)

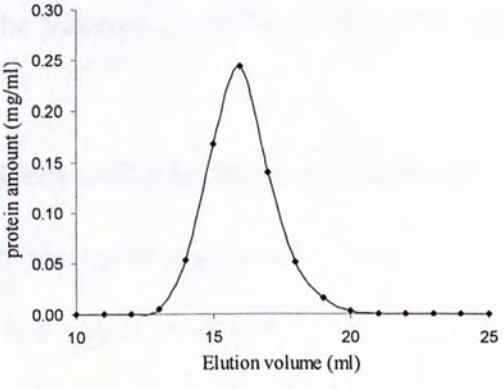

Fig. 3.18 Elution profiles for (a) mixture of BAM-SiPc and LDL (molar ratio of BAM-SiPc to LDL is 1:10) (b) NAD^+ (0.625 nmol) (c) BAM-SiPc (0.2 nmol) (d) LDL (2 nmol). Mixture of BAM-SiPc and LDL was chromatographed on a smaller (1.8 x 9 cm) G-100 Sephadex column (molecular exclusion limit: 150 kDa) while the other Samples were chromatographed on a larger (1.8 x 21 cm) G-100 Sephadex column. In both situations, 20mM aqueous NH_4HCO_3 was used as eluent. Elution of LDL, BAM-SiPc and NAD^+ were monitored by the methods described in Section 2.16.

CHAPTER 4

Discussion

Since the unendurable side effects of using Photofrin® in cancer treatment have been reported, Pc was thought to be a potential replacement in the application of cancer treatment. While metal chelation to the central core of Pc was found to be effective in enhancing the photodynamic activities[52], Pc 4 was one of the most potent PS in killing cancer cells. In recent years, researchers have synthesized many different kinds of phthalocyanine derivatives in an attempt to further enhance the PDT efficacy of the phthalocyanine based PS. BAM-SiPc is a novel second generation phthalocyanine-based PS. Investigation on its photodynamic activities was carried out to test the potential use of BAM-SiPc for clinical application.

4.1 Anti-cancer effect of BAM-SiPc on different cancer cell lines

Long wavelength absorption maximum (> 670 nm), efficiency in producing singlet oxygen are the two major prerequisites for an ideal PS. In previous study, it has been shown that BAM-SiPc possesses these two properties and is not altered by the presence of the axial substitiuents (wavelength absorption maximum: 674 nm; singlet oxygen quantum yield, ϕ_Δ: 0.26)[47]. In terms of anti-cancer activities, BAM-SiPc exhibited potent phototoxicity on a variety of cancer cells including human hepatocarcinoma HepG2 and Hep3B, human colon adenocarcinoma HT29 and T84 and mouse macrophage J774[47] which has cancer-like properties. When the phototoxicity is compared, BAM-SiPc is superior to some of the well-known PS like ALA and Photofrin®. For example, the IC_{80} (i.e. the concentration of drug that results in 20% cell viability) of ALA and Photofrin® against HepG2 were 50 μgml^{-1} and 5

μgml^{-1}, i.e. about 0.3 mM and 4.41 μM respectively (light fluence was fixed at 25 Jcm^{-2})[53]. For BAM-SiPc, the IC_{80} against HepG2 was 0.04 μM (light fluence was fixed at 24 Jcm^{-2}) which was > 7000-fold and > 100-fold more potent than ALA and Photofrin® respectively. In addition, dark toxicity was exerted by ALA and Photofrin® when concentrations greater than IC_{80} were used but BAM-SiPc exhibited no dark toxicity as shown by the result of *in vitro* photodynamic activities assay. As BAM-SiPc exerts potent anti-cancer activities on a broad spectrum of cancer cell lines, it is a good candidate for testing in *in vivo* experiments.

4.2 Tissue distribution of BAM-SiPc in HepG2 bearing nude mice

Biodistribution study of BAM-SiPc was performed to evaluate the tumor selectivity and the retention time of the compound inside the host. It was believed that porphyrin with greater hydrophobicity could bind to the tumor tissue with higher affinity[54-56]. Thus, increasing the hydrophobicity of a PS will enhance its tumor selectivity. However, the steric factor of the compound should also be considered because the photodynamic efficacy of a PS will drop if there is a large bulky side chain which will hinder the uptake by tumor tissue[56]. On the other hand, some researchers had tried to test the potential use of a hydrophilic PS because hydrophobic compounds tend to have higher degree of aggregation which will decrease the phototoxicity of the compound. Although increasing the hydrophilicity of a PS can reduce the aggregation[47,57], it should be noted that hydrophilic PS will clear faster from the host and hence the accumulation by malignant tissue will decrease. Therefore, an ideal PS should have a balanced degree of hydrophobicity and hydrophilicity to compromise the problem of tumor selectivity, aggregation of the compound and the retention of PS in the host so that it could maximize the

phototoxicity to the malignant tissue but will not cause skin photosensitivity due to prolonged retention of PS.

The result of the biodistribution study, showed that BAM-SiPc has a high affinity to the lung and the reticulo-endothelial systems (Fig. 3.2a). It has long been suggested that PS were preferentially accumulated by reticulo-endotheial cells[58]. m-THPC and $mTPP(glu)_3$ are some examples which has been reported in some recent studies[59,60-61]. Brasseur *et al.* claimed that persistent retention of PS by the liver (73% ALClPc ID per gram of tissue for 1 week) could result in hepatic toxicity[62]. Although BAM-SiPc has preferential uptake in liver, a significant amount of BAM-SiPc could be removed from the liver within 24 h (Fig. 3.2a). It was almost completely cleared after 1 week (Fig. 3.2b). In view of such pharmacokinetic properties, hepatic toxicity due to BAM-SiPc was unlikely. However, it should be noted that such speculation should be accompanied by some intrinsic toxicity analyses which will be discussed in Section 4.5.

For the tumor, maximum accumulation of BAM-SiPc was found at 6 h after i.v. injection. The amount of BAM-SiPc accumulated in the HepG2 tumor was persistent even for 24 hr post-injection. At the same time, BAM-SiPc concentration in other organs/tissues dropped significantly except for skin. Since the tumor to tissue BAM-SiPc concentration ratio was better than that at 2 h post-injection, illumination was employed at this time. BAM-SiPc is an amphiphilic PS. At the beginning, it was expected that BAM-SiPc might have good selectivity in tumor uptake and exhibit high photoxicity towards the solid tumor. Although BAM-SiPc could persistently accumulate in HepG2 tumor, the uptake of BAM-SiPc by HepG2 tumor was relatively low (Fig. 3.2a). Such phenomenon may be accounted for by the elevated and rapid PS retention by the reticulo-endothelial system[62]. Regarding to the issue of

selective accumulation of PS in tumor, there were reports emphasizing that some PS could show an impressive tumor to organ/tissue uptake ratio. Chin *et al.* [63] has found that the ratio of Hypocrellin B (a PS) in MGH human bladder tumor versus muscle could be as high as 2.81 but the accumulation of Hypocrellin B in tumor was still lower than other organs/tissues such as liver, spleen and skin. In the study conducted by Masumoto *et al.* [64], amount of ATX-S10Na(II) (a PS) in Colon 26 carcinoma sustained the highest concentration at any time following ATX-S10Na(II) administration when compared with other organs/tissues. Brasseur *et al.* [62] used AlPc-PVA, an AlPc derivative, as a PDT agent in their study. They found that the tumor uptake of of AlPc-PVA could be as high as 15% ID per gram of tissue. Comparing to those findings, it was disappointed to observe that BAM-SiPc showed a relatively low tumor uptake (~ 2%) and low tumor to organ/tissue BAM-SiPc concentration ratio (< 1). This may render its clinical application inefficient[65]. Despite this disappointing finding, the amount of BAM-SiPc present in the tumor tissue could still be significant enough (> 2 nmol per gram of tissue) to exert phototoxicity to malignant tissue and cause tumor cell. death.

Skin photosensitivity can still be induced for up to weeks or months after administration of the commercially available PS[5, 66-67]. Comparatively, BAM-SiPc is a better PS because the rate of clearance of BAM-SiPc was much faster according to the result of biodistribution study. This will bring much convenience to the patient because patients' normal activities can resume a week after BAM-SiPc administration with a low risk of developing skin photosensitivity.

4.3 *In vivo* effect of BAM-SiPc mediated PDT on HepG2 and HT29 tumor growth

There are reports stating the successful application of PDT on eradicating or controlling the tumor growth in animal models. Whitacre *et al.* [20] found that Pc 4 mediated PDT could inhibit the growth of SW480 human colon cancer xenografts in athymic mice. Brasseur *et al.* [62] also reported that a significant growth delay of colon adenocarcinoma Colo-26 tumor could be observed after treating the tumor-bearing mice with PDT using AlPc or its derivatives. The anti-tumor efficacy of BAM-SiPc mediated PDT was evaluated by following the tumor growth for 15 days post-treatment. When HepG2 tumor was treated with BAM-SiPc or laser alone, HepG2 tumor remained unaffected, similar to the "no treatment" control group. A significant tumor regression was observed for the HepG2 tumor PDT treated with BAM-SiPc. The trend and the level of tumor regression (> 80%) may indicate that a complete eradication of HepG2 could be achieved by the dosage of drug and light used in this study (1 $\mu molkg^{-1}$ of BAM-SiPc, total fluence 30 Jcm^{-2}). Thus, BAM-SiPc or laser alone will not exert any cytotoxicity to the tumor cells but a lethal cytotoxicity will be produced when there is a combination of drug administration and illumination on target tissue.

Study about the effect of PDT on the growth of HT29 tumor was conducted in the past by some researchers. Hajri *et al.* [65] showed that a significant tumor growth delay for 3 week could be produced when the HT29 tumor-bearing athymic nude mice were photodynamically treated with Photofrin® and Pheophorbide a ($30mgkg^{-1}$ i.e. 26 $\mu molkg^{-1}$ and 50 $\mu molkg^{-1}$ of body weight for Photofrin® and Pheophorbide a respectively with the laser fluence at 100 Jcm^{-2}). Bourre *et al.* [68] also demonstrated that growth of HT29 tumor could be significantly delayed by PDT with the use of

diphenylchlorin PS (5 $mgkg^{-1}$ of body weight, i.e. 10 $\mu molkg^{-1}$ of body weight with laser fluence at 300 Jcm^{-2}). In our study, *in vivo* BAM-SiPc mediated PDT was also found to be effective in controlling the growth of HT29 tumor. There was a significant growth retardation of HT29 tumors for 10 days post-treatment for the PDT treated group while tumors for the three control groups remained unaffected and grew normally. In terms of dosage of the treatment, BAM-SiPc is better than Photofrin®, Pheophorbide a and diphenylchlorin PS because similar anti-tumor effect could be produced by PDT with BAM-SiPc at a lower drug dose and laser fluence.

In cancer treatment, chemotherapeutic drug can be divided into two classes, cytotoxic and cytostatic. Cytotoxic drugs are drugs that can directly kill the cancer cells while cytostatic drugs are those that can stop the cell from multiplying instead of inducing the cell death. Undoubtedly, BAM-SiPc mediated PDT exerted cytotoxic effect to HepG2 tumor as shown by the significant tumor regression. For HT29, BAM-SiPc mediated PDT seemed to display cytostatic effect because of the presence of tumor growth delay. However, it is more likely that growth retardation instead of regression may be due to a balance between the number of tumor cells died and the number of newly proliferated cells because of the instant cytotoxic effect exerted by ROS produced in PDT[2, 5]. For those tumor cells unaffected by BAM-SiPc mediated PDT treatment, they continued to proliferate and the size of the tumor increased again at 10 days after the treatment. Some tumor cells were unaffected by the treatment. This may be due to the fact that they are located deeply inside the tumor where the laser could not reach to activate BAM-SiPc. It might also be possible that those cells were resistant to PDT treatment. However, reports of PDT-resistant cells were only based on some *in vitro* studies[69-70]. Comparing the response for the treatment by HepG2 and HT29 tumors, BAM-SiPc mediated PDT appeared to be

more effective against HepG2 tumor than HT29 tumor. It could be due to the reason that HepG2 tumor was more efficient in accumulating BAM-SiPc. However, further investigation is necessary to understand why there is difference in the response in these two tumor models. Nevertheless, based on the result of *in vivo* PDT, it is well-demonstrated that BAM-SiPc mediated PDT is effective in controlling the progression of tumor in *in vivo* systems.

The dosage effect of BAM-SiPc and light was also investigated in this study. For the three doses of BAM-SiPc (1 $\mu molkg^{-1}$, 0.5 $\mu molkg^{-1}$, 0.25 $\mu molkg^{-1}$) was chosen in the experiments, only 1 $\mu molkg^{-1}$ could produce significant anti-tumor effect on both HepG2 and HT29 tumor. For the light dose experiment, anti-tumor effect was not obvious at 15 Jcm^{-2}. The laser energy transmitted to the tumor was inadequate and thus the cytotoxicity produced could be tolerated by the tumor cells and hence they survived. Although both 30 Jcm^{-2} and 60 Jcm^{-2} could exhibit significant anti-tumor effect, a burning scar was observed at the site of illumination a day after the treatment when the highest dose in this experiment was used. As there was no dramatic increase in temperature around the site of illumination, the formation of burning scar was likely to be due to photosensitization of the skin by laser with high fluence. Such dose appeared to be too drastic to the host and also the cosmetic effect was unfavourable that would take a very long time to heal. Thus, it was unsuitable to use in PDT treatment. The only optimum drug and light dose used in PDT with BAM-SiPc were thus 1 $\mu molkg^{-1}$ and 30 Jcm^{-2}.

4.4 Analysis of the safety of using BAM-SiPc as a potential agent in PDT

Haematoxylin is a base that will preferentially bind to the acidic components of the cell. Nucleic acids are the highly acidic components found in the nucleus. Thus, nucleus of the cells can be stained by haematoxylin and a dark purple colour will be given. On the contrary, eosin is an acid that will preferentially bind to the basic components of the cell. Many cytoplasmic constituents are basic in nature. Thus, cytoplasm can be stained by eosin in which a pinkish colour will be given. Haematoxylin staining can help identify the integrity of the nuclei structure while eosin serves as a counter stain to enhance the contrast of the nuclei staining. Thus, H & E staining of liver sections will allow us to investigate whether hepatic injury has been induced[71].

Since liver is the organ which accommodates the largest amount of BAM-SiPc, it was chosen for the analysis of the intrinsic toxicity induced by BAM-SiPc. Sinusoidal congestion, cytoplasmic vacuolization, hepatocellular necrosis and neutrophil infiltration are some general features of hepatic damage[72]. It has been reported that hepatic injury would be resulted with high dosage treatment of $ZnPcP_2S_2$ on Wistar rat[73]. Hepatic injury on Syrian golden hamster was also found when treated with veteporfrin combined with high light dose[74]. From the microscopic images of the liver sections, general features for hepatic injury, for example, hepatocellular necrosis, was not apparent for the mice treated with BAM-SiPc or light alone. Similarly, the integrity of the hepatocytes around the region of hepatic artery and its nuclear structure has preserved (Fig. 3.7) for the PDT-treated mice. Also, no significant neutrophil infiltration could be observed for the examined liver sections.

The level of plasma enzyme activities was also utilized as a marker for testing intrinsic toxicity has been induced. As most enzymes are predominantly present inside the cells but not in plasma, the level of plasma enzyme activities was often used as a marker for tracing any organ/tissue damage. ALT and AST are abundant in liver and heart while CK is abundant in cardiac muscle. Thus, ALT , AST and CK were used in this study to analyze whether there was hepatic or cardiac injury[75]. According to the result of enzyme activities assay, treatment with BAM-SiPc or light alone as well as the combined treatment did not induce any hepatic or cardiac injury. Thus, the present protocol of BAM-mediated PDT treatment did not induce any apparent intrinsic toxicity to the host.

Although toxicological analysis has only been done on heart and liver, it is believed that intrinsic toxicity on organs like spleen and kidney was unlikely because the amount of BAM-SiPc accumulated in these organs was lower compared with that in the liver. Thus, significant organ/tissue damage was not likely to be suffered when BAM-SiPc mediated PDT was used in anti-cancer treatment.

4.5 Metabolism of BAM-SiPc

It was found that the rate of uptake of BAM-SiPc gradually decreased with time. Maximal uptake and equilibrium could be achieved at 2 h after adding BAM-SiPc to HepG2 cells (Fig. 3.7). Based on the result, it was expected that the highest phototoxicity can be produced by incubating the cancer cells with BAM-SiPc for 2 h. The 2 h time point was also selected as the reference time point for the study of BAM-SiPc metabolism because it provided greatest sensitivity for the experiment.

In our study, the ability of metabolizing BAM-SiPc was compared between the cancer cells HepG2 and the liver cells WRL-68. It was found that the BAM-SiPc

inside HepG2 cells was not metabolized as indicated by the unchanged fluorescence intensity after 24 h of incubation. The result of incubating BAM-SiPc with the cell lysate was a control used to indicate that any reduction of fluorescence intensity of the sample was not due to chemical reaction or conjugation of BAM-SiPc with intracellular component. The inability in metabolizing BAM-SiPc can provide an explanation for the persistent retention of BAM-SiPc inside the HepG2 solid tumor. Hajri *et al.* [65] suggested that the amount of PS uptake and PS retention would be very different depending on different kinds of PS and tumoral models. In their study, they found that Photofrin® could retain longer inside the cells than pheophorbide a. For pheophorbide a, its concentration in colon cancer cell HT29 were still 3-fold higher than rat intestine cell IEC17 3 days after addition of PS. So, the result of the present study somehow agrees with their findings. In our study, there was reduction in fluorescence intensity when the liver cells WRL-68 taken with BAM-SiPc was further incubated for 24 h. It indicated that BAM-SiPc could be degraded by enzyme-catalyzed reaction or excreted outside from the intracellular compartments. The residual amount of BAM-SiPc and metabolite obtained by organic extraction was too minute for stud ying its *in vitro* photodynamic activity. So, there is no information about whether the metabolite is photoactive or not in this experiment.

One of the possibilities for the difference in metabolizing BAM-SiPc between HepG2 and WRL-68 cells might be that the abnormal intracellular environment of HepG2 cells provides an energy favourable environment for holding BAM-SiPc[14]. The other possibility is that enzymes responsible for metabolizing BAM-SiPc were defective or down-regulated in the cancer cells. BAM-SiPc was unable to be metabolized by HepG2 cells. This can also explain why the PS tends to selectively

accumulate in malignant tissues and persist longer than the normal tissue counterparts.

Studies of drug metabolism are often conducted to evaluate the efficiency for the drug clearance and also whether the drug has been detoxified or a toxic active metabolite has been produced. Drug metabolism often involves biochemical modification or degradation by a series of enzyme-catalyzed reactions. It includes two phases, Phase I and Phase II. Phase I drug metabolism involves chemical reactions such as oxidation, reduction, hydrolysis and cyclization, etc. These reactions are catalyzed by several enzyme systems, mainly the Cytochrome P450 enzyme system. Phase II drug metabolism mainly involves conjugation reactions such as conjugation with glucuronic acid, sulfonates, etc. When the metabolite of the drug after the Phase I reaction is not polar enough for excretion, Phase II reactions will then be carried out to conjugate the drug with a more polar molecule. Metabolite after Phase II reaction will then be readily excreted[76].

Investigation on the metabolism of PS has been conducted for many years. Reports about the metabolism of Photofrin could be traced back to more than a decade ago. Bellnier *et al.* [77] found that Photofrin II was very difficult to be metabolized *in vivo* using DBA/2 Ha-DD mice as the animal model. They also suggested that Photofrin II was primarily excreted through the bile gut pathway. Whelpton *et al.* [78] suggested that 5, 10, 15, 20-tetra [m-hydroxyphenyl] chlorine (m-THPC) could be photochemically oxidized to a polar, hydroxylated derivative and could be detected in the faeces. However, it was later found to be an artifact generated during sample administration, collection, preparation and extraction. They have reported that m-THPC was actually unable to be metabolized and no metabolites could be detected by means of HPLC-electrospray mass spectrometry[79].

Desroches *et al* .[59] and Bellnier *et al.* [80] both have similar claims in their recent studies. For example, Descroches *et al.* [59] has found that m-THPC derivatives were unable to be metabolized in mice while Bellnier *et al.* [80] suggested that no metabolite could be detected in the patient infused with pyropheophorbide-a derivatives or by incubating such derivatives with pooled human microsomes.

In the present study, BAM-SiPc was incubated with mice liver homogenate for the investigation of metabolism of BAM-SiPc. Mice liver homogenate was chosen to mimic the actual situation of the BAM-SiPc metabolism inside the liver. According to the result, BAM-SiPc content decreased with increasing time of incubation. It indicated that BAM-SiPc was metabolized by the native liver homogenate in a time-dependent manner. BAM-SiPc content remained constant when the liver homogenate was first subjected to heat denaturation. It suggested that the reduction in BAM-SiPc content was due to enzyme-catalyzed degradation as all the enzyme activities should be virtually abolished after the heat treatment.

In contrast to many previous reports, BAM-SiPc was found to be metabolized by cultured normal liver cells and mice liver homogenate. However, the metabolite of BAM-SiPc could still be toxic to the host. Also, skin photosensitivity will still be suffered by the patient if the metabolite is photoactive. Laville *et al.* [81, 82] proposed that some PS derivatives could be metabolized by *in vitro* cultured cancer cells and also in an *in vivo* situation. They found that the glycosidic bonds of glycoconjugated porphyrins or chlorin$_{e6}$ could be cleaved by endogenous glycosidases present inside the cancer cells, thus releasing the free porphyrin or chlorin. In that case, phototoxicity could still be induced though the biochemical properties of the PS such as subcellular localization and rate of clearance would be altered. In the present investigation, the metabolite of BAM-SiPc after incubating with liver homogenate

was recovered by organic extraction. It was analyzed by the *in vitro* photodynamic activities assay. It was found that the metabolite was non-toxic both in the dark and in the presence of illumination. Since a non-discriminative extraction method was employed in this study, many difficulties have to be overcome (e.g. the purity of the target compound). At the moment, the metabolite has not been identified. It was not known whether detoxification of BAM-SiPc was by the chemical modification in Phase I reaction or by the conjugation of polar molecules which inactivates the photosensitizing property of BAM-SiPc in Phase II reaction. In the future, liquid chromatography and MALDI-TOF mass spectrometry can be used to trace the identity of the metabolite and that will enable us to understand the detail for the metabolism of BAM-SiPc in liver[79, 81-82]. Nevertheless, combining this finding with the result of the biodistribution study, it is expected that the risk of suffering any adverse side effect is low for the patients administered with BAM-SiPc in PDT.

4.6 Mechanism of the apoptosis triggered by BAM-SiPc mediated PDT

PDT can induce cell death either by apoptosis or necrosis depending on factors such as the dose of drug and light used in the treatment[83-84]. While singlet oxygen is widely accepted as the major cytotoxic agent produced in PDT, the subsequent generation of ROS such as hydroperoxide, superoxide anion and oxygen free radicals can also play a crucial role in inducing cell death[2, 5-6]. In the present study, the DCFDA assay was employed to determine the intracellular ROS production by BAM-SiPc mediated PDT. DCFDA can only be deacetylated by intracellular esterase to 2',7'-dichlorofluorescein (DCF). It is known that DCF does not detect singlet oxygen but rather react with hydroperoxides to give the characteristic fluorescence.

Thus, ROS which has been measured in this study reflected the formation of ROS species by the reaction of singlet oxygen formed earlier after PDT with other molecules[50, 85].

Many studies have reported the role of ROS in inducing cell death. For example, the ROS overproduction induced by p53 over-expression can trigger the downstream pathway of mitochondria-mediated apoptosis[86, 87]. In PDT, the sudden increase in intracellular oxidative stress leads to the oxidation of cellular proteins. These oxidized cellular proteins serve as a death signal to trigger a series of pro-apoptotic events. Lam *et al.* [88] used Pc 4 mediated PDT to trigger apoptosis in the epidermoid carcinoma cells A431. They found that the mitochondrial ROS produced subsequent to PDT treatment would induce mitochondrial inner membrane permeabilization and lead to cell death after a series of downstream events. In the present study, BAM-SiPc mediated PDT could immediately increase the intracellular ROS production in the cancer cell lines (HepG2, Hep3B and HT29). The dose-dependent curves for the survival of the tested cancer cell lines correlated well with ROS production. When comparing the ROS production for each cancer cells with its IC_{50} values of BAM-SiPc, the results were correlated as well. As stated in Section 3.1, the susceptibility of the cancer cells used in this study is in the following order: HT29 > HepG2 > Hep3B which followed the same order for the intracellular ROS production (HT29, > 4-fold; HepG2, > 3-fold; Hep3B, > 2-fold). The difference in the susceptibility to BAM-SiPc mediated PDT for each cancer cell line might be due to their difference in the resistance to oxidative damage. Such phenomenon correlates with the ability of the cell to cope with intracellular oxidative stress, in other words, the efficiency of the cells to scavenge intracellular ROS by the anti-oxidation machinery. Magi *et al.* [85] suggested that the reduced glutathione (GSH)

content is one of the factors which is important for scavenging the ROS produced after PDT. It could also be one of the reasons why there was difference in the susceptibility of the cancer cells towards BAM-SiPc mediated PDT. A more detailed study on screening the potential cellular proteins targeted by BAM-SiPc mediated PDT could be performed to elucidate the signaling events involved in PDT-mediated apoptosis. In some recent studies, several proteins have been identified as the potential target, for example tubulin, β-actin, HSP (heat shock protein) 60, HSP 70, etc. Extensive carbonylation is often found in these proteins after PDT[85, 89].

Some researchers had proposed that apoptosis induced by PDT was a result of cell cycle arrest. Ahmad *et al.* [90] had utilized Pc 4 mediated PDT on A431 cells to study the mechanism of PDT induced cell death. They discovered that there was a significant cell cycle arrest in G_0/G_1 phase and concomitant decrease of cell number in the S-phase. In the same study, they suggested that the occurrence of cell cycle arrest was due to the upregulation of a cyclin kinase inhibitor, namely WAF1/CIP1/p21 which is the key-regulator of G_1 checkpoint to S-phase. Down-regulation of G_1-phase cyclins, cyclin D, cyclin E, cdk2 (cyclin dependent kinase 2) and cdk6 were observed and accompanied by the upregulation of WAF1/CIP1/p21. Cell cycle arrest was finally induced. In a later study, Ahmad *et al.* [91] have also found the involvement of Retinoblastoma (pRb) and E2F family transcription factors (E2F), DP1 and DP2 in Pc 4 mediated cell cycle arrest. Combining with the evidence of the involvement of increased production of nitric oxide species (·NO) [92], they have proposed a model for the Pc 4 mediated cell cycle arrest (Fig. 4.1). Haywood-Small *et al.* [93] had also found that cell cycle arrest in G_0/G_1 phase was also induced when human cervical carcinoma cells SiHa were treated with ZnPc derivatives mediated PDT. In consensus to the findings of Ahmad *et al.* [91] and Haywood-Small *et al.* [93],

cell cycle arrest in G_0/G_1 phase could be detected when HepG2 cells were PDT treated with BAM-SiPc at concentration lower than 0.02 μM. Although the magnitude of the cell cycle arrest of HepG2 cells found in this study (8% compared with solvent control group) was less than that of the Pc 4 – PDT treated A431 cells (> 25% compared with the control), it was convincing to believe that apoptosis triggered by BAM-SiPc mediated PDT was a result of cell cycle arrest. When a BAM-SiPc concentration greater than 0.02 μM was used, significant amount of necrotic or apoptotic cells could be observed one day after PDT treatment. It could be due to the drastic increase in oxidative stress that resulted in extensive protein oxidation. Those oxidized proteins would immediately trigger the apoptotic response. Another possible reason is that ROS floods inside the cells which cause serious and irreversible damage to cell, leading to necrosis. However, such speculation is quite preliminary. It should also be noted that unsynchronized cells were used in this experiment. Experiment should be repeated in order to confirm such speculation and Western blot analysis on cell cycle related proteins should be done to elucidate the intracellular signaling events involved in BAM-SiPc photodynamic therapy mediated apoptosis.

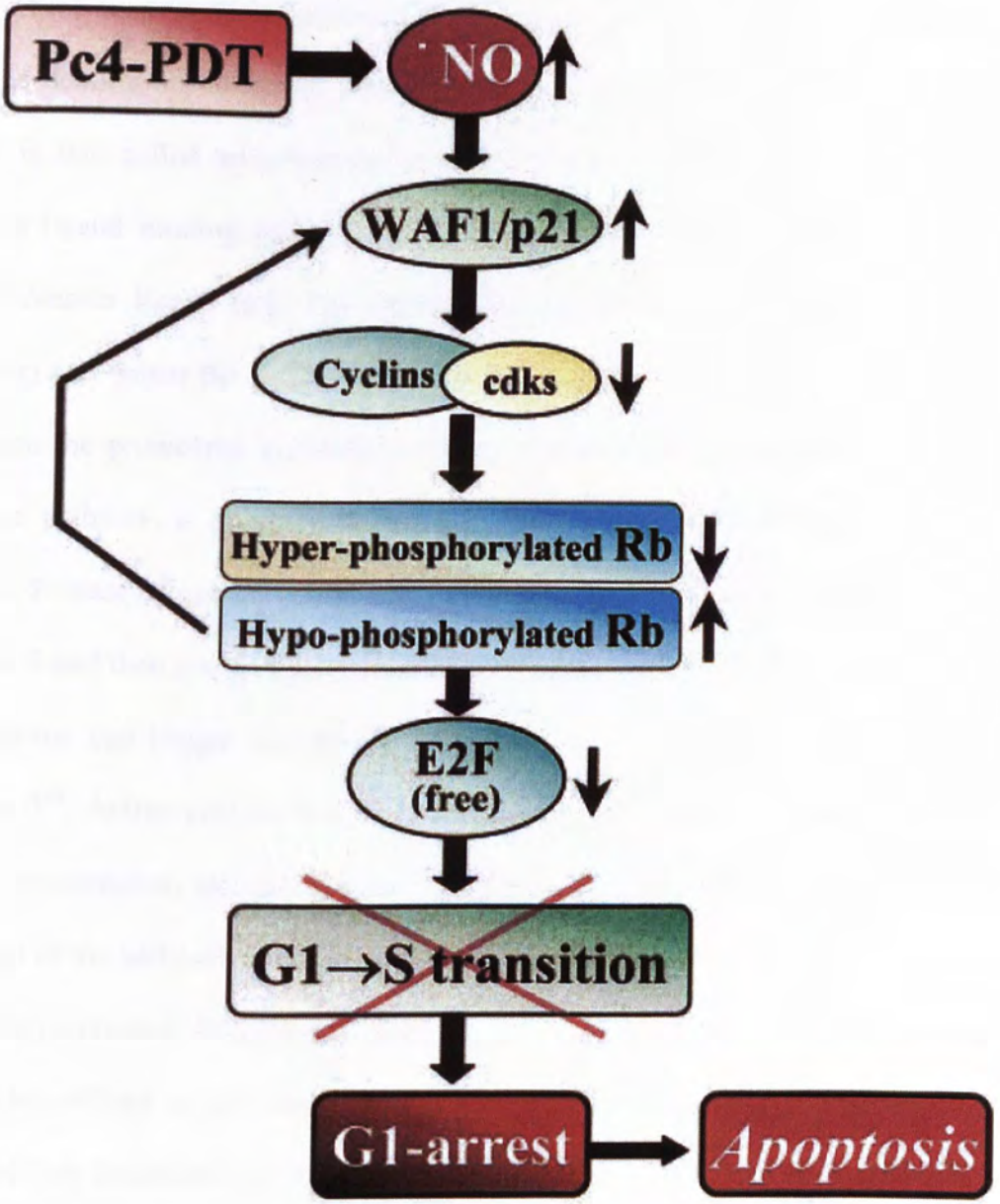

Fig. 4.1 Schematic diagram for proposed model of Pc 4 mediated PDT cell cycle arrest. (Ahmad *et al.*, 1999)

4.7 Death mechanism induced by *in vivo* PDT with BAM-SiPc

There are two major pathways for triggering apoptosis: the extrinsic pathway, i.e. the death receptor ligand binding induced apoptosis and the intrinsic pathway which is also called mitochondria-mediated apoptosis. Extrinsic pathway or death receptor-ligand binding pathway, as the name implies, involves the binding of a death receptor ligand (e.g. Fas ligand) with the death receptor (e.g. Fas-APO-1 receptor) and forms the death inducing signaling complex (DISC). DISC will then stimulate the proteolytic maturation of pro-caspase 8 to active caspase 8. For the intrinsic pathway, it involves the release of cytochrome C from mitochondria to cytosol. Release of cytochrome C will trigger the Apaf-1-mediated activation of pro-caspase 9 and then result in the formation of apoptosome. Both active caspase 8 and apoptosome can trigger the proteolytic cleavage of pro-caspase 3 to form active caspase 3[94]. Active caspase 3 is essential for late stage apoptotic response such as DNA fragmentation and cell surface blebbing[95]. These morphological changes are regarded as the hallmark features of apoptosis.

As mentioned, DNA fragmentation is one of the hallmark features of apoptosis. It can be utilized as an indicator for apoptosis. Double-stranded, low molecular weight DNA fragments and single strand breaks will be produced during the DNA fragmentation in apoptosis. The fragmented DNA could be recognized by terminal deoxynucleotidyl transferase (TdT), which catalyzes the polymerization of nucleotides to free 3'-OH end of the DNA. Incorporation of the fluorescence labels such as fluorescein isothiocyanate (FITC) can help to reveal the presence of these fragmented DNA. Cells which are undergoing late stage apoptosis would be indicated by the green fluorescence nuclei viewed under fluorescence microscope. In previous study, Lai *et al.*[50] suggested that *in vitro* BAM-SiPc mediated PDT could

induce apoptosis in HepG2 cells as shown in the TUNEL assay and the release of pro-apoptotic cyctochrome C to cytosol. However, it is not known whether apoptosis would also be triggered by *in vivo* PDT with BAM-SiPc under our experiment protocol. From the result of the present TUNEL assay, a large amount of TUNEL positive nuclei were observed when the HepG2 tumors were subjected to the combined treatment while only negligible positive signal could be detected for the three control groups. Thus, DNA fragmentation was only triggered by *in vivo* BAM-SiPc mediated PDT but not by BAM-SiPc or illumination alone.

At late stage apoptosis, cellular and nuclear shrinkage, chromatin condensation and prominent nuclear fragmentation with formation of apoptotic bodies can be observed[94, 96]. From the result of H & E staining, nuclear fragmentation could only be observed for the PDT-treated HepG2 tumor (Fig. 3. 16). This confirmed that apoptosis was triggered in HepG2 tumors by *in vivo* BAM-SiPc mediated PDT, though, whether it involved the intrinsic or extrinsic pathway has yet to be determined. In the *in vitro* experiment, it was suggested that mitochondria-mediated apoptosis (intrinsic pathway) played a major role in switching on the apoptosis in HepG2 cells[50]. It is expected that similar signaling pathway will also be induced in the *in vivo* situation.

4.8 Phototoxicity of BAM-SiPc was inhibited in the present of LDL

It has been suggested that addition of LDL with PS can enhance the PS uptake by tumor and hence the PDT efficacy will increase[38]. This hypothesis is supported by the fact that over-expression of LDL receptor is often found in cancer cells[97, 98]. Some researchers also believe that the enhanced photodynamic efficacy of a PS by LDL conjugation is due to the fact that LDL-conjugated PS would facilitate the

delivery to more photosensitive subcellular compartment such as mitochondria[99-101]. Since the tumor uptake of BAM-SiPc was low as shown in the tissue distribution study (Section 3.2), BAM-SiPc was mixed with LDL to see whether the uptake and hence the photodynamic activity would be increased. To our disappointment, phototoxicity of *in vitro* BAM-SiPc mediated PDT against HepG2 actually decreased with the addition of LDL (Fig. 3.18). One possible reason is that the uptake of BAM-SiPc by HepG2 cells was inhibited in the presence of LDL. Another possibility is that the introduction of LDL altered the intracellular trafficking of BAM-SiPc such that it was delivered to a site less susceptible to PDT damage[34, 101]. Our preliminary result showed that there was a 50% reduction of BAM-SiPc uptake in the presence of LDL (data not shown). The decrease in BAM-SiPc uptake could be either due to the inhibition by LDL or the covalent linkage of BAM-SiPc with the apolipoprotein of LDL resulted in reduced receptor recognition as suggested by Urizzi *et al* [34].

Initially, a small scale gel filtration was employed in an attempt to separate free BAM-SiPc and LDL-bound BAM-SiPc. It was thought that the resolution provided by the column was adequate to achieve the separation because the molecular size of LDL is much greater than that of BAM-SiPc (Molecular size of BAM-SiPc and LDL were 717.89 and 2.25 X 10^6 respectively). The elution profile showed that the peaks for LDL and BAM-SiPc overlapped with each other. However, the peak representing free BAM-SiPc was missing in the elution profile. It might be possible that all BAM-SiPc was conjugated with LDL or the resolution of the gel filtration was not good enough to separate BAM-SiPc from LDL. To test this, a larger gel filtration column was used. Again, free BAM-SiPc failed to resolve from free LDL and LDL conjugated BAM-SiPc. It might be due to the aggregation of BAM-SiPc in aqueous solution. Molecular size of the aggregated BAM-SiPc could

be too large and exceeded the size exclusion limit (1.5×10^5) for the G-100 Sephadex gel filtration column. Hence, BAM-SiPc was eluted together with LDL in the void volume. So, gel filtration chromatography of the mixture of BAM-SiPc and LDL was unable to confirm whether LDL has been conjugated with BAM-SiPc in this experiment. Nevertheless, LDL was found to be unable to enhance BAM-SiPc uptake by HepG2 cells and hence the PDT efficacy in our study. As cancer cells often have extra glucose demand to fulfill their energy requirement, conjugation with saccharides can be a possible solution to improve the uptake of BAM-SiPc. Chen *et al.* [102] has successfully improve the tumor selectivity of porphyrin-based PS by conjugation with thioglucose or thiogalactose. Recently, researchers have tried to develop tumor specific antibody conjugated PS to increase the tumor selectivity of a PS because the conjugated antibody can specifically recognize the cancer cells and can be easily derived from antibody phage display library[103]. Such method may help to solve the problem of poor tumor selectivity of BAM-SiPc.

CHAPTER 5

Conclusion and Future Perspective

5.1 Conclusion

Subsequent to the previous study of a novel series of silicon(IV) phthalocyanine derivatives, we have reported in the present study the *in vitro* and *in vivo* photodynamic activities of BAM-SiPc. BAM-SiPc was found to exhibit an extremely high phototoxicity against a wide variety of cancer cells including human hepatocellular carcinoma HepG2 and Hep3B, human colon adenocarcinoma HT29 and T84. Such phenomenon could be attributed to the efficient intracellular ROS production by BAM-SiPc mediated PDT. A dose-dependent cytotoxicity was exerted by PDT with BAM-SiPc, which was also well correlated with the intracellular ROS production as shown by the result of DCFDA assay.

In the *in vivo* study, although there was a persistent accumulation of BAM-SiPc in tumor for 24 h, it was disappointed to observe that the tumor selectivity for BAM-SiPc was low. Despite these, significant regression of HepG2 tumor and growth retardation on HT29 tumor could be clearly seen when they were treated with *in vivo* PDT using BAM-SiPc.

Concerning the death mechanism induced by PDT with BAM-SiPc, preliminary result revealed that cell cycle arrest was induced for BAM-SiPc concentrations between 0.005 μM and 0.02 μM in *in vitro* study. Late stage apoptotic or necrotic change was observed with BAM-SiPc concentrations greater than 0.02 μM. Results of TUNEL assay and H & E histochemical staining revealed that

apoptosis was also induced in HepG2 tumor when the tumor-bearing nude mice were treated with BAM-SiPc mediated PDT.

The phototoxicity against HepG2 cells was reduced in the presence of LDL which could be due to the inhibition of cellular uptake of BAM-SiPc by LDL. However, it has not yet known whether the reduced uptake was due to competitive inhibition of LDL or reduced receptor recognization because of the altered chemical structure by the conjugation to apolipoprotein B. Identification of the presence of LDL-conjugated BAM-SiPc by means of gel filtration chromatography failed. It is because LDL could not be separated from BAM-SiPc. BAM-SiPc aggregated together and was eluted in void volume with LDL. Owing to the fact that the tumor selectivity of BAM-SiPc is low, it is necessary to search for another biomolecule to conjugate with BAM-SiPc or a chemical modification of BAM-SiPc so that the BAM-SiPc uptake by tumor can be enhanced.

In the present study, it was shown that BAM-SiPc can be a potential phthalocyanine-based agent used in clinical PDT for cancer treatment. On the other hand, the present study also provides the foundation for the future development of novel PS, highly active in terms of photodynamic activities but with minimal side effect.

5.2 Future perspective

- ***Eradication of HT29 tumor by repeated PDT treatment with BAM-SiPc***

In *in vivo* PDT, growth retardation on HT29 tumor was observed for 10 days when a single dose of BAM-SiPc was administered to the tumor-bearing nude mice. It is worth to study whether complete eradication of HT29 tumor can be achieved if a repeated treatment of BAM-SiPc mediated PDT is applied at time before the normal

growth of the tumor resumed.

- ***Enhance BAM-SiPc uptake by conjugating with alternate biomolecules***

Since LDL failed to enhance the PDT efficacy of BAM-SiPc, it is necessary to search for other biomolecules such as glucose or insulin[35] for conjuga tion with BAM-SiPc in order to enhance the tumor uptake of BAM-SiPc and hence the PDT efficacy of BAM-SiPc in an *in vivo* system.

- ***Investigation on the intracellular signaling pathway involved in BAM-SiPc mediated PDT induced cell death***

PI staining for cell cycle distribution after PDT with BAM-SiPc should be repeated to confirm the results because cell cycle arrest found in the present study was only a preliminary finding. If it is confirmed, Western blotting for the cell cycle proteins such as cdk2, cyclin D and cyclin E should be done to unveil the possible intracellular signaling events involved in the cell death induced by *in vitro* PDT.

PDT can drastically increase the oxidative stress inside the cells. It has been reported that the intracellular oxidative stress induced by PDT can lead to oxidation or carbonylation of cellular proteins[85, 89]. These oxidized or carbonylated proteins can serve as a signal that triggers apoptosis. Therefore, the amount of oxidized protein formed after PDT with BAM-SiPc can be determined to see if oxidized protein plays an important role in PDT induced cell death. Proteomic analysis on the differential expression of oxidized protein will also provide information on the identity of those oxidized proteins which trigger cell death.

- ***Identification of the metabolite of BAM-SiPc***

In the present study, the identity of metabolite was not yet known. Liquid Chromatography-Mass Spectrometry (LC-MS) could be used so that the chemical structure of the metabolite can be speculated[104]. Based on the chemical structure of the metabolite, we can get an insight on the pathway involved in metabolism of BAM-SiPc.

- ***Anti-tumor immunity related to BAM-SiPc mediated PDT***

PDT can kill the cancer cells by directly inducing cell death and/or shutting down the tumor vasculature which deprives the tumor oxygen and nutrients[104, 105]. Recently, there is much evidence showing that the immune response subsequent to PDT treatment also contributes to cancer cell death. It has been suggested that the apoptotic or necrotic cells formed by PDT will trigger the acute inflammatory response. Neutrophil infiltration and cytokine production such as IL-6, IL10, tumor-necrosis factor-α (TNF-α) are the events which have been linked to tumor cell death[106]. In the future, study on the anti-tumor immunity induced by BAM-SiPc mediated PDT will provide insights on whether acute inflammatory responses mentioned above are induced by BAM-SiPc alone or PDT with BAM-SiPc.

References

1. Lane, N. (2003). New light on medicine. *Scientific American*. 288: 38-45.
2. Dolmans, D. E., Fukumura, D., Jain, R. K. (2003). Photodynamic therapy for cancer. *Nature Review. Cancer*. 3:380-387.
3. Tappeiner, H., Jesionek, A. (1904). Therapeutische versuche mit fluoreszier enden stoffe. *Muench. Med. Wochschr*. 1: 2042-2044.
4. Jesionek, A., Tappeiner, H. (1904). Zur behandlung der haufcarcinome mit fluorescierenden stiffen. *Deut. Arch. Klin. Med*. 82: 223-227.
5. MacDonald, I. J., Dougherty, T. J. (2001). Basic principles of photodynamic therapy. *Journal of Porphyrins and Phthalocyanines*. 5:105-129.
6. Lipson, R. L., Baldes, E. J., Olsen, A. M. (1961). The use of hematoporphyrin in tumor detection. *Journal of The National Cancer Institute*. 26:1-11.
7. Dougherty, T. J. (1974). Activated dyes as antitumor agents. *Journal of The National Cancer Institute*. 52:1333-1336.
8. Rouhi, A. M. (1998). Let there be light and let it heal. *Chemical & Engineering News*. 76:22-27.
9. Moseley, H., Allen, J. W., Ibbotson, S., Lesar, A., McNeill, A., Camacho-Lopez, M. A., Samuel, I. D. W., Sibbett, W., Ferguson, J. (2006). Ambulatory photodynamic therapy: a new concept in delivering photodynamic therapy. *British Journal of Dermatology*. 154: 747-750.
10. Brown, S. B., Brown, E. A., Walker, I. (2004). The present and future role of photodynamic therapy in cancer treatment. *Lancet Oncology*. 5: 497-508.
11. Richter, A.M., Cerruti-Sola, S., Sternberg, E. D., Dolphin, D., Levy, J. G. (1990). Biodistribution of tritiated benzoporphyrin derivative (^{3}H-BPD-MA), a potent photosensitizer, in normal and tumor bearing mice. *Journal of Photochemistry and Photobiology. B: Biology*. 5:231-244.
12. Brown, S.D., Mellish, K.J. (2001). Verteporfin: a milestone in ophthalmology and photodynamic therapy. *Expert Opinion on Pharmacotherapy*. 2:351-361
13. Messmer, K., J., Abel, S. R. (2001). Verteporphyrin for age-related macular degeneration. *Annals of Pharmacotherapy*. 35: 1593-1598.
14. Dougherty, T. J., Gomer, C. J., Henderson, B. W., Jori, G., Kessel, D., Korbelik, M., Moan, J., Peng, Q. (1998). Photodynamic Therapy. *Journal of The National Cancer Institute*. 90: 889-905.
15. Kuebuler, A., Hasse, T., Staff, C., Kahle, B., Rheinwald, M., Muhling, J. (1999). Photodynamic therapy of primary nonmelanomatous skin tumors of the head

and neck. *Lasers in Surgery and Medicine*. 25:60-68.

16. Allemann, E., Brasseur, N., Kudrevich, S. V., Madeleine, C. L., Van Lier, J. E. (1997). Photodynamic activities and biodistribution of fluorinated zinc phthalocyanine derivatives in the murine EMT-6 tumor model. *International Journal of Cancer*. 72: 289-294.
17. Fabris, C., Soncin, M., Miotto, G., Fantetti, Chiti, G., Dei, d., Roncucci, G., Jori, G. (2006). Zn(II)-phthalocyanines as phototherapeutic agents for cutaneous diseases. Photosensitization of fibroblasts and keratinocytes. *Journal of Photochemistry and Photobiology, B: Biology*. 83: 48-54.
18. Artarsky, S., Dimitrova, S., Bonnett, R., Krysteva, M., (2006). Immobilization of zinc phthalocyanines in silicate matrices and investigation of their photobactericidal effect on *E. coli*. *Scienctific World Journal*. 6: 374-82.
19. George, J. E. 3rd, Ahmad, Y., Varghai, D., Li. X., Berlin, J., Jackowe, D., Jungermann, M., Wolfe, M. S., Lilge, L., Totonchi, A., Morris, R. L., Peterson, A., Lust, W. D., Kenney, M. E., Hoppel, C. L., Sun, J., Oleinick, N.L., Dean, D. (2005). Pc 4 photodynamic therapy of U87-derived human glioma in the nude rat. *Lasers in Surgery and Medicine*. 36: 383-389.
20. Whitacre, C. M., Feyes, d. K., Satoh, T., Grossmann, J., Mulvihill, J. W., Mukhtar, H., Oleinick, N. L. (2000) Photodynamic therapy with the phthalocyanine photosensitizer Pc 4 of SW480 human colon cancer xenografts in athymic mice. *Clinical Cancer Research*. 6: 2021-2027.
21. Colussi, V. C., Feyes, D.K., Mulvihill, J. W., Li, Y. S., Kenney, M. E., Elmets, C. A., Oleinick, N. L., Mukhtar, H. (1999). Phthalocyanine 4 (Pc 4) photodynamic therapy of human OVCAR-3 tumor xenografts. *Photochemistry and Photobiology*. 69: 236-41.
22. Borgatti-Jeffreys, A., Hooser, S. B., Miller, M. A., Lucroy, M. D. (2007). Phase I clinical trial of the use of zinc phthalocyanine tetrasulfonate as a photosensitizer for photodynamic therapy in dogs. *American Journal of Veterinary Research*. 68: 399-404.
23. Boyle, R. W., Dolphin, D. (1996). Structure and biodistribution relationships of photodynamic sensitizers. *Photochemistry and Photobiology*. 63: 469-485.
24. Hilf, R., Warne, N. W., Smail, D. B., Gibson, S. L. (1984). Photodynamic inactivation of selected intracellular enzymes by hematoporphyrin derivative and their relationship to tumor cell viability *in vitro*. *Cancer Letter*. 24: 165-172.
25. Singh, G., Jeeves, W. P., Wilson, B. C., Jang, D. (1987). Mitochondrial photosensitization by Photofrin II. *Photochemistry and Photobiology*. 46:

645-659.

26. Chatterjee, S. R., Srivastava, T. S., Kamat, J. P., Devasagayam, T. P. A. (1997). Lipid peroxidation induced by novel porphyrin plus light in isolated mitochondria: possible implications in photodynamic therapy. *Molecular and Cellular Biochemistry*. 166: 25-33.
27. Margaron, P., Gregoire, M., Scasnar, V., Ali, H., Van Lier, J. E. (1996). Structure-photodynamic activity relationships of a series of 4-substituted zinc phthalocyanines. *Photochemistry and Photobiology*. 63: 217-223.
28. Cauchon, N., Tian, H., Langlois, R., La Madeleine, C., Martin, S., Ali, H., Hunting, D., Van Lier, J. E. (2005). Structure-photodynamic activity relationships of substituted zinc trisulfophthalocyanines. *Bioconjugate Chemistry*. 16: 80-89.
29. Brasseue, N., Langlois, R., La Madeleine, C., Ouellet, R., Van Lier, J. E. (1999). Receptor-mediated targeting of phthalocyanines to macrophages via covalent coupling to native or maleylated bovine serum albumin. *Photochemistry and Photobiology*. 69: 345-352.
30. Hamblin, M. R., Miller, J. L., Ortel, B. (2000). Scavenger-receptor targeted photodynamic therapy. *Photochemistry and Photobiology*. 72: 533-540.
31. Huang, J. D., Fong, W. P., Chan, E. Y. M., Choi, M. T. M., Chan, W. K., Chan, M. C., Ng, D. K. P. (2003). Photodynamic activities of a dicationic silicon(IV) phthalocyanine and its bovine serum albumin conjugates. *Tetrahedron Letters*. 44: 8029-8032.
32. Polo, L., Valduga, G., Jori, G., Reddi, E. (2002). Low-density lipoprotein receptors in the uptake of tumor photosensitizers by human and rat transformed fibroblasts. *The international Journal of Biochemistry & Cell Biology*. 34: 10-23.
33. Schmidt-Erfurth, U., Diddens, H., Birngruber, R., Hasan, T. (1997). Photodynamic targeting of human retinoblastoma cells using covalent low-density lipoprotein conjugates. *British Journal of Cancer*. 75: 54-61.
34. Urizzi, P., Allen, C. M., Langlois, R., Ouellet, R., La Madeleine, C., Van Lier, J. E. (2000). Low-density lipoprotein-bound aluminium sulfophthalocyanine: targeting tumor cells for photodynamic therapy. *Journal of Porphyrins and Phthalocyanines*. 4: 1-7.
35. Sharman, W. M., Van Lier, J. E., Allen, C. M. (2004). Targeted photodynamic therapy via receptor mediated delivery systems. *Advanced Drug Delivery Systems*. 56: 53-76.
36. Akhlynina, T. V., Rosenkranz, A. A., Jans, D. A., Sobolev, A. S. (1995) Insulin-mediated intracellular targeting enhances the photodynamic activity of

chlorine e6. *Cancer Research*. 55: 1014-1019.

37. Akhlynina, T. V., Jans, D. A., Rosenkranz, A. A., Statsyuk, N. V., Balashova, I. Y., Toth, G., Pavo, I., Rubin, A. B., Sobolev, A. S. (1997). Nuclear targeting of chlorine e6 enhances its photosensitizing activity. *Journal of Biological Chemistry*. 272: 20328-20331.
38. Sobolev, A. S., Jans, D. A., Rosenkranz, A. A. (2000). Targeted intracellular delivery of photosensitizers (review). *Progress in Biophysics & Molecular Biology*. 73:51-90.
39. DeClerck, Y. A., Mercurio, A. M., Stack, M. S., Chapman HA, Zutter MM, Muschel RJ, Raz A, Matrisian LM, Sloane BF, Noel A, Hendrix MJ, Coussens L, Padarathsingh M. (2004). Proteases, extracellular matrix, and cancer: a workshop of the path B study section. *American Journal of Pathology*. 164: 1131-1139.
40. Koblinski, J. E., Ahram, M., Sloane, B. F. (2000). Unraveling the role of proteases in cancer. *Clinica Chimica Acta.* 291: 113-35.
41. Lynch, C. C., L. M., Matrisian, L. M. (2002). Matrix metalloproteinases in tumor-host cell communication. *Differentiation*. 70: 561-73.
42. Choi, Y., Weissleder, R., Tung, C. H. (2006). Selective antitumor effect of novel protease-mediated photodynamic agent. *Cancer Research*. 66: 7225-7229.
43. Zamora-León, S. P., Golde, D. W., Concha, I. I., Rivas, C. I., Delgado-López, F., Baselga, J., Nualart, F., Vera, J. C. (1996). Expression of the fructose transporter GLUT5 in human breast cancer. *Proceedings of the National Academy of Sciences, USA*. 93: 1847-1852
44. Kumamoto, K., Goto, Y., Sekikawa, K., Takenoshita, S., Ishida, N., Kawakita M., Kannagi, R. (2001). Increased expression of UDP-galactose transporter messenger RNA in human colon cancer tissues and its Implication in Synthesis of Thomsen-Friedenreich Antigen and Sialyl Lewis A/X Determinants. *Cancer Research*. 61: 4620-4627.
45. Lo, P. C., Huang, J. D., Cheng, D. Y. Y., Chan, E. Y. M., Fong, W. P., Ko, W. H., Ng, D. K. P. (2004). New amphiphilic silicon(IV) phthalocyanines as efficient photosensitizers for photodynamic therapy: synthesis, photophysical properties, and *in vitro* photodynamic activities. *Chemistry: A European Journal*. 10: 4831-4838.
46. Chandler, J. D., Williams, E. D., Slavin, J. L., Best, J. D., Rogers, S. (2003). Expression and localization of GLUT1 and GLUT12 in prostate carcinoma. *Cancer*. 97: 2035-2042.
47. Lo, P. C., Leung, S. C. H., Chan, E. Y. M., Fong, W. P., Ko, W. H., Ng, D. K. P. (2007). Photodynamic effects of a novel series of silicon(IV) phthalocyanines

against human colon adenocarcinoma cells. *Photodiagnosis and Photodynamic Therapy*. 4: 117-123.

48. Almeida, R. D., Manadas, B. J., Carvalho, A. P., Duarte, C. B. (2004). Intracellular signaling mechanisms in photodynamic therapy. *Biochimica et Biophysica Acta*. 1704: 59-86.
49. Ahmad, N., Gupta, S., Feyes, D. K., Mukhtar, H. (2000). Involvement of Fas (APO-1/CD95) during photodynamic-therapy-mediated apoptosis in human epidermoid carcinoma A431 cells. *Journal of Investigative Dermatology*. 115: 1041:1046.
50. Lai, J. C., Lo, P. C., Ng, D. K. P., Ko, W. H., Leung, S. C. H., Fung, K. P., Fong, W. P. (2006). BAM-SiPc, a novel agent for photodynamic therapy, induces Apoptosis in Human Hepatocarcinoma HepG2 Cells by a Direct Mitochondrial Action. *Cancer Biology & Therapy*. 5: 413-418.
51. Tada, H., Shiho, O., Kuroshima, K., Koyama, M., Tsukamoto, K. (1986). An improved colorimetric assay for interleukin 2. *Journal of Immunological Methods*. 93: 157 –165.
52. Patrice, T. (2003). Photodynamic Therapy. Cambridge: Royal Society of Chemistry.
53. Vonarx-Coinsman, V., Foultier, M. T., Xavier de Brito, L., Morlet, L., Gouyette, A., Patrice, T. (1995). HepG2 human hepatocarcinoma cells: an experimental model for photosensitization by endogenous porphyrins. *Journal of Photochemistry and Photobiology B: Biology*. 30: 201-208.
54. Jori, G. (1990). Factors controlling the selectivity and efficiency of tumor damage in photodynamic therapy. *Lasers in Medical Science*. 5: 115-120.
55. Brasseur, N., Nguyen, T. L., Langlois, R., Oullet, R., Marengo, S., Houde, D., Van Lier, J. E. (1994). Synthesis and photodynamic activities of silicon 2, 3-naphthalocyanine derivatives. *Journal of Medicinal Chemistry*. 37: 415-420.
56. Soncin. M., Busetti, A., Reddi, E., Jori, G., Rither, B. D., Kenney, M. E., Rodgers, M. A. J. (1997). Pharmacokinetic and photodynamic properties of axially substituted Si(IV)- tetradibenzobarreleno- octabutoxyphthalocyanines. *Journal of Photochemistry and Photobiology B: Biology*. 40: 163-167.
57. Lee, P. P. S., Huang, J. D., Wu, C., Fong, W. P., Ng, D. K. P. (2003). Synthesis, characterization, biodegradation and *in vitro* photodynamic activities of silicon(IV) phthalocyanines conjugated axially with poly(ε-caprolactone). *Macromolecules*. 36: 7527-7533.
58. Gomer, C. J., Dougherty, T. J. (1979). Determination of [^{3}H]- and [^{14}C] hematoporphyrin derivatives distribution in malignant and normal tissue.

Cancer Research. 39: 146-151.

59. Desroches, M. C., Bautista-Sanchez, A., Lamotte, C., Labeque, B., Auchere, D., Farinotti, R., Maillard, P., Grierson, D. S., Prognon, P., Kasselouri, A. (2006). Pharmacokinetics of a tri-glucoconjugated 5, 10, 15 -(meta) -trihydroxyphenyl -20-phenyl porphyrin photosensitizer for PDT. A single dose study in the rat. *Journal of Photochemistry and Photobiology B: Biology*. 85: 56-64.
60. Bourdon, O., Laville, I., Carrez, D., Croisy, A., Fedel, P., Kasselouri, P., Prognon, P. Legrand, P., Blais, J. (2002). Biodistribution of meta-tetra(hydroxyphenyl)chlorin incorporated into surface-modified nanocapsules in tumor-bearing mice. *Photochemical and Photobiological Sciences*. 1: 709-714.
61. Ronn, A. M., Batti, J., Lee, C. J., Yoo, D., Siegel, M. E., Nouri, M., Lofgren, L. A., Steinberg, B. M. (2002). Comparative biodistribution of meta-tetra(hydroxyphenyl)chlorine in multiples species: clinical implications for photodynamic therapy. *Lasers in Surgery and Medicine*. 20: 437-442.
62. Brasseur, N., Ouellet, R., La Madeleine, C., Van Lier, J. E. (1999). Water-soluble aluminium phthalocyanine-poymer conjugates for PDT: photodynamic activities and pharmacokinetics in tumor-bearing mice. *British Journal of Cancer*. 80: 1533-1541.
63. Chin, W., Lau, W., Cheng, C., Olivo, M. (2004). Evaluation of Hypocrelin B in a human bladder tumor model in experimental photodynamic therapy: Biodistribution, light dose and drug-light interval effects. *International Journal of Oncology*. 25: 623-629.
64. Masumoto, K., Yamada, I., Tanaka, H., Fujise, Y., Hashimoto, K. (2003). Tissue distribution of a new photosensitizer ATX-S10Na(II) and effect of a diode laser (670nm) in photodynamic therapy. *Lasers in Surgery and Medicine*. 18: 134-138.
65. Hajri, A., Wack, S., Meyer, C., Smith, M. K., Leberquier, C., Kedinger, M., Aprahamian, M. (2002). *In vitro* and *In vivo* efficacy of Photofrin® and Pheophorbide a, a Bacteriochlorin, in photodynamic therapy of colonic cancer cells. *Photochemistry and Photobiology*. 75: 140-148.
66. Dougherty, T. J., Cooper, M. T., Mang, T. S. (1990). Cutaneous phototoxic occurrences in patients receiving Photofrin. *Lasers in Surgery and Medicine*. 10: 485-488.
67. Moriwaki, S. I., Misawa, J., Yoshinari, Y., Yamada, I., Takigawa, M., Tokura, Y. (2001). Analysis of photosensitivity in Japanese cancer-bearing patients receiving photodynamic therapy with porfimer sodium (Photofrin). *Photodermatology, Photoimmunology, Photomedicine*. 17: 241-243.

68. Bourre, L., Simonneaux, G., Ferrand, Y., Thibaut, S., Lajat, Y., Patrice, T. (2003). Synthesis, and *in vitro* and *in vivo* evaluation of a diphenylchlorin sensitizer for photodynamic therapy. *Journal of Photochemistry and Photobiology B: Biology*. 69: 179-192.
69. Singh, G., Espiritu, M., Shen, X. Y., Hanlon, J. G., Rainbow, A. J. (2001). *In Vitro* induction of PDT resistance in HT29, HT1376 and SK-N-MC Cells by various Photosensitizers. *Photochemistry and Photobiology*. 73: 651-656.
70. Zacal, N., Espiritu, M., Singh, G., Rainbow, A. J. (2005). Increased BNip3 and decreased mutant p53 in cisplatin-sensitive PDT-resistant HT29 cells. *Biochemical and Biophysical Research Communications*. 331: 648-657.
71. Gartner, L. P., Hiatt, J. L. (2007). Introduction to histology and basic histological techniques. *Colour Textbook of Histology*. 3rd edition. Saunders Elsevier. p.2
72. Crockett, E. T., Spielman, W., Dowlatshahi, S., He, J. (2006). Sex differences in inflammatory cytokine production in ischemia-reperfusion. *Journal of inflammation*. 3: 16.
73. Zhang, Z., Jin, H., Bao, J., Fang, F., Wei, J., Wang, A. (2006). Intravenous repeated-dose toxicity study of ZnPcS2P2-based-photodynamic therapy in Wistar rats. *Photochemical and Photobiological Sciences*. 5: 1006-1017.
74. Ayaru, L., Wittmann, J., Macrobert, A. J., Novelli, M., Bown, S. G., Pereira, S. P. (2007). Photodynamic therapy using verteporfin photosensitization in the pancreas and surrounding tissues in the Syrian golden hamster. Pancreatology. 7: 20-27.
75. Mayne, P. D. (1994). Plasma enzyme in diagnosis. *Clinical Chemistry in Diagnosis and Treatment*. 6th edition. Edward Arnold. pp300-312.
76. Rodriguez-Antona, C., Ingelman-Sundberg, M. (2006). Cytochrome P450 pharmacogentics and cancer. *Oncogene*. 25: 1679-1691.
77. Belliner, D. A., Ho, Y-K., Pandey, R. K., Missert, J. R., Dougherty, T. J. (1989). Distribution and elimination of Photofrin II in mice. *Photochemistry and Photobiology*. 50: 221-228.
78. Whelpton, R., Michael-titus, A. T., Jamdar, R. P., Abdillahi, K., Granhn, M. F. (1996). Distribution and elimination of radiolabeled temoporfin in a murine tumor model. *Photochemistry and Photobiology*. 63: 885-891.
79. Cai, H., Wang, Q., Luo, J., Lim, C. K. (1999). Study of temoporfin metabolism by HPLC and electrospray mass spectrometry. *Biomedical chromatography*. 13: 354-359.

80. Bellnier, D. A., Greco, W. R., Loewen, G. M., Nava, H., Oseroff, A. R., Pandey, R. K., Tsuchida, T., Dougherty, T. J. (2003). Population pharmacokinetics of the photodynamic therapy agent 2-[1-hexyloxyethyl]-2-devinyl pyrophephorbide-a in cancer patients. *Cancer Research.* 63: 1806-1813.

81. Laville, I., Pigaglio, S., Blais, J.-C., Loock, B., Maillard, Ph., Grierson, D. S., Blais, J. (2004). A study of the stability of tri(glucosyloxyphenyl)chlorine, a sensitizer for photodynamic therapy, in human colon tumoural cells: a liquid chromatography and MALDI-TOF mass spectrometry analysis. *Bioorganic & Medicinal Chemistry.* 12: 3673-3682.

82. Laville, I., Pigaglio, S., Blais, J.-C., Doz, F., Loock, B., Maillard, Ph., Grierson, D. S., Blais, J. (2006). Photodynamic efficiency of diethylene glycol-linked glycoconjugated porphyrins in human retinoblastoma cells. *Journal of Medicinal Chemistry.* 49: 2558-2567.

83. Fabris, C., Valduga, G., Miotto, G., Borsetto, L., Jori, G., Garbisa, S., Reddi, E. (2001). Photosensitization with zinc (II) phthalocyanine as a switch in the decision between apoptosis and necrosis. *Cancer Research.* 61: 7495-7500.

84. Marchal, S., Fadloun, A., Maugain, E., D'Hallewin, M. A., Guillemin, F., Bezdetnaya, L. (2005). Necrotic and apoptotic features of cell death in response to Foscan photosensitization of HT29 monolayer and multicell spheroids. *Biochemical Pharmacology.* 69: 1167-1176.

85. Magi, B., Ettorre, A., Liberatori., S., Bini, L., Andreassi, Frosali, S., Neri, P., Pallini, V., Di Stefano, A. (2004). Selectivity of protein carbonylation in the apoptotic response to oxidative stress associated with photodynamic therapy: a cell biochemical and proteomic investigation. *Cell Death and Differentiation.* 11: 842-852.

86. Johnson, T. M., Yu, Z. X. Ferrans, V. J., Lowenstein, R. A., Finkel, T. (1996). Reactive oxygen species are downstream mediators of p53-dependent apoptosis. *Proceedings of the National Academy of Sciences, USA.* 93: 1848-1852

87. Macip, S. M., Igarashi, M., Berggren, T., Yu, J., Lee, S. W., Aaronson, S. A. (2003). Influence of induced reactive oxygen species in p53-mediated cell fate decision. *Molecular Cell biology.* 23: 8576-8585.

88. Lam, M., Oleinick, N. L., Nieminen, A.-L. (2001). Photodynamic therapy-induced apoptosis in epidermoid carcinoma cells: reactive oxygen species and mitochondrial inner membrane permeabilization. *The Journal of Biological Chemistry.* 276: 47379-47386.

89. Sakharov, D. V., Bunschoten, A., Van Weelden, H., Wirtz, K. W. A. (2003). Photodynamic treatment and H_2O_2-induced oxidative stress result in different patterns of cellular protein oxidation. *European Journal of Biochemistry*. 270: 4859-4865.

90. Ahmad, N., Feyes, D. K., Agarwal, R., Mukhtar, H. (1998). Photodynamic therapy results in induction of WAF1/CIP1/p21 leading to cell cycle arrest and apoptosis. *Proceedings of the National Academy of Sciences, USA*. 95: 6977-6982.

91. Ahmad, N., Gupta, S., Mukhtar, H. (1999). Involvement of retinoblastoma (Rb) and E2F transcription factors during photodynamic therapy of human epidermoid carcinoma cells A431. *Oncogene*. 18: 1891-1896.

92. Gupta, S., Ahmad, N., Mukhtar, H. (1998). Involvement of nitric oxide during phthalocyanine (Pc4) photodynamic therapy-mediated apoptosis. *Cancer Research*. 58: 1785-1788.

93. Haywood-small, S. L., Vernon, D. I., Griffths, J., Schofield, J., Brown, S. B. (2006). Phthalocyanine-mediated photodynamic therapy induces cell death and a G_0/G_1 cell cycle arrest in cervical cancer cells. *Biochemical and Biophysical Research Communication*. 339: 569-576.

94. Kroemer, G., Martin, S. J. (2005). Caspase-independent cell death. *Nature Medicine*. 11: 725-730.

95. Janicke, R. U., Sprengart, M L., Wati, M. R., Porter, A. G. (1998). Caspase-3 is required for DNA fragmentation and morphological changes associated with apoptosis. *The Journal of Biological Chemistry*. 273(16): 9357-9360.

96. Kroemer, G., El-Deiry, W. S., Golstein, P., Peter, M. E., Vaux, D., Vandenabeele, P., Zhivotovsky, B., Blagosklonny, M. V., Malorni, W., Knight, R. A., Piacentini, M., Nagata, S., Melino, G. (2005). Classification of cell death: recommendations of the nomenclature committee on cell death. *Cell Death and Differentiation*. 12: 1463-1467.

97. Vitols, S., Gahrton, G., Bjorkholm, M., Peterson, C. (1985). Hypocholesterolaemia in malignancy due to elevated low-density lipoprotein-receptor activity in tumour cells: evidence from studies in patients with leukaemia. *Lancet*. 2: 1150-1154.

98. Vitols, S., Sodeberg-Reid, K., Masquelier, M., Sjostrom, B., Peterson, C. (1990). Low density lipoprotein for delivery of a water-insoluble alkylating agent to malignant cells. *In vitro* and *in vivo* studies of a drug-lipoprotein complex. *British Journal of Cancer*. 62: 724-729.

99. Jori, G., Reddi, E. (1993). The role of lipoproteins in the delivery of tumor-targeting photosensitizers. *International Journal of Biochemistry*. 25: 1369-1375.
100. Zhou, C., Milanesi, C., Jori, G. (1988). An ultrastructural comparative evaluation of tumors photosensitized by porphyrins administered in aqueous solution, bound to liposomes or to lipoproteins. *Photochemistry and Photobiology*. 48: 487-492.
101. Obochi, M. O. K., Boyle, R. W., Van Lier, J. E. (1993). Biological activities of phthalocyanines. XIII. The effects of human serum components on the *in vitro* uptake and photodynamic activity of zinc phthalocyanine. *Photochemistry and Photobiology*. 57: 634-640.
102. Chen, X., Hui, L., Foster, D. A., Drain, C. M. (2004). Efficient synthesis and photodynamic activity of porphyrin-saccharide conjugates: targeting and incapacitating cancer Cells. *Biochemistry*. 43: 10918-10929.
103. Staneloudi, C., Smith, K. A., Hudson, R., Malatesti, N., Savoie, H., Boyle, R. W., Greenman, J. (2007). Development and characterization of novel photosensitizer : scFv conjugates for use in photodynamic therapy of cancer. *Immunology*. 120: 512-517.
104. Heinfling-Weidtmann, A., Reemtsma, T., Storm, T., Szewzyk, U. (2001). Sulfophthalimide as major metabolite formed from sulfonated phthalocyanine dyes by the white-rot fungus *Bjerkandera adusta*. *FEMS Microbiology Letters*. 203: 179-183.
105. Krammer, B. (2001). Vascular effects of photodynamic therapy. *Anticancer Research*. 21: 4271-4277.
106. Dolmans, D. E., Kadambi, A., Hill, J. S., Waters, C. A., Robinson, B. C., Walker, J. P., Fukumura, D., Jain, R. K. (2002) Vascular accumulation of a novel photosensitizer, MV6401, causes selective thrombosis in tumour vessels after photodynamic therapy. *Cancer Research*. 62: 2151-2156.
107. Castano, A. P., Mroz, P., Hamblin, M. R. (2006). Photodynamic therapy and anti-tumour immunity. *Nature Reviews. Cancer*. 6: 535-545.